DEVELOPMENT OF NON-MOTORIZED GRABBER MECHANISM FOR UNMANNED AERIAL VEHICLES

MUHAMMED SAMED KÖROĞLU

AUGUST 2022

ÇANKAYA UNIVERSITY

GRADUATE SCHOOL OF NATURAL AND APPLIED SCIENCES

DEPARTMENT OF MECHANICAL ENGINEERING

MASTER'S THESIS IN

MECHANICAL ENGINEERING

DEVELOPMENT OF NON-MOTORIZED GRABBER MECHANISM FOR UNMANNED AERIAL VEHICLES

MUHAMMED SAMED KÖROĞLU

AUGUST 2022

ABSTRACT

DEVELOPMENT OF NON-MOTORIZED GRABBER MECHANISM FOR UNMANNED AERIAL VEHICLES

KÖROĞLU, Muhammed Samed
M.Sc., Department of Mechanical Engineering

Supervisor: Assist. Prof. Dr. Özgün SELVİ
August 2022, 112 pages

In this thesis, we aimed to make research and design regarding a grabber mechanism which is going to be used especially on unmanned aerial vehicles. Throughout the thesis process, we plan to apply methods of optimization, synthesis, analysis, CAD and manufacturing to design a novel grabber system for today's rising technology; drones and unmanned similar aerial vehicles. According to prior art, numerous grabber mechanisms has been created with different manners for air vehicles which can be controllable via electricity motors or similar actuators. Most encountered versions of grabber design for drones can be counted like servo or DC motor actuated claws, integrated robotic arms/manipulators, roller systems, motor driven grippers, magnetic latching grippers and so on. In our thesis, we target to solve the current problems of this kind of mechanisms as of over-weighting, flight stability failures, volume limitations for grabber placing, failures due to complexity of current mechanisms etc. The new concept thesis is created to cover mentioned problems by working on a novel non-motorized linkage model which is similar to latch mechanism. Thanks to this approach, problems can be minimized or pulled down to acceptable limits.

Keywords: Drone, Gripper, Non-Motorized, Aerial Vehicle

ÖZ

İNSANSIZ HAVA ARAÇLARI İÇİN BİR MOTORSUZ TUTUCU MEKANİZMA GELİŞTİRMESİ

KÖROĞLU, Muhammed Samed
Yüksek Lisans, Makine Mühendisliği Anabilim Dalı

Tez Yöneticisi: Dr. Özgün SELVİ
Ağustos 2022, 112 sayfa

Bu tezde özellikle insansız hava araçlarında kullanılacak bir tutucu mekanizması ile ilgili araştırma ve tasarım yapmayı amaçladık. Tez süreci boyunca, günümüzün yükselen teknolojisi; insansız hava araçları ve benzeri insansız hava araçları için yeni bir tutucu sistemi tasarlamak için optimizasyon, sentez, analiz, CAD ve üretim yöntemlerini uygulamayı planladık. Önceki tekniğe göre, drone araçları için elektrik motorları veya benzeri aktüatörler ile kontrol edilebilen, farklı şekillerde çok sayıda tutucu mekanizma oluşturulmuştur. Drone sistemleri için tutucu tasarımlarının en çok karşılaşılan versiyonları, servo veya DC motorla çalıştırılan pençeler, entegre robotik kollar/manipülatörler, makara sistemleri, motor tahrikli tutucular, manyetik mandallı tutucular vb. gösterilebilir. Tezimizde bu tür mekanizmaların gereğinden fazla ağır olması, uçuş stabilitesi bozukluklarına yol açması, tutucunun yerleştirilmesi için hacim sınırlamaları, mevcut mekanizmaların karmaşıklığından kaynaklanan arızalar vb. sorunlarını çözmeyi hedefledik. Bir mandal mekanizmasına benzer motorsuz bir mekanizma modeli üzerinde çalışılarak belirtilen sorunlar en aza indirilebilir veya tasarım için kabul edilebilir sınırlara çekilebilir.

Anahtar Kelimeler: Uçangöz, Tutucu, Motorsuz, Hava Aracı

ACKNOWLEDGEMENT

I would like to express my sincere gratitude to my parents for their support and sacrifice to me. Your memories would ever shine in my mind.

Special thanks to my supervisor Dr. Özgün SELVİ for the excellent guidance and providing me with an excellent atmosphere to conduct this research. My special gratitude also goes to the rest of the thesis committee for the encouragement and insightful comments.

TABLE OF CONTENTS

LIST OF TABLES

LIST OF FIGURES

LIST OF ABBREVIATIONS AND SYMBOLS

Symbols

F:	Force
F(N):	Normal Force
μ:	Frictional constant
G:	Weight of objects
∝:	Angle values
cm:	Centimeter
mm:	Milimeter
m/s:	Meter per second
km/h:	Kilometer per hour
mAh:	Ampere per hour
V:	Voltage
Wh:	Watt hour
N:	Newton
m:	Mass / Meter
g:	Gravitational acceleration
k:	Spring constant
M:	Moment

Abbreviations

CAD:	Computer Aided Design
DC:	Direct Current
AI:	Artificial Intelligence
UAV:	Unmanned aerial vehicle
DOF:	Degree of freedom
COG:	Center of gravity
COT:	Center of thrust
IDE:	Integrated development environment

PLA:	Polylactic acid
MDF:	Medium density fibreboard

CHAPTER I

INTRODUCTION

In today's world, aerial transportation gains an important role in different places of life. In cases where human interaction is hard, conveyance speeds are vital or in situations causing big expenses while loads are required to be hauled, aerial transportation and depending on these unmanned aerial vehicles turns to be necessity. These unmanned systems are gradually entering our lifes more and more in conditions such that natural disasters, epidemics or pandemics, internet shopping, surveillance demands, firefighting, aerial photography, military observations or military gunned tasks etc. For example, near to end of 2019, in COVID-19 pandemic, which has been affected whole world strongly and resulted millions of people's death, humanity needed these aerial vehicles more than ever such that in quarantine conditions some important internet shopping companies like Amazon, Alibaba.com etc. have preferred drone systems to transport trade goods to different coordinates. That companies use AI technologies and simple box systems in their drones to complete the whole process without human interference.

Figure 1: Amazon's delivery drone with simple box system [1]

Depending on mentioned situations, both in civil and military base projects, aerial load carriage operations come to a pioneer development item. These aerial based operations are made by two main air vehicle configurations as fixed wing and rotary wing flying vehicles. Fixed wing structures do carriage operations generally by fixed storage sections inside, like cargo planes and fixed wing UAVs which are carrying useful loads. Rotary wing designs, which are mostly known as drones among people, do load transportation tasks with various type of methods. One is fixed storage type transportation that is just like in the fixed wing vehicles, other ones are gripper mechanisms that are driven with various sources like electricity, pressurized air, gasoline, magnetism etc. Mentioned gripper systems composed from sections including electricity motors, actuators or any other electricity-based components connecting to a linkage structure to do load carriage. These gripper designs can work seamlessly under any conditions on mentioned aerial vehicles serving remote control facility as well. However, current mechanisms developed for grabbing loads need additional space and create additional weight for an aerial vehicle which is undesirable thing when we talk about a flying human made object. Additional space and extra weights mean we will need more power and design area for a flight, which will cause us more expenses and ineffectiveness in design process. Besides, it may cause frequent breakdowns in system, which may be highly dangerous for a flying vehicle when we talk about flight dynamics. There are few experimental works in which grippers are created in different techniques which are like scissor type, manipulator arm type, roller type etc. But simply they stayed in beta form, more clearly, they couldn't be used in daily life base just because they were not able to provide quickness, flight stability and design simplicity. Moreover, as stated before all these said mechanisms have a power system to control grabbers/grippers, so these systems prevent flight stability and directly affect the vehicle's weight in negative way which is most substantial parameter of an aerial devices.

1.1 OBJECTIVE

In this thesis, we targeted to solve mentioned current problems of electrically, pneumatically driven scissor type, manipulator arm type, roller type mechanisms which are stated as over-weighting, flight stability failures due to incompact design, volume limitations for gripper placing, breakdowns due to complexity of current mechanisms etc. Our new concept will be designed to cover mentioned problems by

thinking on a simple non-motorized mechanism model, which will be similar to latch mechanism. Thanks to this approach, problems can be minimized or pulled down to limits that may be acceptable in a project according to designer's preference. Our gripper design considered to be working especially on rotary wing aerial vehicles but system can also be adapted to any upper assemblies that serving grabbing function like robotic arms. Desired gripper mechanism would also be useful in production lines that require single movement having hold and release logic for different loads. As mentioned, in design process, we will consider a gripper system which is going to be similar to latch mechanisms. In other words, grabbing motion will be completed without need to any electricity, pressurized air or similar power sources. We planned to provide power source for gripper directly from motion of rotary wing vehicle itself. For example, in case we have a quadcopter, we can do load grabbing and releasing functions with two simple acts of quadcopter, which may be ascending and descending moves of drone. Thus, it is possible that power need for gripper may be provided directly from these motions of quadcopter. With this simple movement of aerial vehicle, also locking function of load can be successfully applied for desired mechanism in flight moment. Our system will be templated basically under these limitations. Clearly, it is obvious thing that removing motorized systems, electrical installations and their components will minimize drone's weight and that will directly affect flight quality. Moreover, design will help to prevent over-weighting, flight stability failures, volume limitations for grabber placing, failures due to complexity of current mechanisms.

With this thesis, it is targeted to reach a point that drone will grab the loads in very quick way. Therefore, a latch linkage which should be appropriate to a desired given propeller-drone is going to be created and integrated to desired vehicle.

One another purpose is to encourage the people, researchers who are willing to work in this field and to carry the concept better points.

1.2 ORGANIZATION OF THESIS

This thesis contains six chapters. Our thesis starts from literature search regarding current technologies and techniques about unmanned aerial conveyance systems and reaches to creation of novel non-motorized gripper mechanism for rotary wing aerial vehicles in the end.

Chapter 1 is including brief history of unmanned aerial conveyance projects and mentioning main objectives of thesis regarding the field.

Chapter 2 refers prior art, current technologies and basic principles for aerial load conveyance systems in more detailed manner.

In Chapter 3; design limitations, conceptual works and whole major design processes are involved for desired gripper system.

Chapter 4 is including fabrication stages for final design.

Chapter 5 is related with testing steps for desired gripper. The chapter is also involving test results, evaluations and comparison of the thesis with current works.

Chapter 6 draws a conclusion for whole work done in this thesis.

CHAPTER II

PRIOR ART

2.1 APPLIED CONCEPTS IN CURRENT TECHNOLOGIES

In prior art, numerous load conveyance systems have been created for unmanned air vehicles including different shapes which can be controlled via electricity motors or similar actuators as remotely or in self-determination manner which is in other words, artificial intelligence supported way. Most encountered version of carriage designs for these vehicles can be expressed as motor actuated claws, integrated robotic arm/manipulators, rope roller systems, motor driven grippers, magnetic latching grippers and so on. Generally, we can separate current aerial gripper mechanisms into two parts by their active or passive characteristics. Active mechanisms do grasp with their links which are actively moving to grab target objects. These mechanisms provide their power from electricity (Like battery, accumulator etc.), directed air (Pneumatically driven systems), gasoline-based sources (Cylinder motor connected systems) or sun (Solar panels are used on aerial vehicles to provide power for links of gripper) etc. Passive mechanisms do grasp an object while they don't have a movable component inside. Magnetics or piezoelectricity-based mechanisms are example for passive gripper systems.

2.1.1 Active Gripper Systems Developed for Aerial Vehicles

As of our literature search regarding current active gripper systems, we can encounter similar mechanical configurations which are claw-like systems, manipulator-like systems or hybrid systems which combining both claw-manipulator type system characteristics into one mechanism. Sometimes, these mechanisms are not created in rigid way which are mostly used in old techniques. Such that, soft linkages, bistable mechanisms or compliant based structures are also new developing trends in this fields.

2.1.1.1 Rigid Mechanical Gripper Systems

As referred, rigid mechanical gripper systems are generally including claw-like systems, manipulator-like systems or hybrid systems. There are also recreated gripper configurations from historically famous mechanisms like “Scotch Yoke” [2]. Besides, self-catcher hook structures which provide their power from drone itself, also tried in the field [3]. Rigid mechanical gripper mechanisms are today most encountered and matured configurations in aerial grasping tasks.

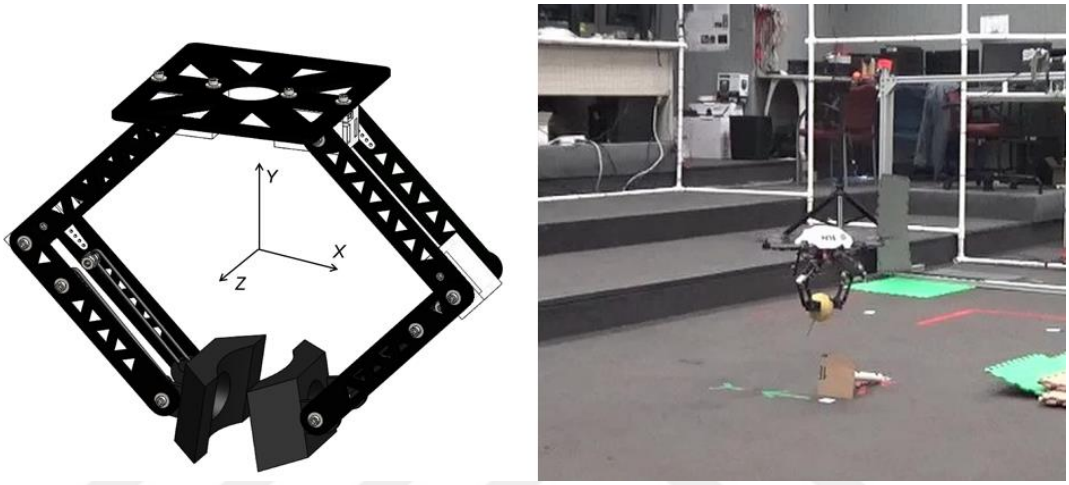

Figure 2: Hybrid and actively compliant manipulator/gripper systems for air vehicles [4]

Figure 3: Drone gripper system recreated by using famous “Scotch Yoke Mechanism” [2]

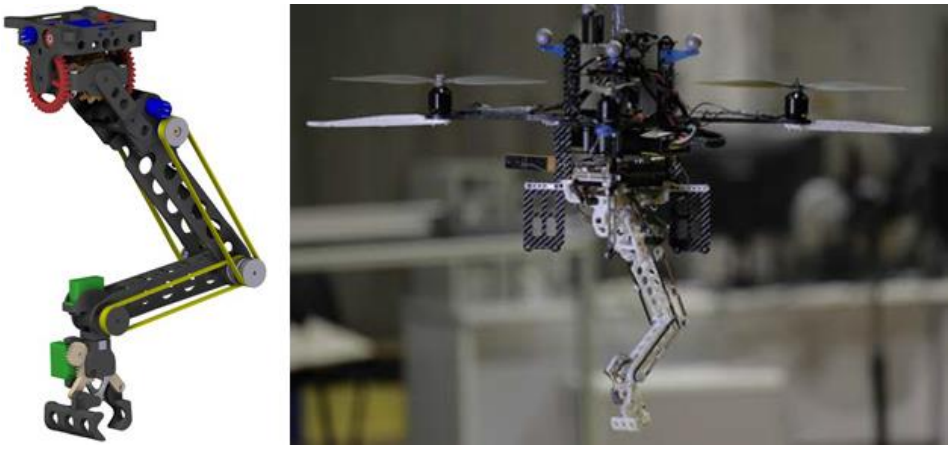

Figure 4: 5-DoF Robot Arm for Aerial Manipulation [5]

Figure 5: Motor actuated claw system mounted bottom of drone, which composed from servo motors to grasp an object [6]

Figure 6: Self-catcher hook system mounted bottom of drone, which provide required power directly from aerial vehicle's ascending or descending motion [3][7]

Figure 7: Origami inspired drone arm which can be collapsed or expanded in origami manner [8]

Figure 8: A motorized hybrid claw-arm system mounted bottom of drone [9]

2.1.1.2 Soft Gripper Systems

Soft gripper systems are new leading mechanisms used in aerial vehicles. These mechanisms decrease number of complex components in system, moreover it provides a light-weight usage for grasping an object. It is easier to supply power in wide range compare to rigid mechanical grippers in soft gripper systems. In other words, they are more flexible systems such that control of this kind systems are easier.

It is also possible better grasping in soft systems because in most cases we have more grasping surfaces on a load.

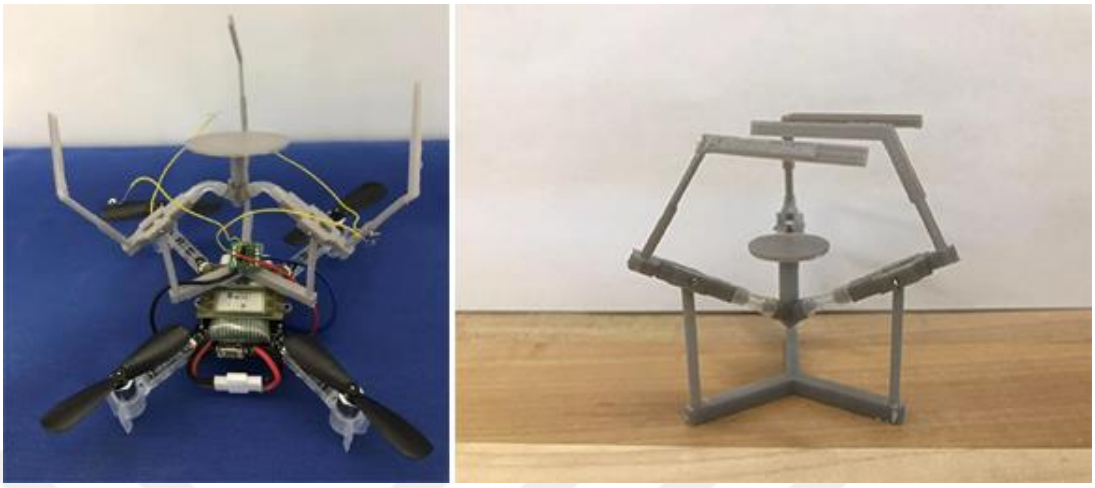

Figure 9: Compliant bistable gripper for aerial perching and grasping [10]

2.1.2 Passive Gripper Systems Developed for Aerial Vehicles

Passive mechanisms don't have an actively moving part inside. These mechanisms do grip functions with their passive driving characteristics such as magnetism, piezoelectricity etc. Practically, these kinds of graspers are being widely used in recycling plants to separate ferromagnetic metals from garbage. These passive systems are also adapted for aerial conveying systems in new experimental works and academic studies. Although passive systems are successful on grabbing an object and can take actions quickly, they require additional mechanisms when they are to release an object. For example, one thesis that includes magnetic grab-release function uses additional servo motor-crank complex to solve releasing object problem. That proposed system uses permanent magnets for grasping, and a novel dual-impulsive release mechanism, for achieving drop [11].

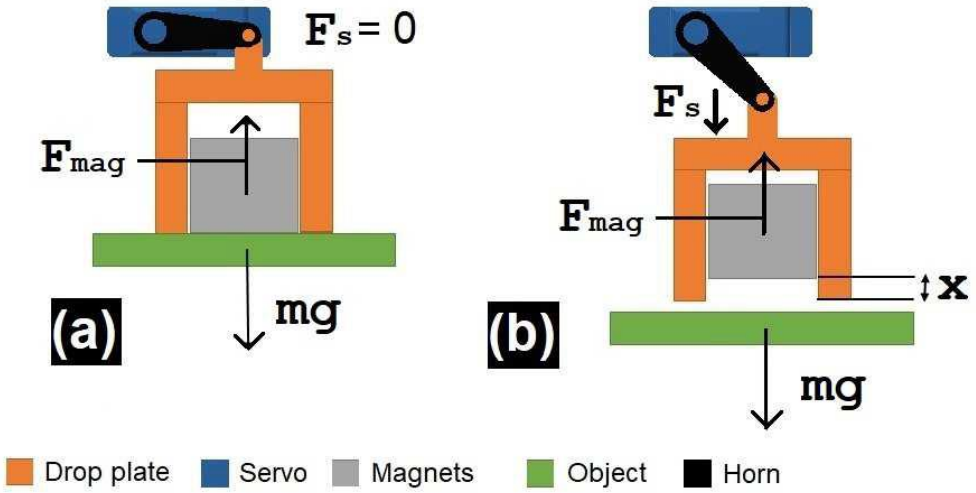

Figure 10: Impulsive release mechanism by merging both servo motor and magnet system for using in aerial transporting of objects [11]

2.2 BASIC LOGIC BEHIND GRASPING AN OBJECT

2.2.1 Gripper Arm-Load Grasping Condition

Grasping an object simply based on a force equation including friction between touching surfaces. Considering a simple gripper structure which has two grasping arms;

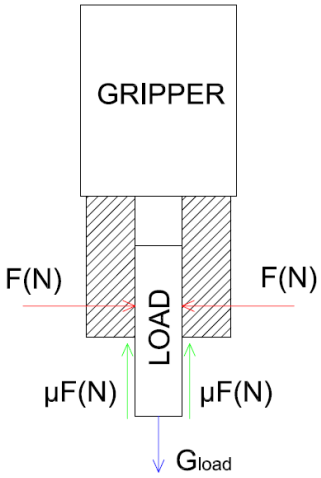

Figure 11: Gripper arm load grasping position schematic

Here F(N) can be denoted as pressing force of gripper arms which is also F_{normal}. Static friction coefficient between surfaces is "μ" and "μ×F(N)" is friction force between load and arms. Load can be stay stationary between arms, if force condition is;

$$2 \times \mu F(N) \geq G_{load} \quad (2.1)$$

Similarly, if we consider a four-legged gripper;

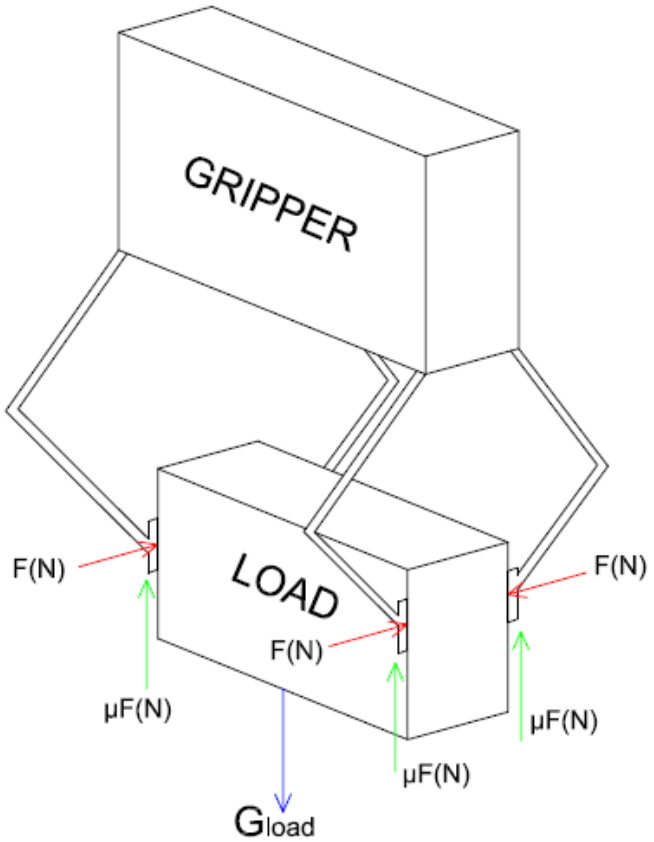

Figure 12: Four-legged gripper arm load grasping position schematic

Grasping condition becomes;

$$4 \times \mu F(N) \geq G_{load} \quad (2.2)$$

When gripper arm numbers are increased, same balance situation is kept to be preserving to hold the load successfully. This approach is all applied for even with different type of arms.

2.2.2 Determination of Static Friction Between Surfaces

Static friction coefficient between surfaces can be provided from a very simple experiment as shown;

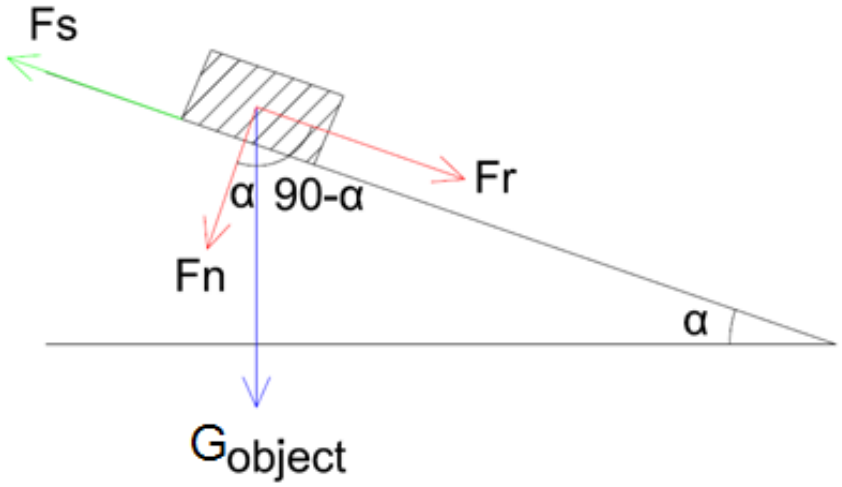

Figure 13: Inclined platform experiment for extracting friction coefficient between surfaces

Experiment procedure;

A flat platform is put on any ground surface and an object is put on that platform. Gradually some inclination is given to platform. When object starts to slide along the platform, α angle in that moment is saved. Tangent value of α gives us static friction coefficient called "μ_s". By this way, static friction coefficient between different surfaces can be found. We can prove tan(α) = μ_s equation from;

In moment of $F_S = F_R$, object starts to slide along the platform;

$$\mu_S \times G_{Object} \times cos(\propto) = G_{Object} \times cos(90-\propto) \quad (2.3)$$

$$\mu_S \times cos(\propto) = cos(90-\propto) \quad (2.4)$$

$$\mu_S = \frac{cos(90-\propto)}{cos(\propto)} = \tan(\propto) \quad (2.5)$$

2.3 LITERATURE SEARCH FOR POSSIBLE NON-MOTORIZED GRIPPER SYSTEMS

2.3.1 Mechanisms Having Middle Contact Limbs for Transmission of Force to Gripper Arms

By thinking our design purposes, we have determined to design a gripper mechanism which can be driven via drone's ascending and descending motions. This motion should be transmitted by a touch system inside the mechanism and reverted to arms as pressing force on the target load. For example, when our aerial vehicle approaches to touch the load by its limb, that limb (Will be called "pressure pad" after

this point.) should transfer that touch motion to gripper arms to grasp the load as a reaction. By this way, we can create a gripper model which doesn't need an external motor/actuator driving. It is also desired to create at least four arms to grab the object better. Under these circumstances, a new literature search has been made for similar mechanisms providing these conditions. Sample mechanisms are shown in Figure 14 and Figure 15.

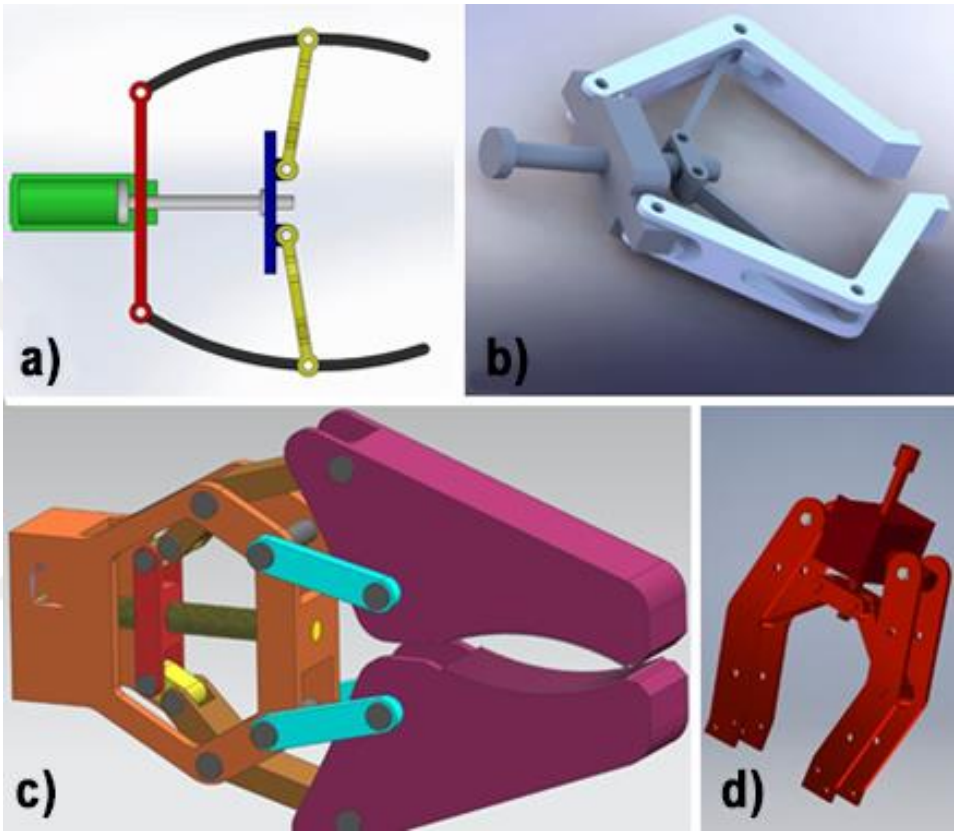

Figure 14: Mechanisms driven by force transfer rod on middle to drive gripper arms (a is pneumatic-hydraulic gripper [12], b is a rod driven robotic arm gripper [13], c is screw driven robot gripper [14], d is motorized rod driven gripper model [15])

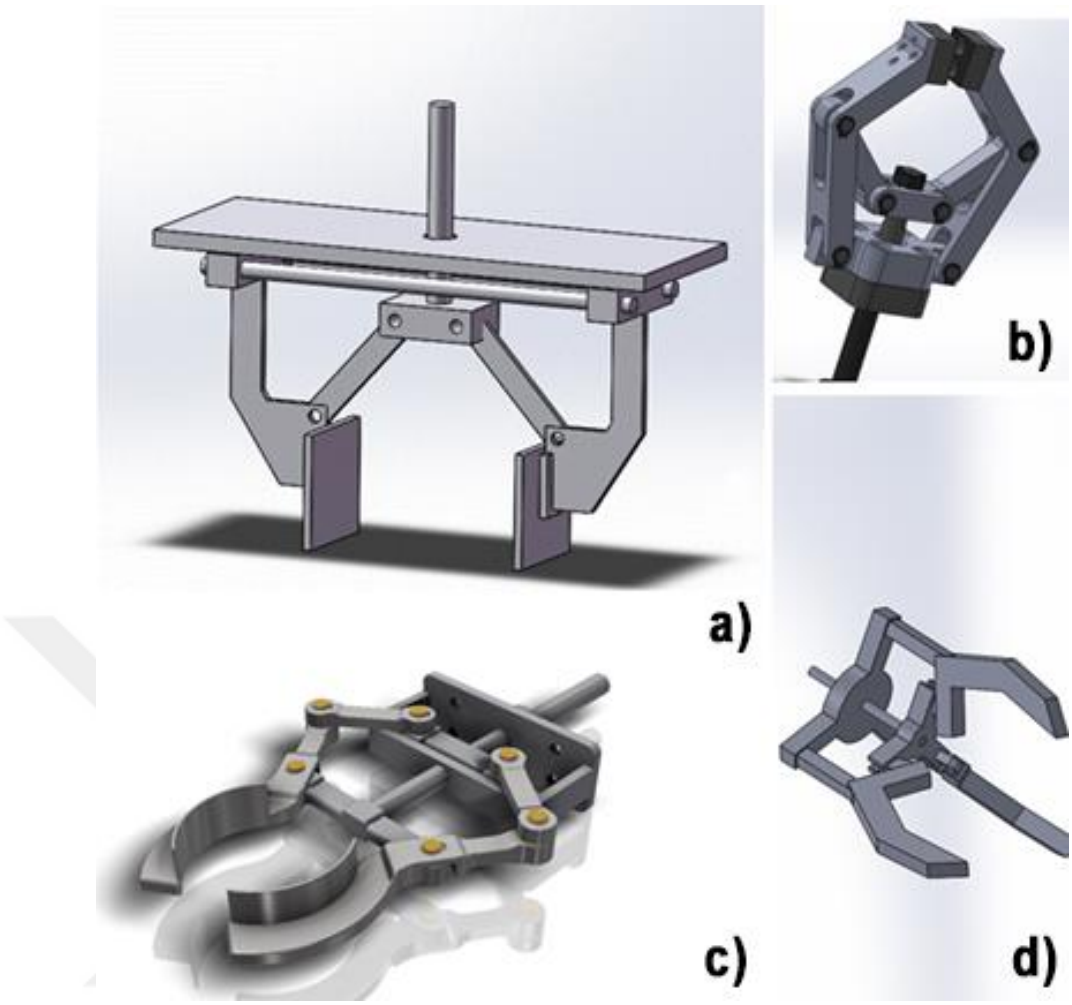

Figure 15: Mechanisms driven by force transfer rod on middle to drive gripper arms (a is plunger activated gripper [16], b is pneumatic gripper [17], c is middle stick driven robot gripper [18], d is three legged gripper [19])

In searched linkage literature, all these eight models include a middle force transfer rod to drive gripper arms in mechanism. In these linkages, middle force transfer rods are driven by screw structures, pneumatic pressure effects or with direct linear forces created by motors or similar actuators. In our project, force transfer rod will be driven via force originated from load-pressure pad contact which is going to direct forces to arm members to provide movements as collapsing or expanding of gripper arms. Some of mentioned mechanisms are close to what we are aiming in this project. However, none of these mechanisms can't provide self locking-unlocking function in mechanisms. For this reason, an additional mechanism literature search for self-locking-unlocking is needed as well.

2.3.2 Mechanisms Having Self Locking-Unlocking Abilities

A force transfer rod driven function is desired feature in this project as referred before. However, we also expect in this project self locking-unlocking feature as stated. Therefore, we made an extra search for possible mechanisms for this. At first, we thought about ball pen mechanisms that can provide motion of what we are demanding in this project. As known, ball pen mechanisms can make both locking and unlocking actions with two clicks respectively. In other saying, if a force touches twice to the button of ball pen systems, one can get lock-unlock functions together. Typical ball pen mechanisms have few configurations. These configurations are actually different versions of cam-follower couplings. All these configurations provide push-push action by applying cam movements in periodic way. Linear mechanism in Figure 16 (Figure b, Figure e) are easiest ones for quick prototyping. Because they have a linear path which can be easily modified for any project. So, these linear-based systems can easily be adapted for our project as well. Rest configurations are mostly cylindrical structures and relatively hard to apply for every project. Possible mechanisms after literature scan are seen in Figure 16.

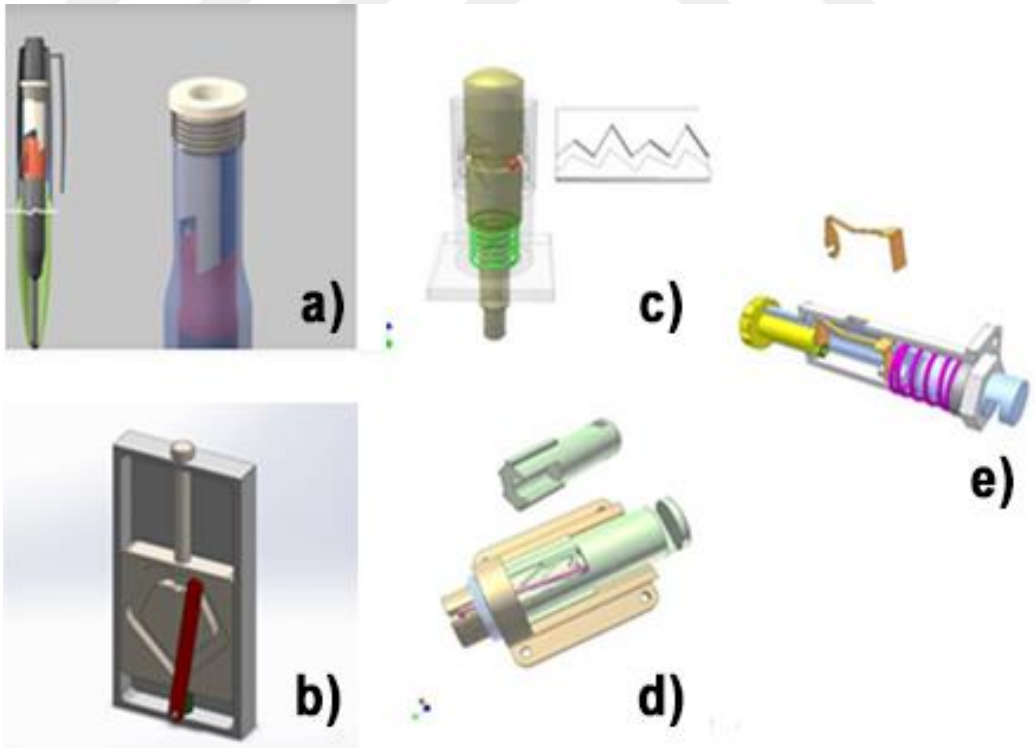

Figure 16: Various ball pen mechanisms having push-push function (a is ballpoint pen mechanism [20], b is linear push- push button mechanism [21], c is cylindrical push-push button mechanism having peripheral cam path [22], d is cylindrical push-push button mechanism having cam follower inside [23], e is push-turn button mechanism [24])

CHAPTER III

DESIGN STAGE

3.1 DETERMINATION OF LIMITATIONS

3.1.1 Selection of Aerial Vehicle

To design our final gripper model, we need to get a reference aerial vehicle to determine main dimensional limitations and future tests. So, we can create a reference gripper placement template by that way. For this purpose, we have selected a quadcopter weighting over 500 grams for having a significant lifting power. Full specifications for selected drone are;

Drone name: MJX Bugs 16 Pro (Known as "Aden FX67 Pro" in Turkish market)
Drone Weight: 612 grams (Battery and propellers included)
Sizes: 295*80*87 mm (Closed form), 395*395*87 mm (Opened form)
Max. Ascending Velocity: 3m/s
Max. Descending Velocity: 2 m/s
Max. Velocity: 40 km/h
Max. Altitude: 120 m
Max. Tilt Angle: 35 degrees
Max. Angular Velocity: 45 degrees/s
Working temperature: 0-40 Centigrade degrees
Drone Battery: 3200 mAh
Working Voltage: 11.4 V
Power: 36.45 Wh
Drone Battery Weight: +-208 grams

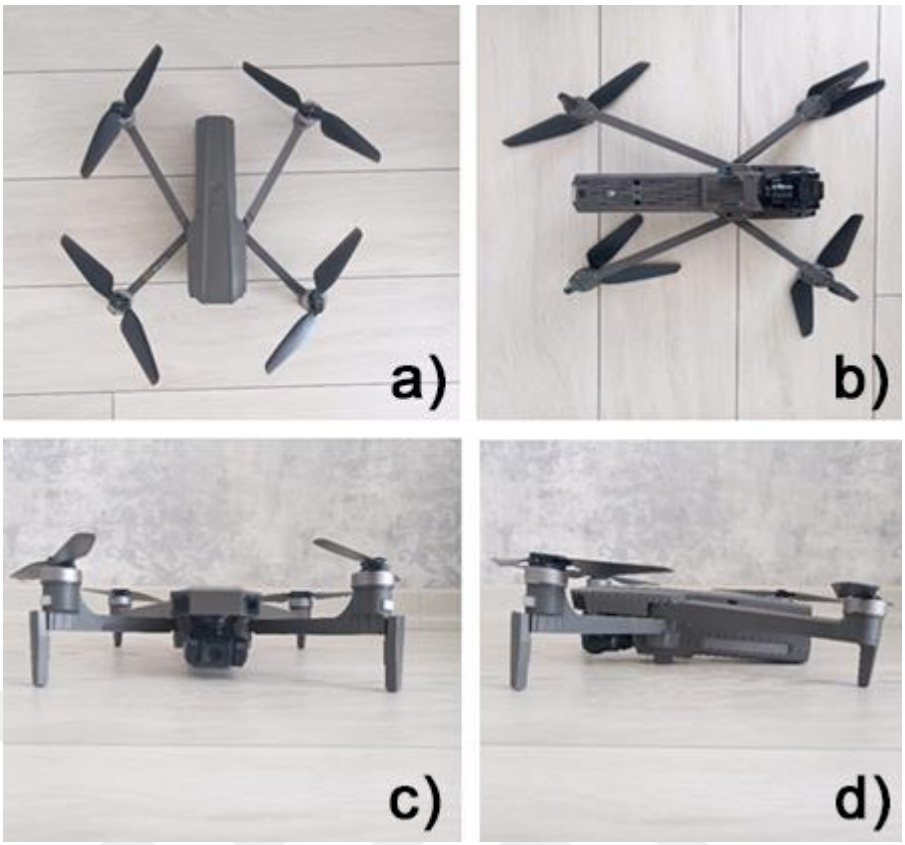

Figure 17: Drone views from a) top, b) bottom, c) front and d) side respectively

3.1.2 Determination of Drone Lifting Capacity

Although drone lifting capacities changes one drone to another, a general rule about lifting capacities of quadcopters is that sum of all motor power can lift up to two times of quadcopter weight. For example, if we have drone weighting 500 grams, that means our drone lifting capacity should be 1 kilogram. That means, we will have 250 grams lifting capacity for each motor. Extra lifting capacity provides us better control capability on our aerial vehicle and more spaces for additional useful loads which may be different cameras, batteries for extending flight time or support structures [25].

This rate can be expressed as thrust to weight ratio. For a good flight with full control, this ratio should be kept 2:1. Greater ratio means we will have better control on drone. For example, in an aerial shooting, 2:1 ratio may be good for a smooth performance. These ratios should be far higher when we are to use FPV drones which can be 3:1, 4:1, 5:1 and even 7:1 because we will need more nimble characteristics on these vehicles for that cases [25]. So, briefly it is seen that drone lifting capacity can be considered as twice as the drone's weight due to our search.

3.1.3 Determination of Drone Thrust Center (COT)

Center of Thrust (COT) point can be determined on a quadcopter by simply drawing cross lines between motors. Intersection point of these cross lines defines the thrust center of quadcopter [26].

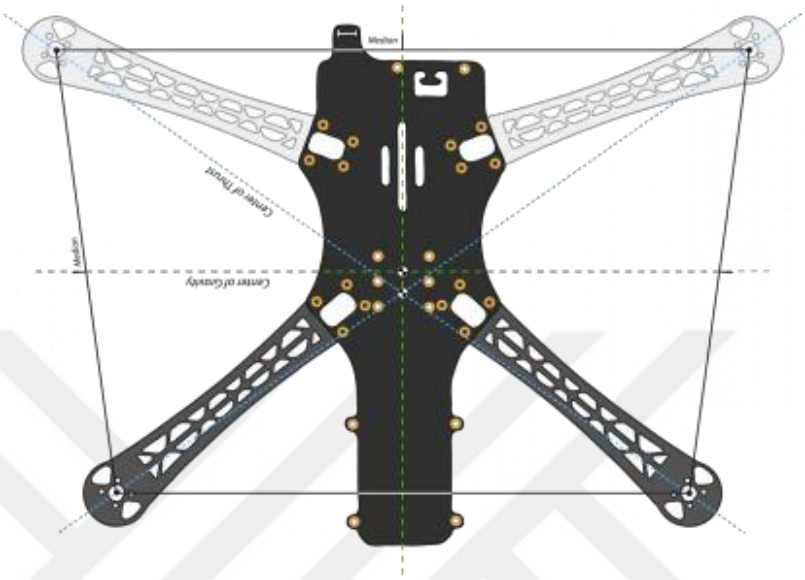

Figure 18: Thrust center calculation for a drone [26]

3.1.4 Determination of Center of Gravity for a Drone (COG)

Center of Gravity for an aerial vehicle should be calculated carefully for a stable flight. Especially, this phenomenon gets more important when we plan to hang an object to quadcopter. Similarly, Center of Gravity (COG) for a quadcopter can be defined like the same way with finding Center of Thrust (COT), however there are some differences about application.

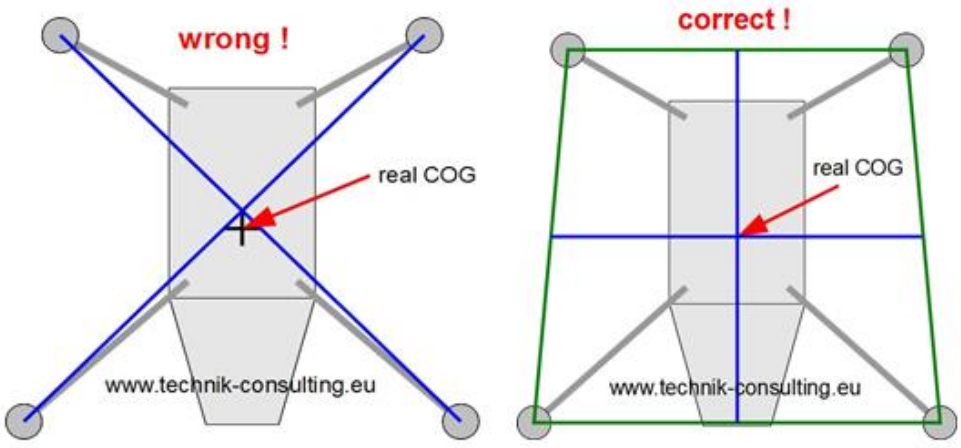

Figure 19: Determination center of gravity for a drone [27]

In left side of Figure 19, it is seen same diagonal method which was told in finding Center of Thrust (COT) as well. However, for some quadcopters this method doesn't always show Center of Gravity (COG) precisely. Instead in the right-side figure, there is a better way to detect Center of Gravity (COG). To find gravity center of a quadcopter, first, green lines are created between motors as in the figure. Then, new blue lines whose starting points should be placed in middle lines of that green lines. Intersection point of these blue lines shows us Center of Gravity (COG) for that quadcopter in better way [27].

Another alternative method to find gravity center of any object is to hang the object with rope from chosen object's any arbitrary point. Center of gravity point for that object should be somewhere placed on rope's vertical projection when object becomes balanced and no more rotate about that axis.

So, by using these basic guidelines about finding drone's center of gravity or thrust center, same line drawing methods and rope hanging methods have been applied for our quadcopter. Due to both methods, our center of gravity and thrust center are found approximately in same point as shown in Figure 20.

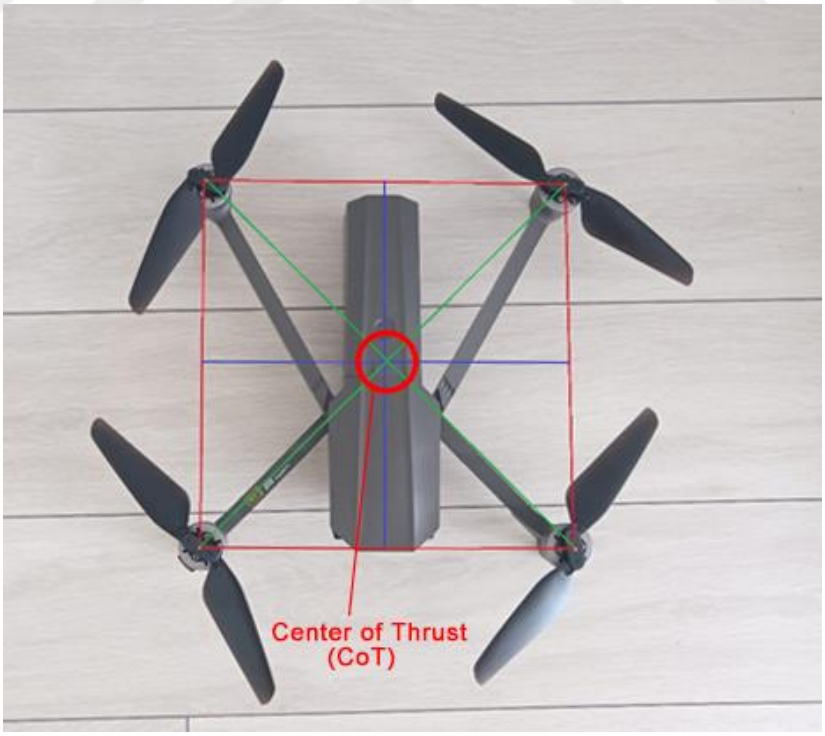

Figure 20: Thrust center for our quadcopter

Determined thrust center and center of gravity points are required instruments especially in CAD stage of design.

3.1.5 Estimated Gripper Placement on Drone

After determination of drone's thrust center and mass center (Mass center and thrust center are determined to be nearly in same point by methods mentioned before), placements of expected sample gripper and load which has 5x5 cm cross section on drone have been proposed like in Figure 21.

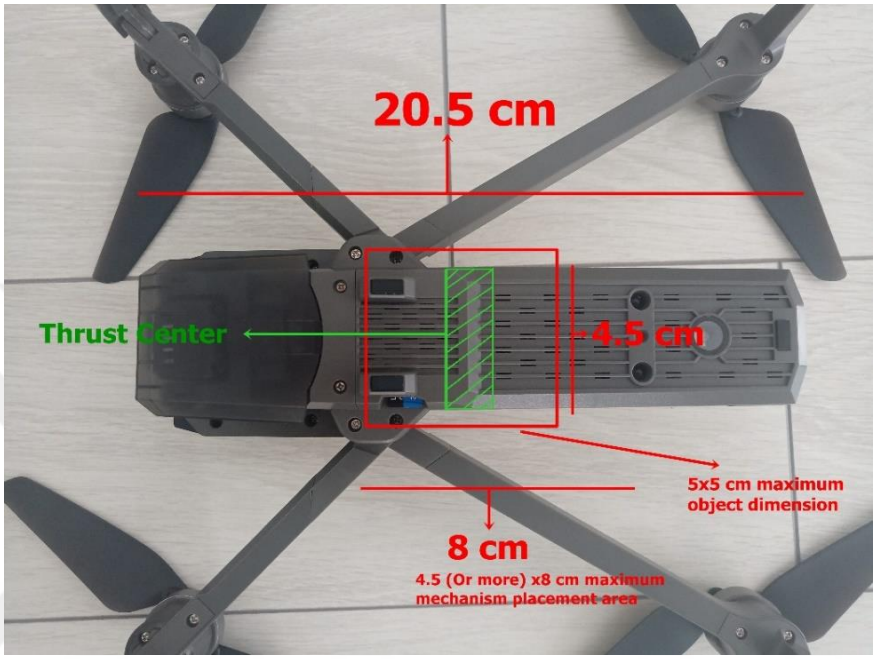

Figure 21: Gripper and load placement sections on bottom of quadcopter

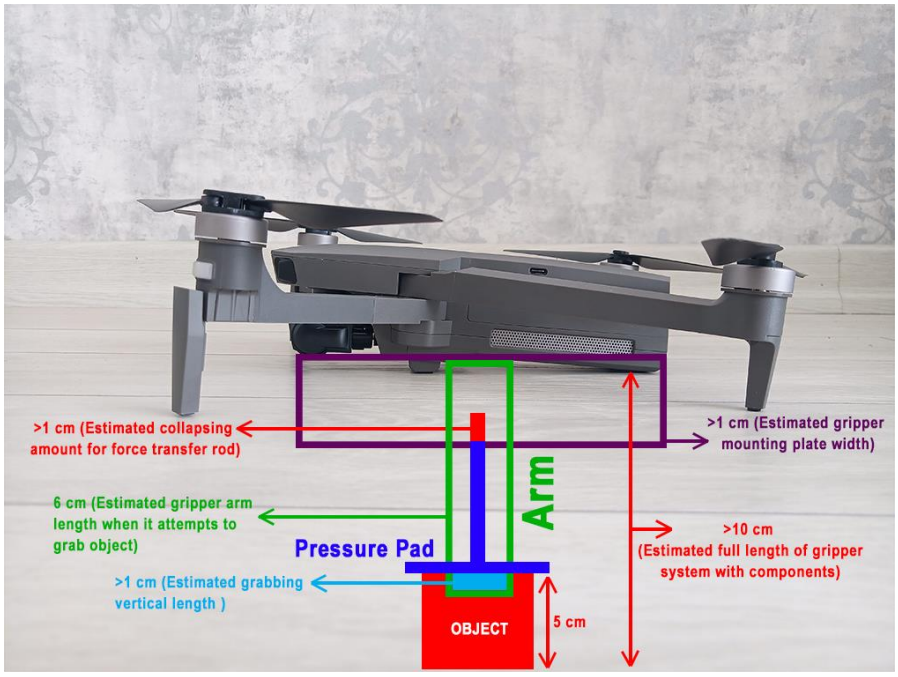

Figure 22: Estimated gripper placement sections on our quadcopter due to limitations

3.2 CONCEPTUAL DESIGN

After determination of basic limitations and reference template of chosen aerial vehicle, proper alternative mechanism ideas are also illustrated in sketchy way. This step is required to help us about imagination for general lines of aimed gripper linkage. So, four alternative concepts are also determined to be useful in scope of this thesis before creation of target design.

3.2.1 Concept-1

A concept including safety part (1), pressure pad (2), load releasing buttons (3), gripper arms (4), pressure stick (5) (Force transfer rod), chassis (6), springs (7). Gripper which is assembled to bottom of drone approaches to a load by help of drone descending motion to grab the load. Pressure pad should be placed just over the load and drone should start to descend to provide touch between pressure pad and load. As drone continues to descend, load will push the pad to embed safety part inside chassis structure for a short distance. When safety part is embedded inside the chassis, gripper arms start to be collapsed for grabbing the load in proper position because embedded safety part is no more creates an obstacle to limit arms. When grabbing done, drone will rise to carry the load to desired position. When drone reaches to desired position, final person who will receive the load can push the load releasing arm to release the load in desired way.

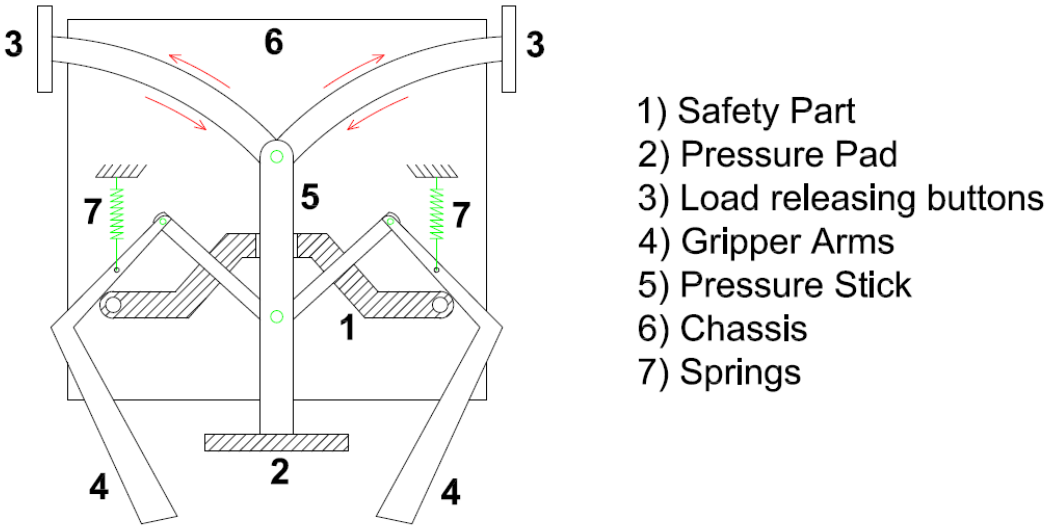

Figure 23: Concept-1

3.2.2 Concept-2

Concept-2 is similar to Concept-1 but it serves simpler working principle. In this concept, pressure pad will be pushed like in Concept-1. Here, pushed pad will drive a magnet system and will provide arms to be collapsed. For releasing the arm, electromagnet poles are changed remotely to drop the load by exploiting reverse magnet principle. Therefore, an unlocking mechanism will be operational to release the load. This mechanism promises fewer mechanical components but requires additional electronics ingredients for remote control.

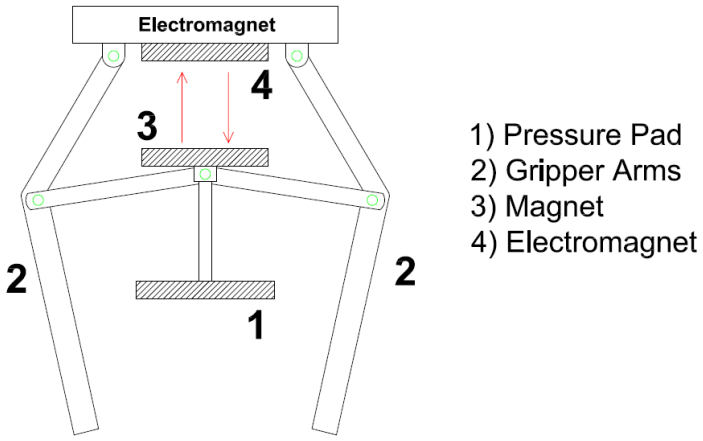

Figure 24: Concept-2

3.2.3 Concept-3

Concept-3 includes another electromagnet-based idea without a pressure pad. Here electromagnet system directly has effect on gripper arms to be collapsed or expanded. The concept provides lesser mechanical links but needs more powerful electromagnetic drive demand.

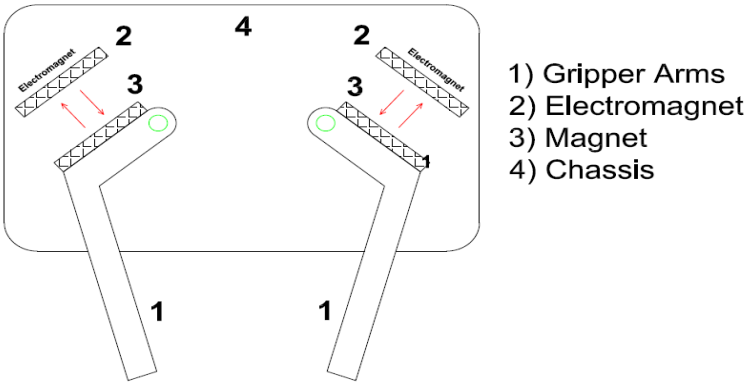

Figure 25: Concept-3

3.2.4 Concept-4

Concept-4 is composed of a soft tube arm couple which can be driven via ferromagnetic powders. Ferromagnetic powder chamber includes powders which can be directed via electromagnet system to fill tube arms with ferromagnetic powders for collapsing the arms. Reverse procedure will cause arms to be expanded. This loop will make loads to be grasped and released.

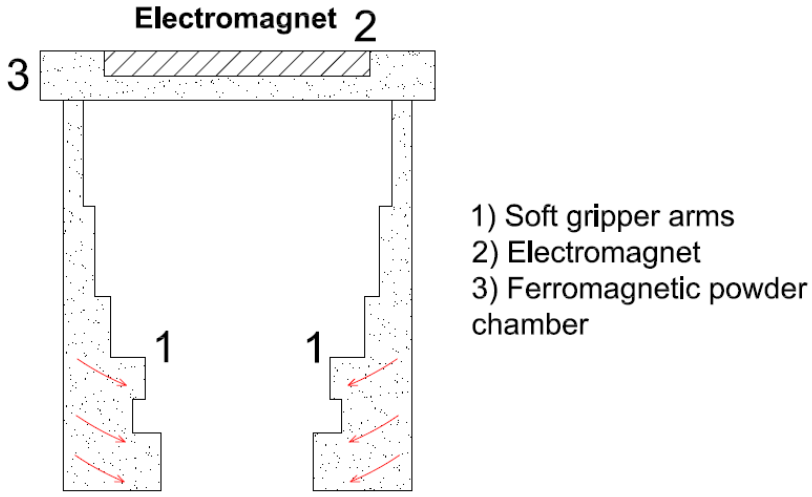

Figure 26: Concept-4

After thinking about these four alternative configurations, for a non-motorized system design, as stated before, it was found efficient to design a concept including a pressure pad, a self locking-unlocking mechanism and a mechanism having at least four arms for providing a better grasping surface. By looking at our first considerations, a mechanical gripper which is mostly under interest of mechanical science instead some other possible heavy electro or pneumatic systems will be designed to do aimed tasks.

3.3 CREATING A TEMPLATE GRIPPER MECHANISM TO DO THE GIVEN TASK

After determination of pre-assumed demands for our gripper (Having pressure pad system, self-locking-unlocking function and condition of providing gripper energy directly from aerial vehicle itself), we planned to design a sample gripper to complete a given short task. The task is determined to be lifting and carrying a small surprise egg plastic case with our planned template gripper. For making this, package CAD

software Solid Works is used to simulate the action. At first approach, a standard push-push button which is used for electricity switch mechanisms as well has been integrated to the computer program to take it as reference part on design process. Our push-push button mechanism has a standard spring translocation amount which should be taken into account in the process. In our case, maximum interval for spring translocation is 5 mm and unlocking interval was nearly 1 mm. So, in result of a CAD process, a concept created like in Figure 27.

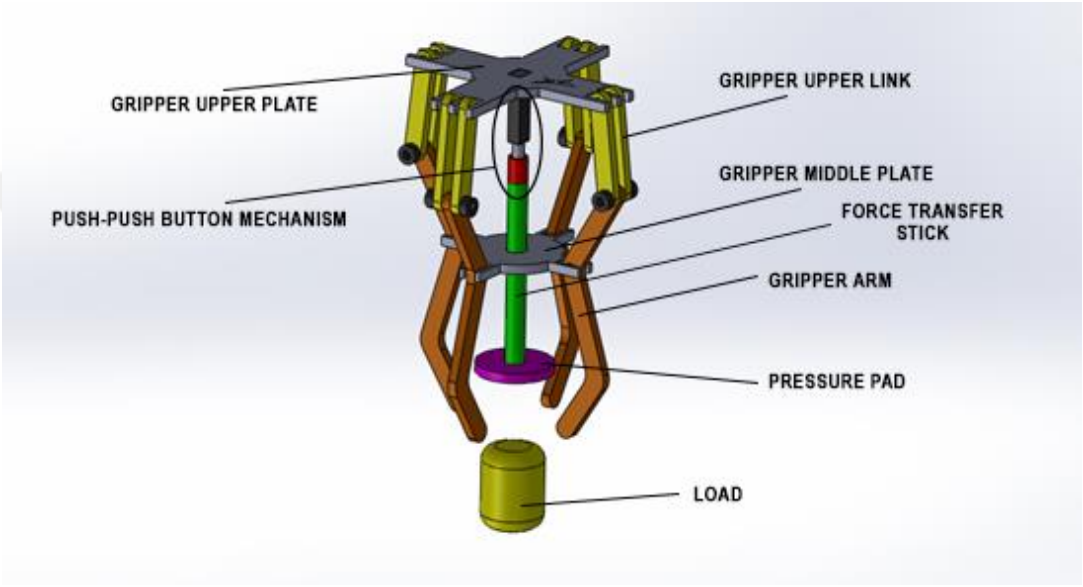

Figure 27: Designed template gripper to make defined task

As shown in Figure 27, big grey plate is gripper upper plate which will be mounted to possible aerial vehicle bottom, small grey plate is movable plate that connected to arms and force transfer rod with green colour, yellow links are gripper upper links connected to gripper upper plate, gripper lower links (Arms) is shown with orange colour, pressure pad is shown with purple colour, section with red head and black body show button mechanism, yellow egg symbolizes an object to be grasped.

When CAD simulation completed, technical drawings are prepared for each part for to be laser cutting by using 5 mm plyboard material. The wood material is believed to be powerful enough to take such small force loads on gripper. Button mechanism has been fixed on gripper with glues and adhesive tapes. Hinge structures and force transfer rod are made with plastic straw. A soft foam material attached gripper leads to reach desired frictional force on arms. Just because button locking mechanism has a locking 1 mm distance, foam material is used to soften the grabbing function on load.

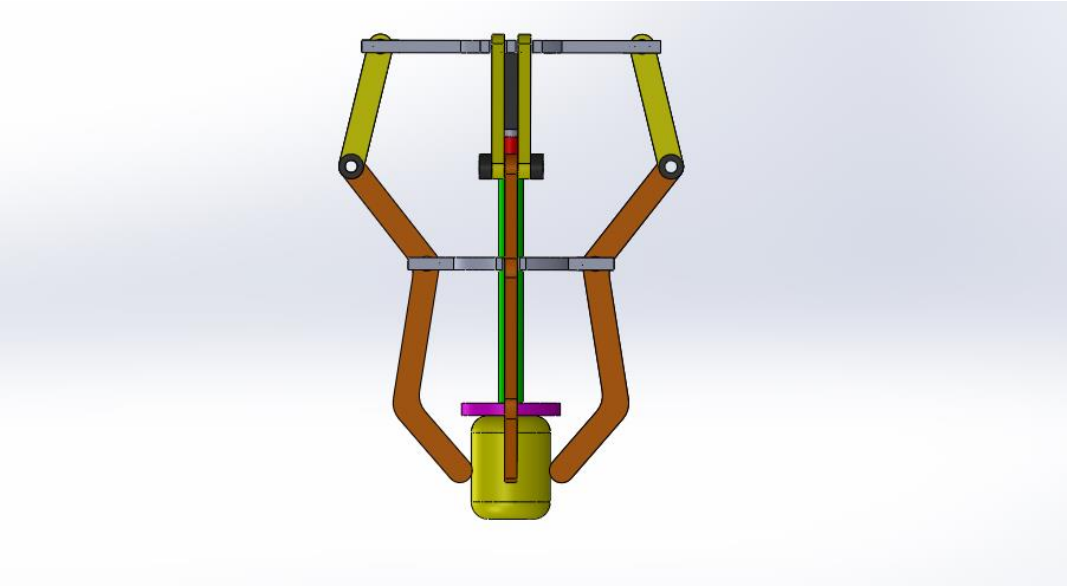

Figure 28: Designed sample gripper while it is grasping the object

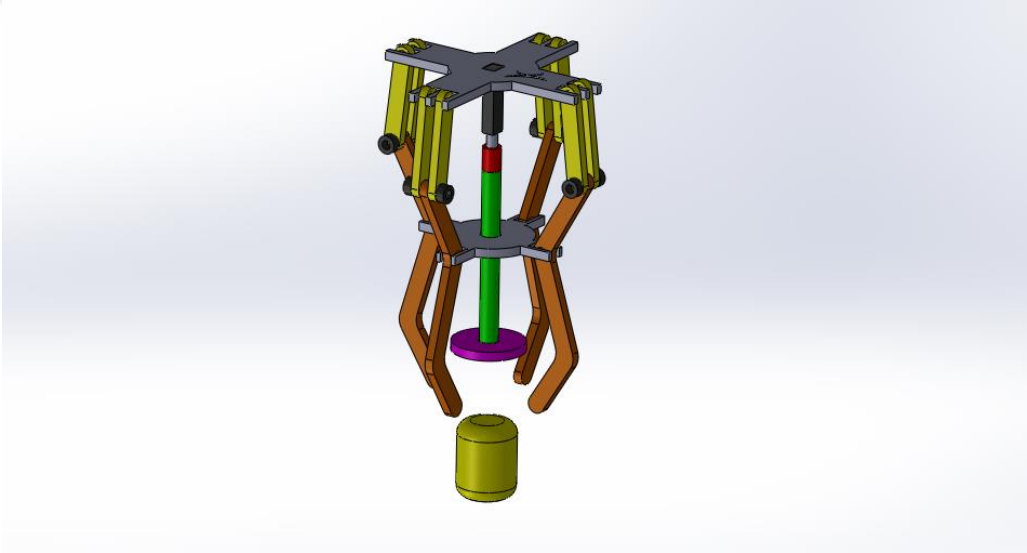

Figure 29: Designed template gripper to make defined task

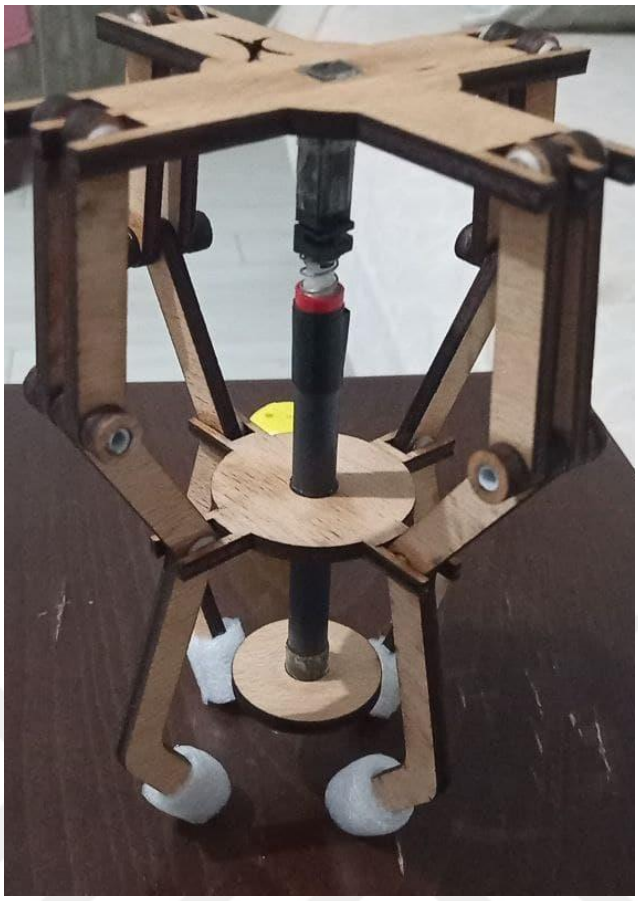

Figure 30: Wood material is used for prototyping the desired template gripper

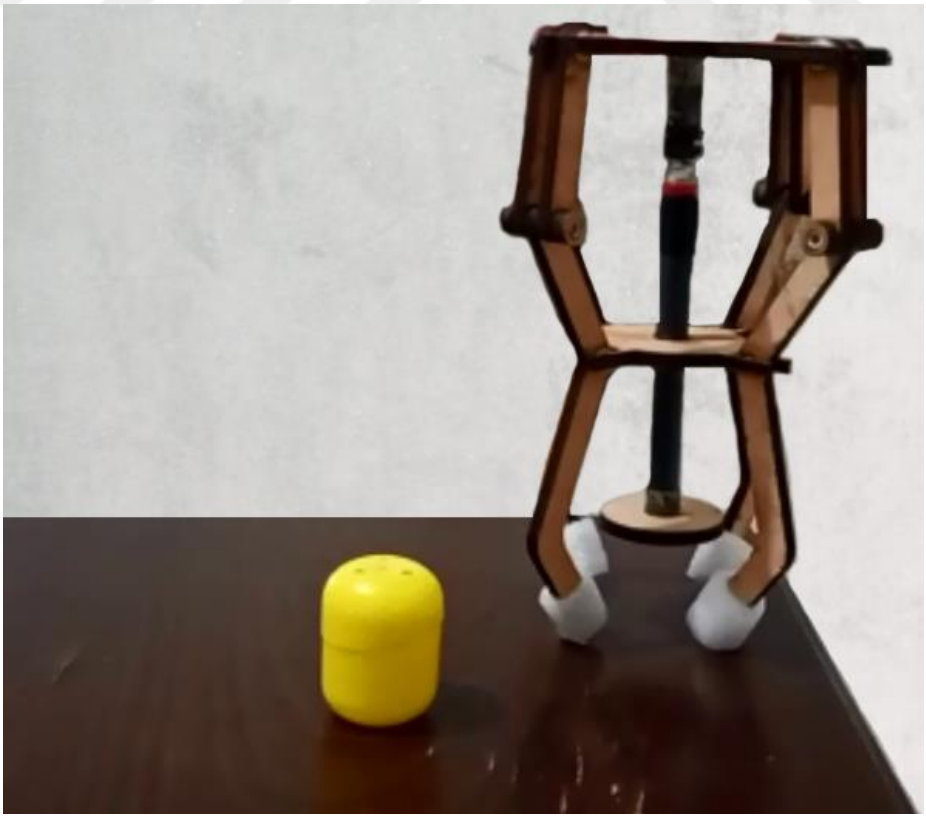

Figure 31: Wood template gripper and sample load

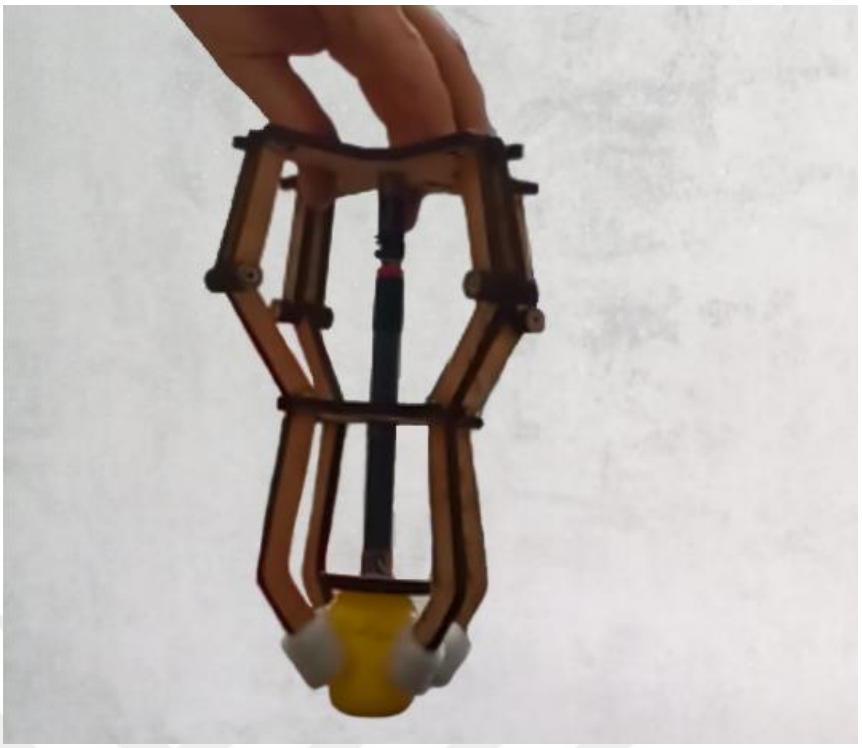

Figure 32: Wood template gripper is grasping sample load

System is working very similar to ball pen system. Working stages of mechanism are;

1- Gripper approaches to yellow egg load and pressure pad applies a force on load. This force causes connected force transfer road to move upward together with gripper middle plate. This upward move of force transfer rod locks the push-push button mechanism as well. In the end of motion, load is grasped and locked between arms.
2- Locked load can now be carried to desired location.
3- Locked load between arms can be released by repeating stage 1. A force again applied on locked load to drive push-push button to release the locked load. In other words, push-push button's this move causes both arms to expand and pressure pad to be pushed by force transfer rod.

3.4 FREE BODY DIAGRAMS FOR ESTIMATED MECHANISM

3.4.1 Free Body Diagram for Load

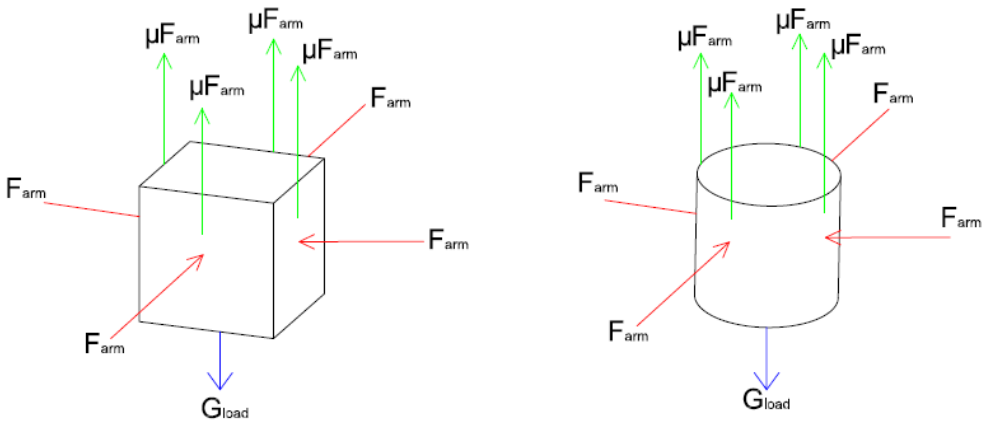

μ: Friction coefficient between gripper arm and load

F_{arm}: Gripper arm pressing force to the load

μF: Frictional Force = F_s

$\mu F_{arm} \times 4 \geq G_{load}$ (Gripper arm load grasping condition)

Figure 33: Free body diagram for loads

3.4.2 Free Body Diagram for Gripper Arms

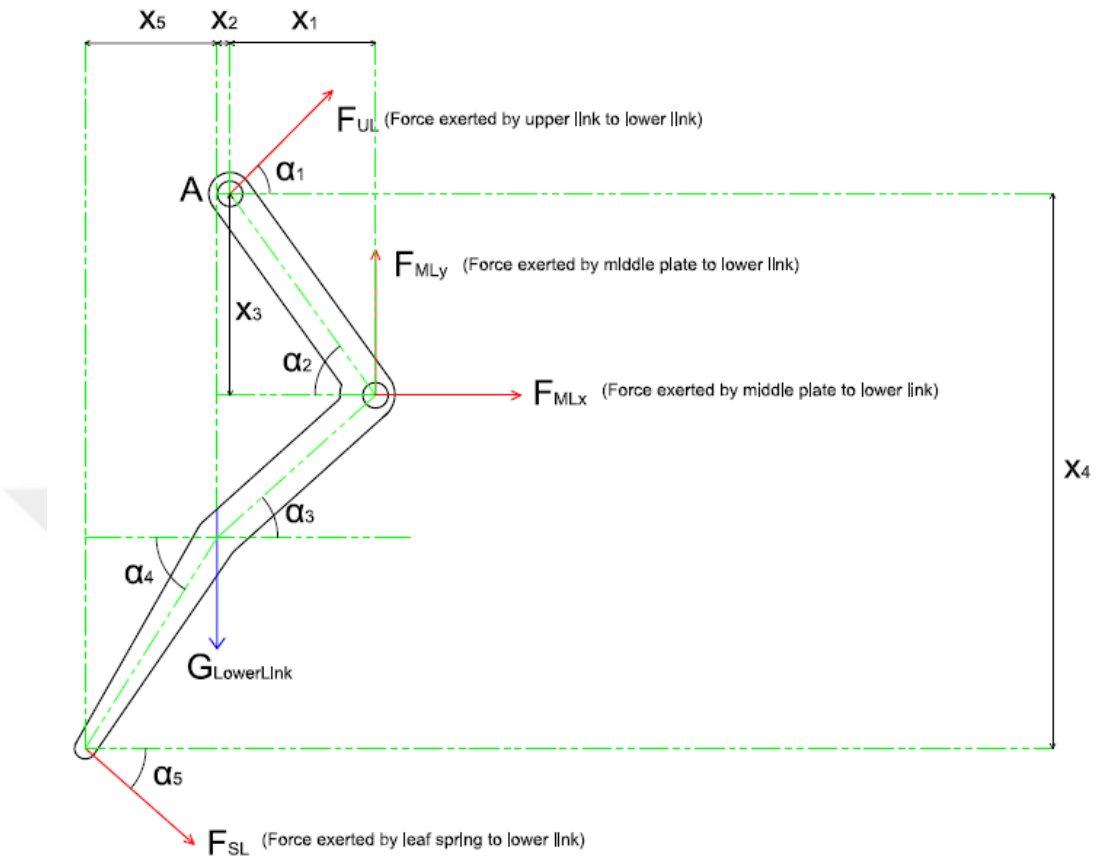

Figure 34: Free body diagram for arm link

Force Equations:

$$\sum F_X = 0\ ;\ F_{UL} \times cos(\propto_1) + F_{ML_X} + F_{SL} \times cos(\propto_5) = 0 \qquad (3.1)$$

$$\sum F_Y = 0\ ;\ F_{UL} \times sin(\propto_1) + F_{ML_Y} + F_{SL} \times sin(\propto_5) + G_{LowerLink} = 0 \qquad (3.2)$$

Moment Equation:

$$\sum M_A = 0\ ;\ F_{ML_Y} \times X_1 + G_{LowerLink} \times X_2 + F_{ML_X} \times X_3 + F_{SL_X} \times X_4 + F_{SL_Y} \times X_5 = 0 \qquad (3.3)$$

3.4.3 Free Body Diagram for Griper Upper Link

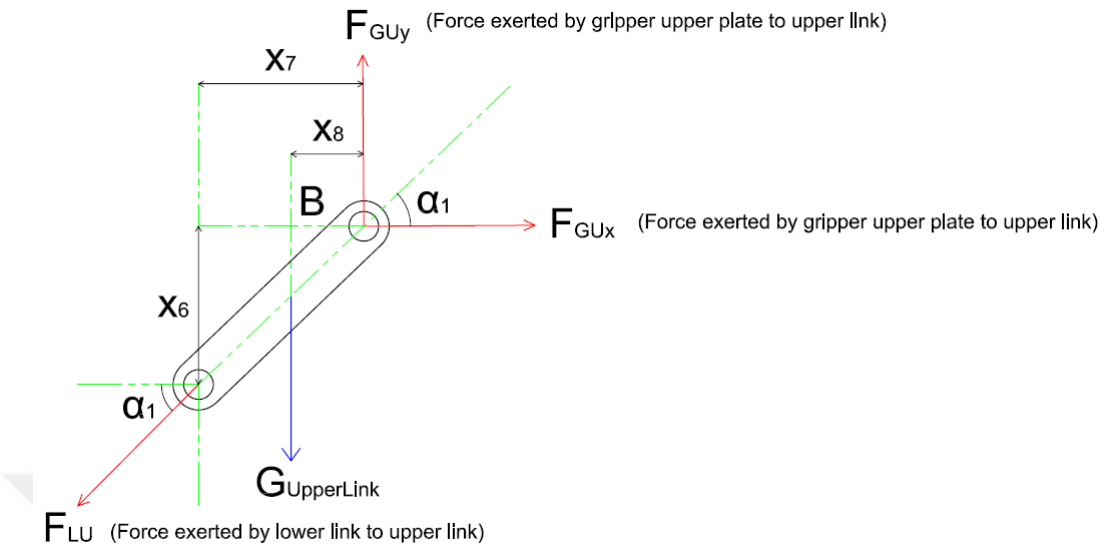

Figure 35: Free body diagram for gripper upper link

Force Equations:

$$\sum F_X = 0\ ;\ F_{LU} \times cos(\propto_1) + F_{GU_X} = 0 \qquad (3.4)$$

$$\sum F_Y = 0\ ;\ F_{LU} \times sin(\propto_1) + F_{GU_Y} + G_{UpperLink} = 0 \qquad (3.5)$$

Moment Equation:

$$\sum M_B = 0\ ;\ F_{LU_X} \times X_6 + F_{LU_Y} \times X_7 + G_{UpperLink} \times X_8 = 0 \qquad (3.6)$$

3.4.4 Free Body Diagram for Gripper Upper Plate

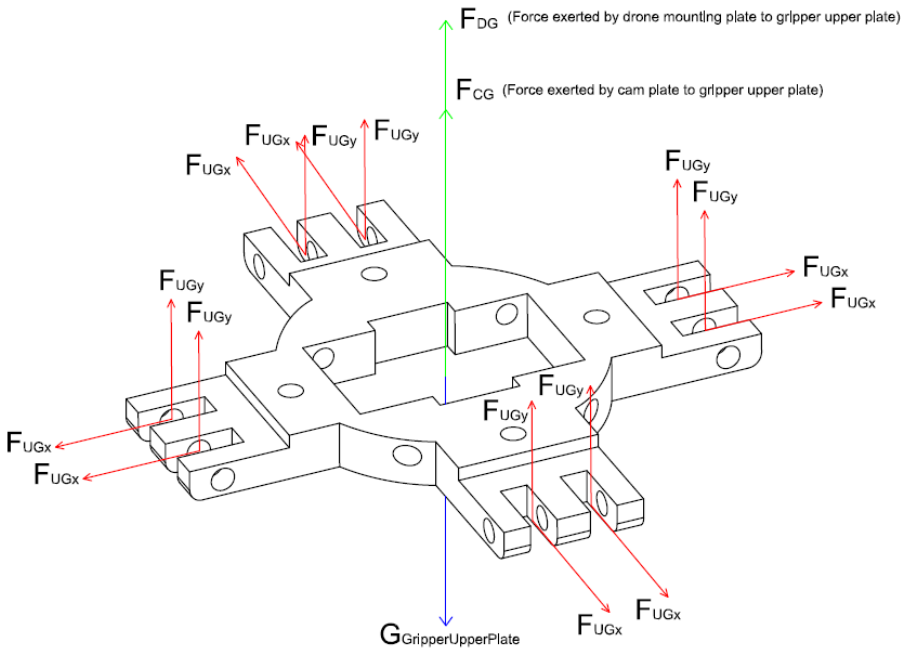

Figure 36: Free body diagram for gripper upper plate

Force Equation:

$$\sum F_Y = 0\ ;\ F_{UG_Y} \times 8 + G_{GripperUpperPlate} + F_{CG} + F_{DG} = 0 \qquad (3.7)$$

3.4.5 Free Body Diagram for Gripper Middle Plate

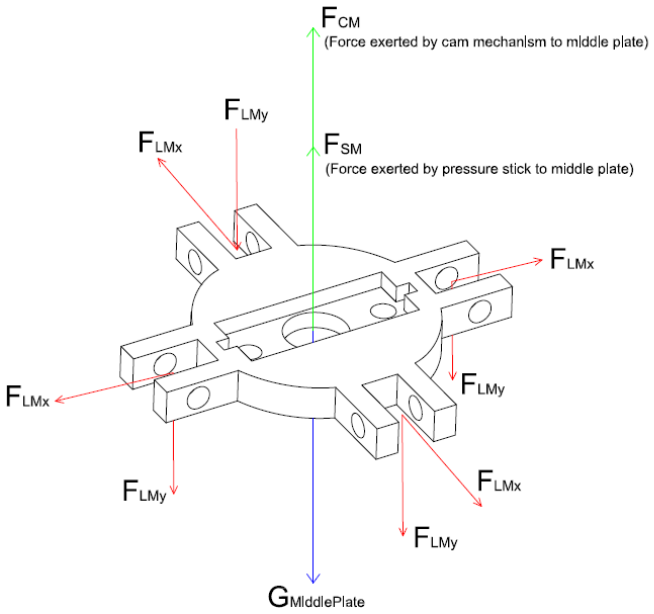

Figure 37: Free body diagram for gripper middle plate

Force Equation:

$$\sum F_Y = 0\ ;\ F_{CM} + F_{SM}\ +\ F_{LM_Y} \times 4 + G_{GripperMiddlePlate} = 0 \qquad (3.8)$$

3.4.6 Cam Mechanism

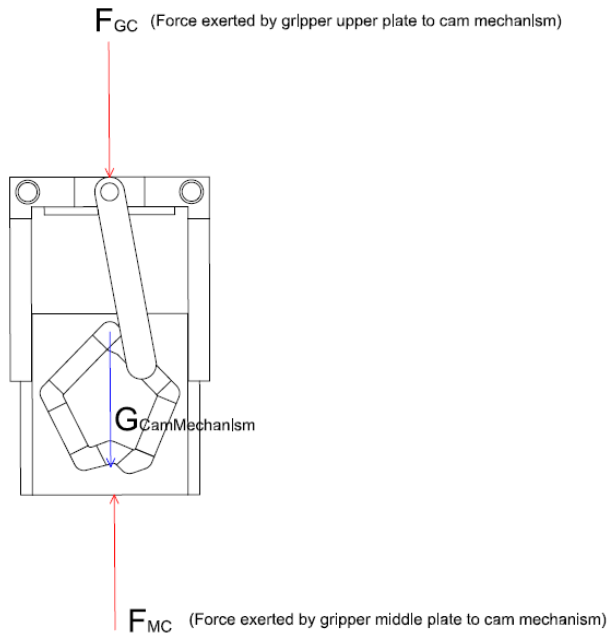

Figure 38: Free body diagram for cam mechanism

Force Equation:

$$\sum F_Y = 0\ ;\ F_{MC} + F_{GC}\ +\ G_{CamMechanism} = 0 \qquad (3.9)$$

3.4.6.1 Cam Channel

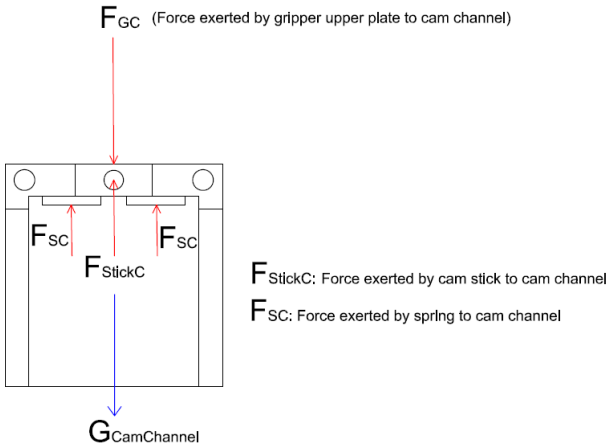

Figure 39: Free body diagram for cam channel

Force Equation:

$$\sum F_Y = 0\ ;\ F_{SC} + F_{GC} + F_{StickC} + G_{CamChannel} = 0 \qquad (3.10)$$

3.4.6.2 Cam Stick

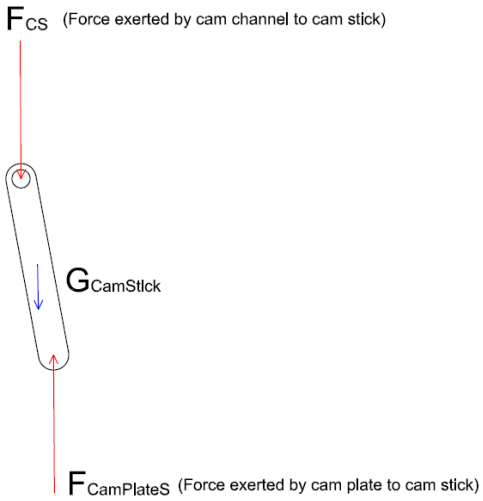

Figure 40: Free body diagram for cam stick

Force Equation:

$$\sum F_Y = 0\ ;\ F_{CS} + F_{CamPlateS} + G_{CamStick} = 0 \qquad (3.11)$$

3.4.6.3 Cam Plate

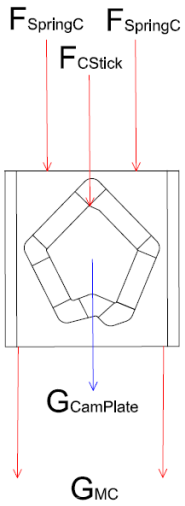

Figure 41: Free body diagram for cam plate

Force Equation:

$$\sum F_Y = 0\ ;\ F_{CStick} + F_{SpringC}\ +\ G_{CamPlate} + \ G_{MC}\ = 0 \qquad (3.12)$$

3.4.7 Force Transfer Rod

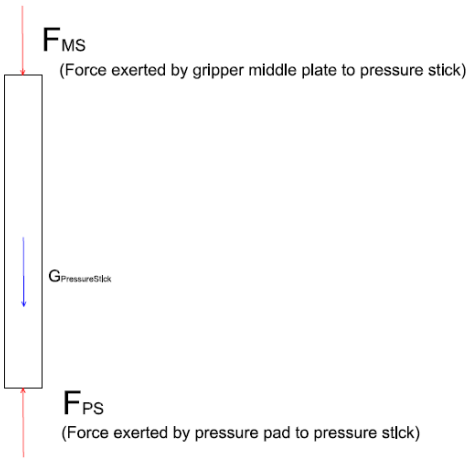

Figure 42: Free body diagram for force transfer rod

Force Equation:

$$\sum F_Y = 0\ ;\ F_{MS} + F_{PS}\ +\ G_{PressureStick} = 0 \qquad (3.13)$$

3.4.8 Pressure Pad

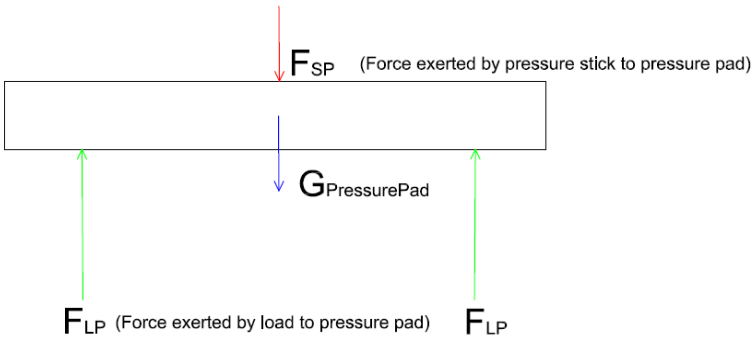

Figure 43: Free body diagram for pressure pad

Force Equation:

$$\sum F_Y = 0\ ;\ F_{SP} + F_{LP}\ +\ G_{PressurePad} = 0 \qquad (3.14)$$

3.4.9 Leaf Spring

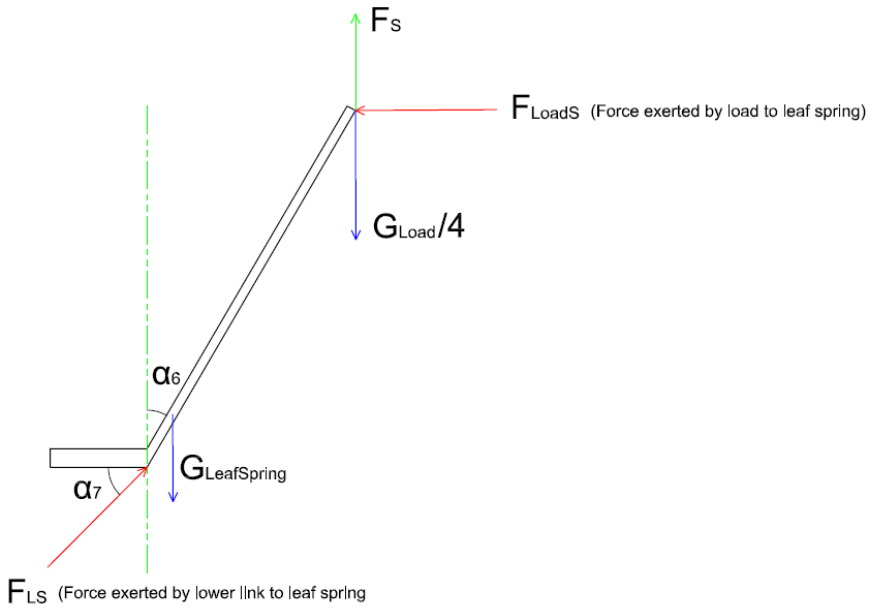

Figure 44: Free body diagram for leaf spring

Force Equations:

$$\sum F_X = 0\ ;\ F_{LS} \times cos(\propto_7)\ +\ F_{LoadS} = 0 \qquad (3.15)$$

$$\sum F_Y = 0\ ;\ F_{LS} \times sin(\propto_7)\ +\ F_S +\ G_{LeafSpring} + \frac{G_{Load}}{4} = 0 \qquad (3.16)$$

3.5 MEASURING DRONE FLIGHT CHARACTERISTICS

3.5.1 Measuring Drone Pressing Force on a Load

For measuring the pressing force of drone on a load, we determined to use a precision scale. So, a hook structure is designed to be attached to top of drone. Then, precision scale is fastened to the hook. By holding precision scale with hand, drone is taken off as rising a short distance. Following this movement, drone is lowered with highest acceleration while reading the value on precision scale. This experiment is repeated several times and value is measured 500 grams averagely (It should be mentioned that drone's high dynamic motion made hard a precise measuring. 500 grams value which is averagely equal to 4.905 N is found after several measurements.).

It is thought that drone's high dynamic motion may also cause gripper's wrong action while drone placing over the load. So, desired gripper is planned to be tried with also robotic arm which will simulate drone's movements. To simulate gripper on

robotic arm, MPU6050 module is determined to be used. MPU6050 is composed of 3 axes gyros and 3 axes angular accelometer sensors. These abilities provide module to show us drone flight parameters in terms of mean or maximum accelerations.

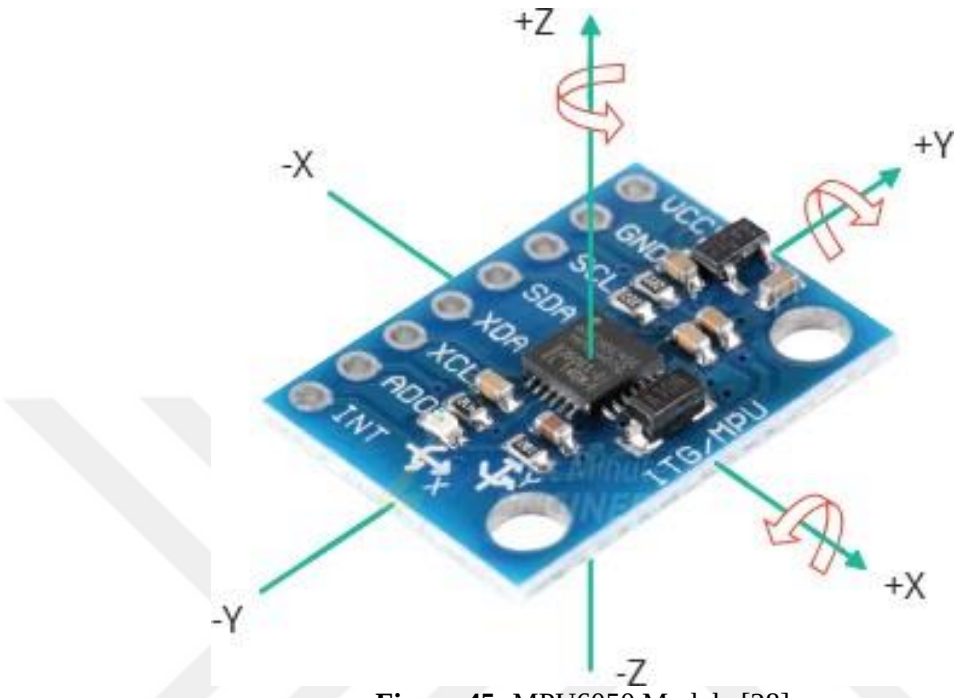

Figure 45: MPU6050 Module [28]

3.5.2 MPU6050 Module Preparation

It is desired that MPU6050 will be mounted bottom of our quadcopter and it is arranged to be sending acceleration and velocity parameters to a computer remotely. By this way, collected data may be categorized and charted in a package program to simulate drone's flight. We can get linear acceleration (m/s^2), angular velocity (degree/seconds) and angular acceleration from derivation of angular velocity ($degree/s^2$) with the module. MPU6050 sensor can easily be integrated to any Arduino card. For remote data transferring, there are several methods exist. One of them is HC06 Bluetooth module which can also be easily integrated to Arduino module also. All Arduino and composed systems are be powered from 9V battery. Desired circuit is built like in Figure 46.

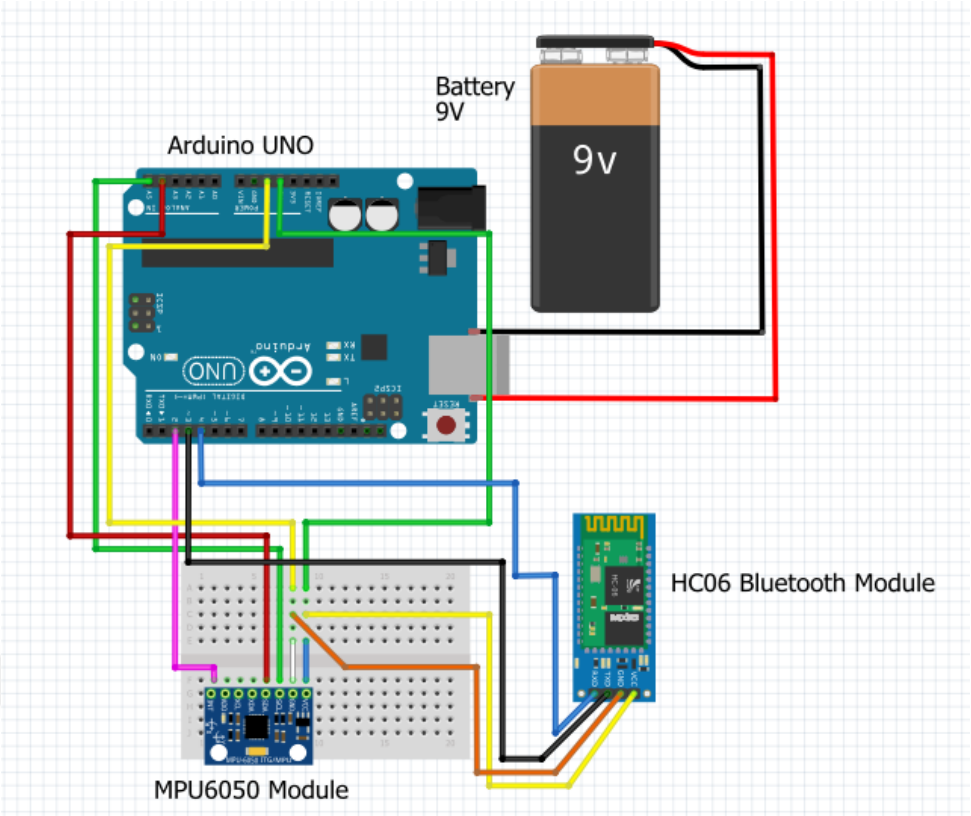

Figure 46: Circuit design on Fritzing Software

Written code for this circuit (In this work, Adafruit_MPU6050.h library has been used.) is added in Appendix part. Our circuit is get prepared as seen in Figure 47.

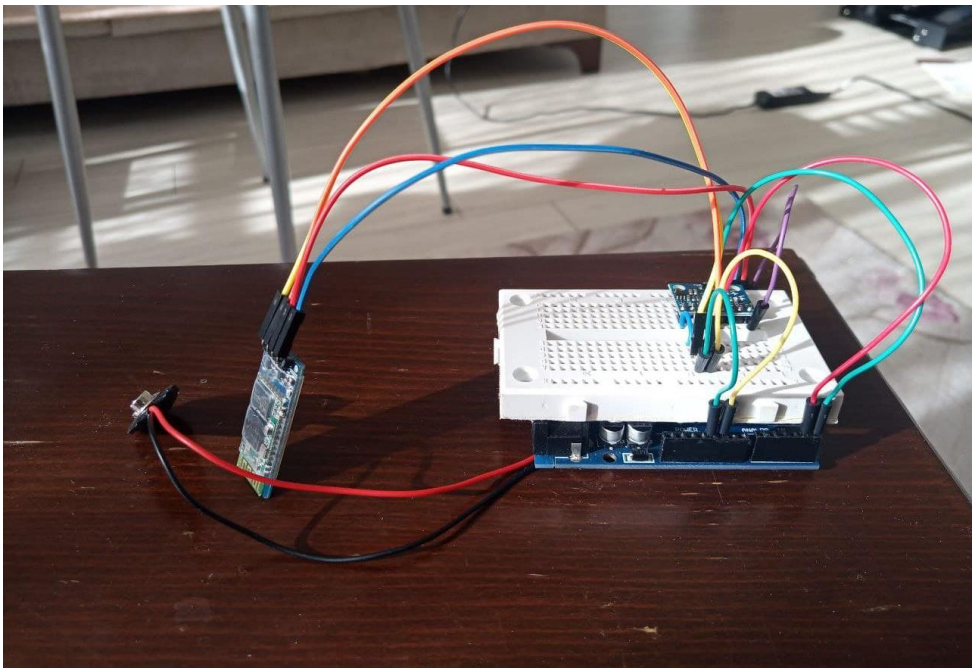

Figure 47: Arduino circuit preparation

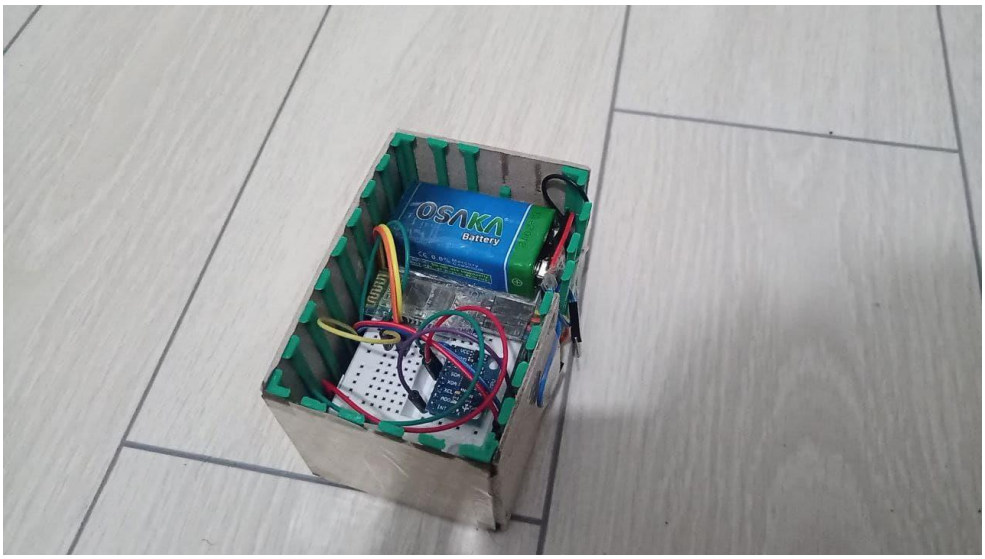

Figure 48: Cardboard box for placing Arduino circuit inside

Our sample data reading from circuit on serial port of Arduino IDE as seen in Figure 49. This test is applied with hand before mounting the circuit to quadcopter.

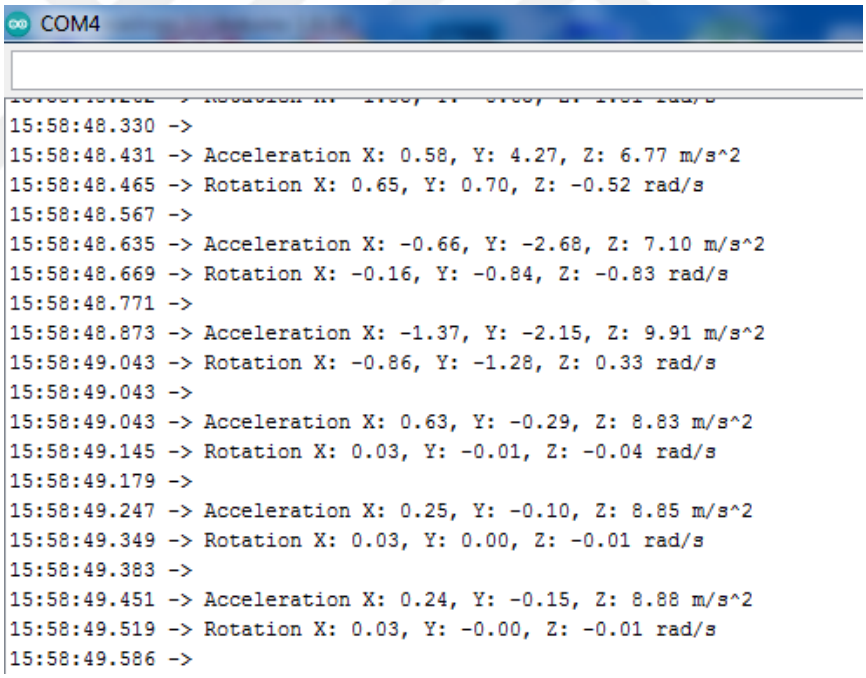

Figure 49: Sample data reading on Arduino IDE serial port

When we see our circuit works well on case of trial, we mounted our circuit in a cardboard box to the bottom of drone as seen in Figure 50.

Figure 50: Prepared Arduino circuit and the quadcopter (Extra 3D printed legs made for extending drone's bottom distance from the ground.)

Figure 51: Prepared Arduino circuit mounted on our drone (An adhesive band has been used for mounting the circuit to bottom of drone tightly)

With integrated circuit, six flight trials made as following; "Free Flight 1", "Free Flight 2", "Free Flight 3", "Up-Down" between –z and +z axes, "Turning" around only z axis and only planar movement between –y and +y or –x and +x axes. These trials are expected to give us drone characteristics in various flights. Especially, ultimate acceleration values can be obtained in a normal flight of our quadcopter.

Collected datas on serial port of Arduino IDE are transferred to Excel environment to rearrange them. Mentioned six flights are grouped as creating tables, then charts have been made by using values from there. Sample created table in Excel can be seen as in Figure 52.

	Variables			Variables			Variables		
Measur.	aX(m/s^2)	aY(m/s^2)	aZ(m/s^2)	RotX(rad/s)	RotY(rad/s)	RotZ(rad/s)	AngAX(rad/s^2)	AngAY(rad/s^2)	AngAZ(rad/s^2)
1	-0.01	-2.77	0.02	0.03	-0.01	-0.01	0.00	0.00	0.00
2	0.02	-2.78	0.02	0.03	-0.01	-0.01	0.00	0.10	0.00
3	0.01	-2.77	0.03	0.03	0.00	-0.01	0.00	-0.10	0.00
4	0.00	-2.75	0.04	0.03	-0.01	-0.01	0.00	0.00	0.00
5	0.02	-2.79	0.00	0.03	-0.01	-0.01	0.00	0.00	0.00
6	0.00	-2.75	0.02	0.03	-0.01	-0.01	0.00	0.00	0.00
7	0.00	-2.79	0.06	0.03	-0.01	-0.01	0.00	0.00	0.00
8	0.01	-2.77	0.01	0.03	-0.01	-0.01	0.00	0.00	0.00
9	0.02	-2.78	0.04	0.03	-0.01	-0.01	0.00	0.00	0.00
10	0.02	-2.78	0.01	0.03	-0.01	-0.01	0.00	0.00	0.00
11	0.02	-2.81	0.04	0.03	-0.01	-0.01	0.00	0.00	0.00
12	0.01	-2.78	0.03	0.03	-0.01	-0.01	0.00	0.00	0.00
13	0.03	-2.77	0.00	0.03	-0.01	-0.01	0.00	0.00	0.00
14	0.02	-2.77	0.03	0.03	-0.01	-0.01	0.00	0.00	0.00
15	0.04	-2.79	0.03	0.03	-0.01	-0.01	0.00	0.00	0.00
16	0.01	-2.78	0.04	0.03	-0.01	-0.01	0.00	0.00	0.00
17	0.02	-2.79	0.03	0.03	-0.01	-0.01	0.00	0.00	0.00
18	0.02	-2.75	0.02	0.03	-0.01	-0.01	0.00	0.10	0.00
19	0.04	-2.79	0.00	0.03	0.00	-0.01	0.00	0.00	0.00
20	0.03	-2.78	0.02	0.03	0.00	-0.01	0.00	-0.10	0.00
21	0.02	-2.79	0.01	0.03	-0.01	-0.01	0.00	0.00	0.00
22	0.00	-2.78	0.01	0.03	-0.01	-0.01	0.00	0.00	0.00
23	0.02	-2.78	0.02	0.03	-0.01	-0.01	0.00	0.10	0.00
24	0.02	-2.77	0.03	0.03	0.00	-0.01	0.00	0.00	0.00
25	0.04	-2.78	0.03	0.03	0.00	-0.01	0.00	-0.10	0.00
26	0.02	-2.77	0.04	0.03	-0.01	-0.01	0.00	0.00	0.00
27	0.03	-2.79	0.02	0.03	-0.01	-0.01	0.00	0.00	0.00

Figure 52: Rearranged datas on Excel

Figure 53 shows sample created charts in Excel.

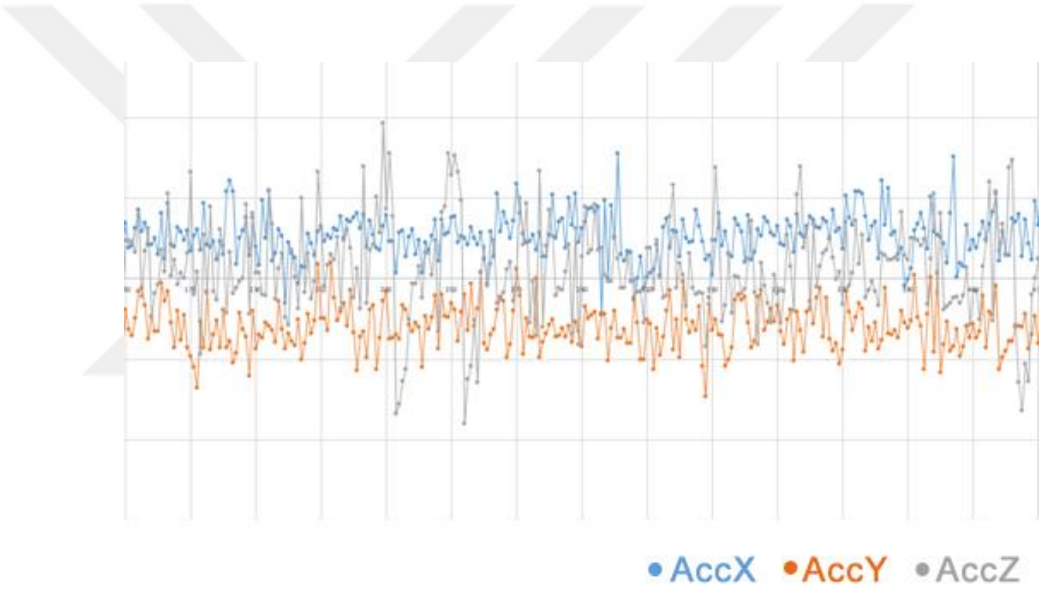

Figure 53: Created acceleration chart on Excel in time domain

3.5.3 Free Flight Trials

In these trials, quadcopter is tried under a normal flight. These flights include motions of quadcopter freely moving around an environment for a minute. Trials are applied for three times to determine values in trustful ranges. Linear acceleration, angular velocity and angular acceleration values are determined in result of these trials. Maximum and minimum numbers are extracted from these measurements as ultimate points.

In the end of “Free Flight 1” measurement results are;

Table 1: Ultimate values for “Free Flight 1”

	Linear Acceleration (m/s^2)		
	aX(m/s^2)	aY(m/s^2)	aZ(m/s^2)
Maximum	2.57	4.04	3.93
Minimum	-0.45	-1.99	-1.80
	Angular Velocity (rad/s)		
	RotX(rad/s)	RotY(rad/s)	RotZ(rad/s)
Maximum	2.66	1.50	0.62
Minimum	-1.13	-1.42	-0.43
	Angular Acceleration (rad/s^2)		
	AngAX(rad/s^2)	AngAY(rad/s^2)	AngAZ(rad/s^2)
Maximum	26.40	18.60	5.60
Minimum	-28.40	-16.50	-6.20

In the end of “Free Flight 2” measurement results are;

Table 2: Ultimate values for “Free Flight 2”

	Linear Acceleration (m/s^2)		
	aX(m/s^2)	aY(m/s^2)	aZ(m/s^2)
Maximum	1.91	2.54	3.19
Minimum	-1.83	-3.81	-1.99
	Angular Velocity (rad/s)		
	RotX(rad/s)	RotY(rad/s)	RotZ(rad/s)
Maximum	1.44	1.27	0.62
Minimum	-1.32	-1.42	-1.48
	Angular Acceleration (rad/s^2)		
	AngAX(rad/s^2)	AngAY(rad/s^2)	AngAZ(rad/s^2)
Maximum	16.30	15.70	13.60
Minimum	-15.10	-21.50	-21.00

In the end of “Free Flight 3” measurement results are;

Table 3: Ultimate values for “Free Flight 3”

	Linear Acceleration (m/s^2)		
	aX(m/s^2)	aY(m/s^2)	aZ(m/s^2)
Maximum	1.84	1.01	10.36
Minimum	-4.18	-1.29	-1.96
	Angular Velocity (rad/s)		
	RotX(rad/s)	RotY(rad/s)	RotZ(rad/s)
Maximum	1.49	1.33	1.38
Minimum	-1.19	-1.61	-0.45
	Angular Acceleration (rad/s^2)		
	AngAX(rad/s^2)	AngAY(rad/s^2)	AngAZ(rad/s^2)
Maximum	18.90	16.90	10.50
Minimum	-18.90	-26.40	-13.50

3.5.4 Specific Flights

These trials are made for just to do specific motions with quadcopter. Flights are including “Up-Down” motion through -Z and +Z direction, “Left-Right-Front-Back” motion through -Y and +Y or -X and +X directions, “Turning” motion along Z axis. Linear acceleration, angular velocity and angular acceleration values are determined in result of these trials as well. Maximum and minimum numbers are provided in the end of specific flights too. One thing should be known that, precise specific behaviours are not possible with our quadcopter because we control our air vehicle manually and due to many conditions other short complex motions may happen accidentally before we do our target motion. So, we applied our test movements precise as possible.

In the end of “Up-Down” motion measurement results are;

Table 4: Ultimate values for “Up-Down”

	Linear Acceleration (m/s^2)		
	aX(m/s^2)	aY(m/s^2)	aZ(m/s^2)
Maximum	4.35	5.89	15.81
Minimum	-6.00	-11.30	-3.14
	Angular Velocity (rad/s)		
	RotX(rad/s)	RotY(rad/s)	RotZ(rad/s)
Maximum	1.33	0.81	0.54
Minimum	-0.70	-0.95	-0.46
	Angular Acceleration (rad/s^2)		
	AngAX(rad/s^2)	AngAY(rad/s^2)	AngAZ(rad/s^2)
Maximum	12.50	8.70	7.60
Minimum	-9.90	-11.70	-10.00

In the end of “Left-Right-Front-Back” motion measurement results are;

Table 5: Ultimate values for “Left-Right-Front-Back”

	Linear Acceleration (m/s^2)		
	aX(m/s^2)	aY(m/s^2)	aZ(m/s^2)
Maximum	1.74	8.87	2.80
Minimum	-3.68	-4.64	-3.21
	Angular Velocity (rad/s)		
	RotX(rad/s)	RotY(rad/s)	RotZ(rad/s)
Maximum	2.31	1.46	0.75
Minimum	-1.41	-1.48	-0.93
	Angular Acceleration (rad/s^2)		
	AngAX(rad/s^2)	AngAY(rad/s^2)	AngAZ(rad/s^2)
Maximum	24.20	16.10	8.20
Minimum	-27.90	-19.00	-8.50

In the end of “Turning” motion measurement results are;

Table 6: Ultimate values for “Turning”

	Linear Acceleration (m/s^2)		
	aX(m/s^2)	aY(m/s^2)	aZ(m/s^2)
Maximum	3.22	12.04	2.06
Minimum	-0.96	-5.71	-2.33
	Angular Velocity (rad/s)		
	RotX(rad/s)	RotY(rad/s)	RotZ(rad/s)
Maximum	0.97	0.94	0.94
Minimum	-0.88	-0.81	-1.13
	Angular Acceleration (rad/s^2)		
	AngAX(rad/s^2)	AngAY(rad/s^2)	AngAZ(rad/s^2)
Maximum	11.10	10.60	8.80
Minimum	-11.00	-13.30	-15.20

3.6 FINAL DESIGN STAGE

After collected quadcopter parameters with MPU6050 module, calculations and assumptions are collected together for creating final design by using first wood model as our template too. Firstly, we divided into steps every motion of desired gripper.

3.6.1 Mechanism Working Stages

3.6.1.1 Step 1: Gripper Pad Load Pressing Position

In this step, our gripper which is attached to the bottom of drone approaches right to the target object. Meanwhile, the forces acting on the gripper are; the force generated by the total gripper weight, buoyancy force by quadcopter, forces arise from acceleration caused by drone flight, and in connection, forces effected by air resistance. When gripper gets in touch with the load by its pressure pad (Purple marked in Figure 54), pressure pad transmits the force to force transfer rod (Green marked in Figure 54), then force transfer rod transfer force to gripper arms by help of middle plate (Grey marked in Figure 54). This step continues up to cam mechanism (Push-push button mechanism) to lock the load.

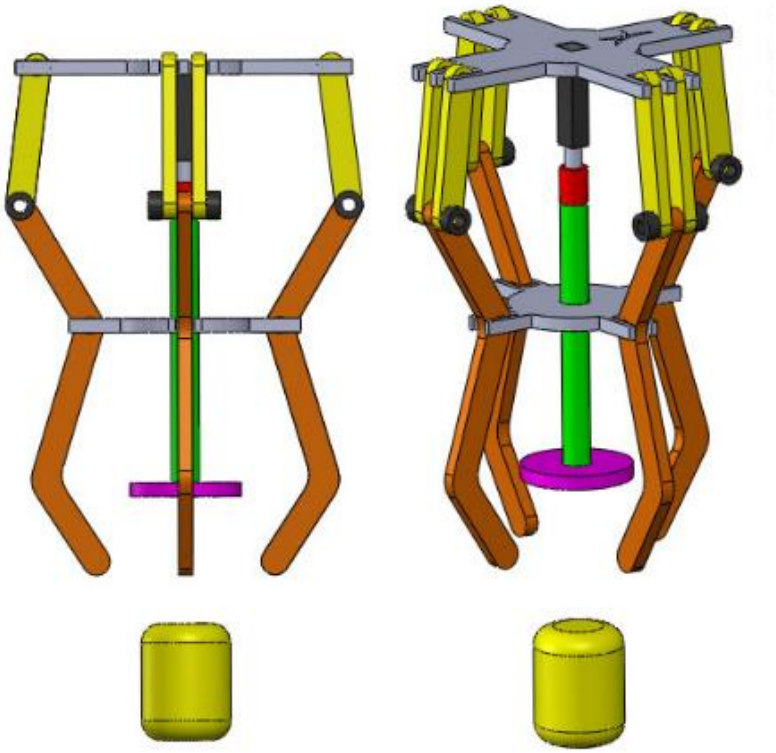

Figure 54: Step-1 Representation

3.6.1.2 Step 2: Gripper Load Grasping Position

The gripper pressure pad comes on the object and presses the object with the drone pressing force in Step-1 as mentioned. Step-1 continues up to cam mechanism locks the arm in case of grasping the load (Step-1 ends with a sound which created by cam mechanism as “click”). In locked position, load can be carried to desired location by aerial vehicle. The spring inside the cam mechanism is in compressed position at this time.

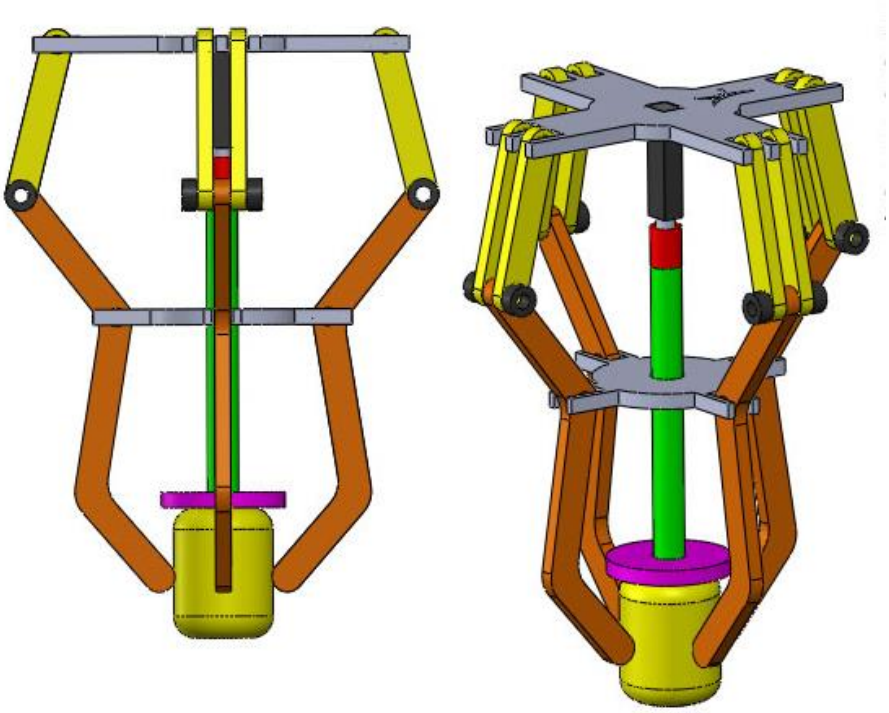

Figure 55: Step-2 Representation

3.6.1.3 Step 3: Gripper Releases the Load

Drone approaches the ground level to leave the load which received via the gripper for conveying another location. Drone descends until the payload makes contact with the ground. When the load-ground contact occurs, drone lowers a little more and puts pressure on the load. At the same time, that pressure must also overcome friction between the surfaces of drone arm and the object. Concurrently, the pressure pad compresses the spring a little, causing a “click” sound again. The cam mechanism unlocks the existing lock and allows the spring to be opened. The opened spring pushes force transfer rod and causes the middle plate to open its arms. The opened arms release the object then finally object is moved from one point to another by an aerial vehicle.

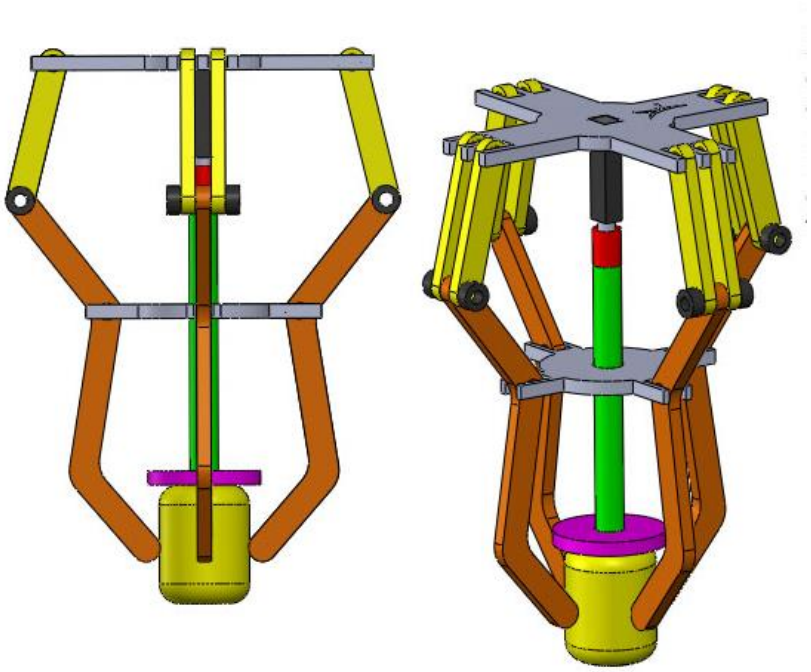

Figure 56: Step-3 Representation

3.6.2 Predesign Stage on Computer Environment

After determination of first dimensional limitations, gripper basic functions and working stages, next move is to create final gripper with CAD by help of Solid Works package software. For patterning, firstly, our drone is modelled one by one in CAD environment. So, with one by one model of our quadcopter, we can build all gripper components on this referencing drone model in Solid Works.

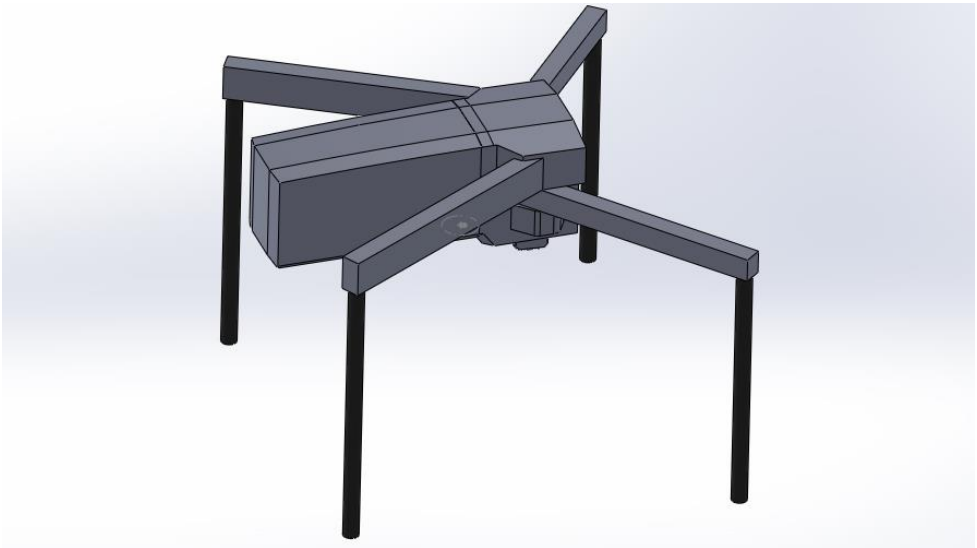

Figure 57: CAD modelling of our quadcopter as for referencing part (From side) (Drone head, propeller and similar details are neglected because of no necessity in placement plan)

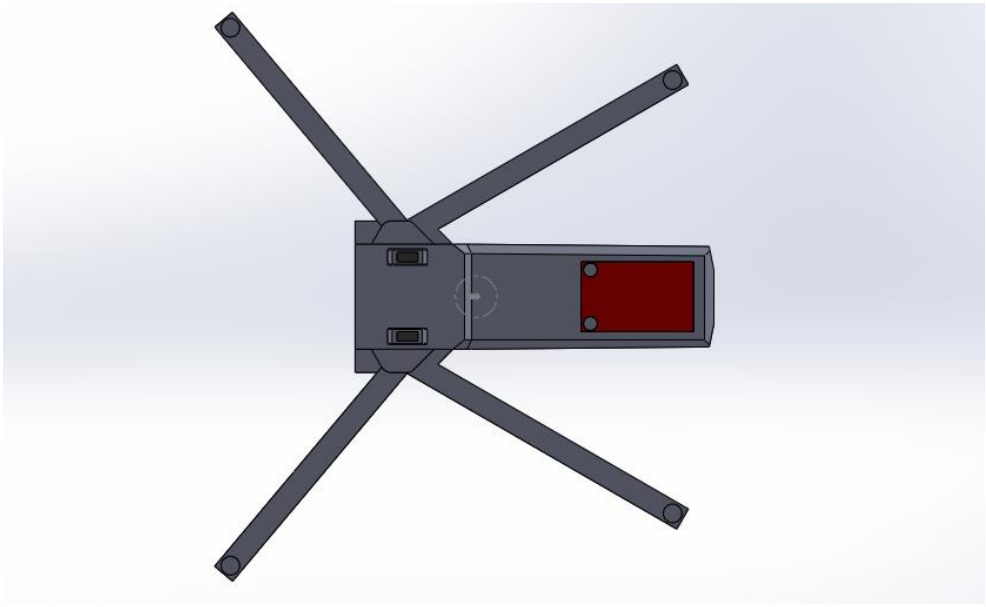

Figure 58: CAD modelling of our quadcopter as for referencing part (From bottom) (Drone head, propeller and similar details are neglected because of no necessity in placement plan)

Then, according to mass center of drone which was determined before, a chassis for mounting of gripper has been designed as light as possible like in Figure 59.

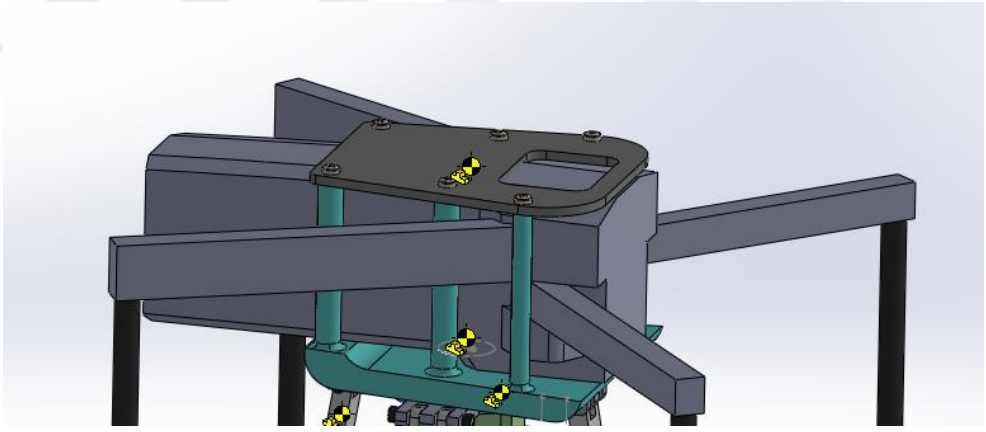

Figure 59: Gripper chassis placements on our drone (In figure upper chassis and lower chassis are seen with yellow signed mass centers)

The process has been expanded for modelling gripper structure. Here most important part is to calculate gripper arm motions according to pressure pad's movement. This design problem is solved by help of Solid Works real time simulation feature. By trial and error; linkage lengths, angles and step positions created under first dimensional limitations.

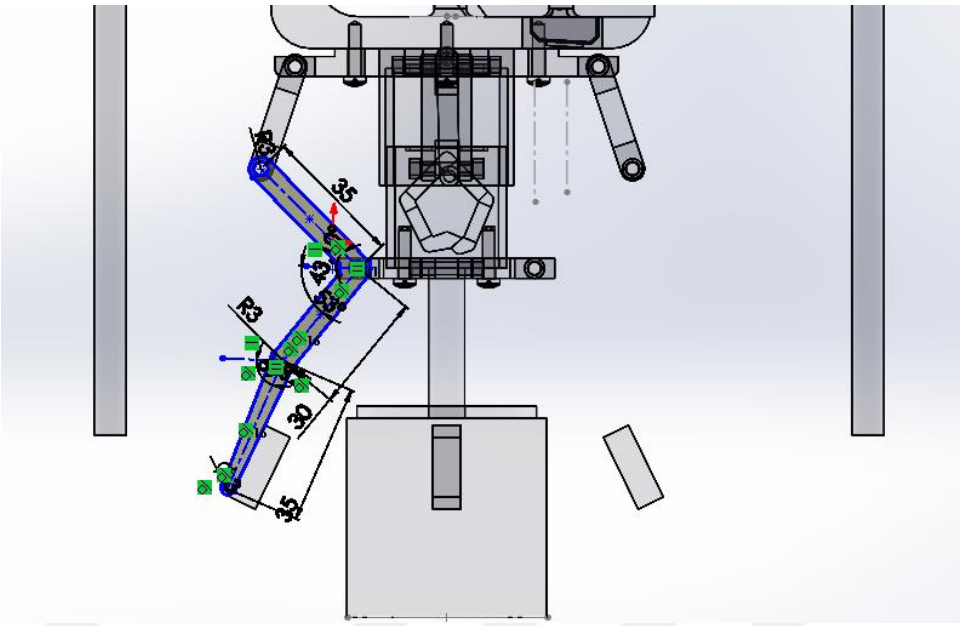

Figure 60: Gripper linkage dimensioning on CAD assembly

Real time simulations are applied only for one arm, just because other arms will be the same. Same design approaches can be easily applied for other arms as well. From simulations we get force transfer rod displacement values optimally as; x1: 22.65 mm (Spring's first displacement according to force transfer rod's displacement), x2: 2,60 mm (Spring's second displacement for locking condition) and net displacement: 20.05 mm (Spring displacement under locking condition.). As considered here, when drone approaches to load for touching with its pressure pad, desired grasping scenario will happen. According to determined linkage parameters, a ball pen mechanism cam profile design made. With this cam profile, locking-unlocking motions will be done through displacement range. Cam profile and slider system are seen as;

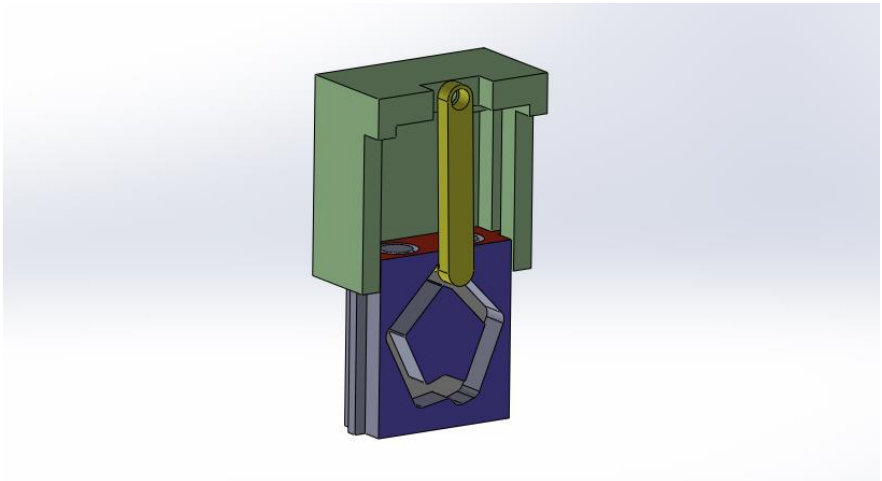

Figure 61: Cam assembly inside the gripper

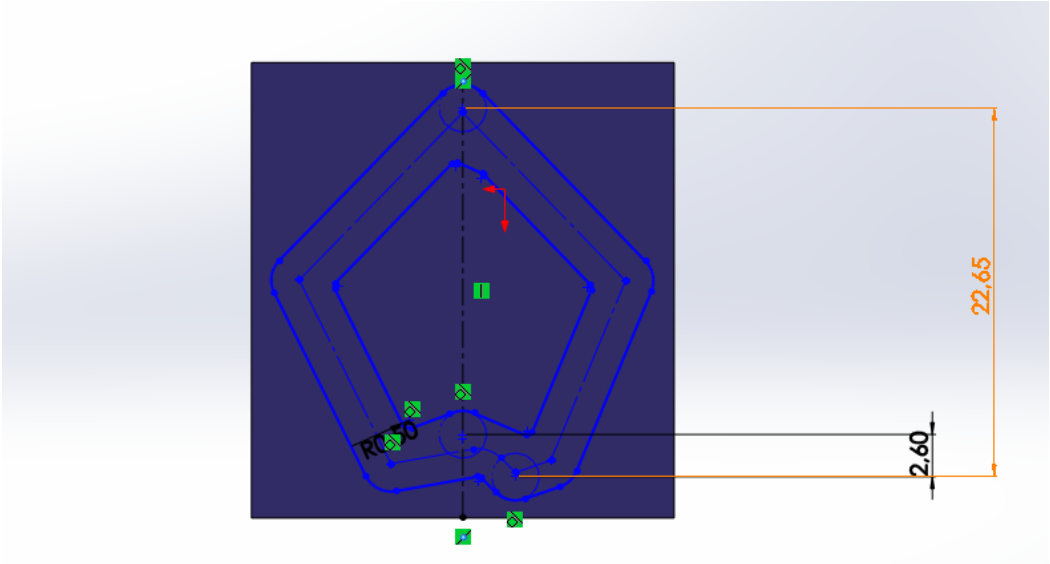

Figure 62: Cam plate path profile showing x1 and x2 displacement values

Follower stick (With yellow colour in Figure 61) will follow the path of cam as force transfer rod moves. Cam path depth may be created samely in any level inside the plate. But this makes follower stick's movement sometimes complicated (It may result wrong or reverse follower motions). So, for solving this problem we made guide ramped profile inside the cam for follower stick's smooth motion. By adding this, we get more accurate follower stick motion, and prevent stick's wrong motions that we don't desire.

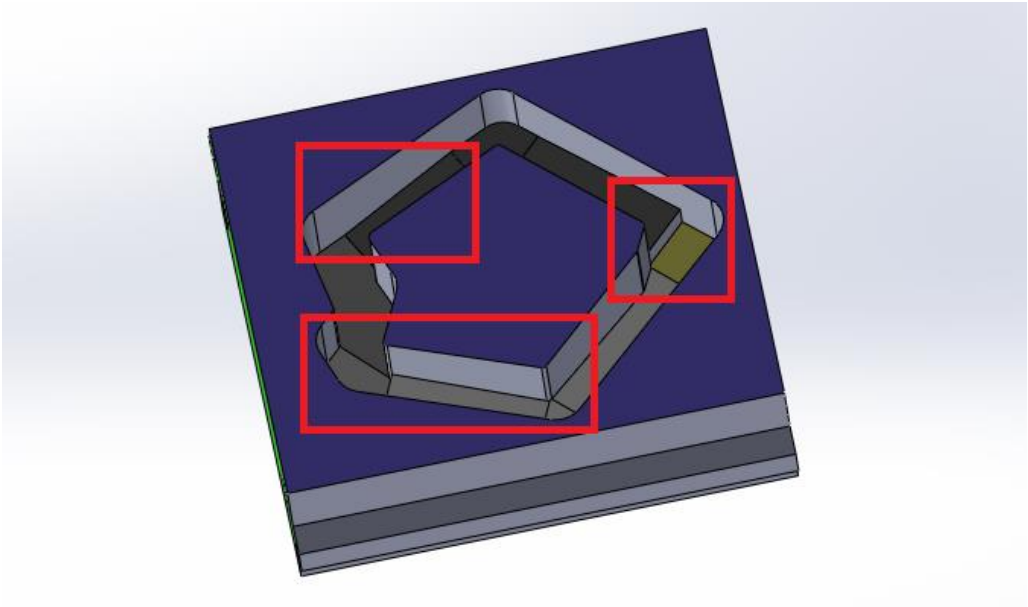

Figure 63: Cam plate path with guide ramped profile for follower stick

So, after fully define most important parts (Which are linkage parameters and cam mechanism) in the project. We get a sample gripper like in Figure 64.

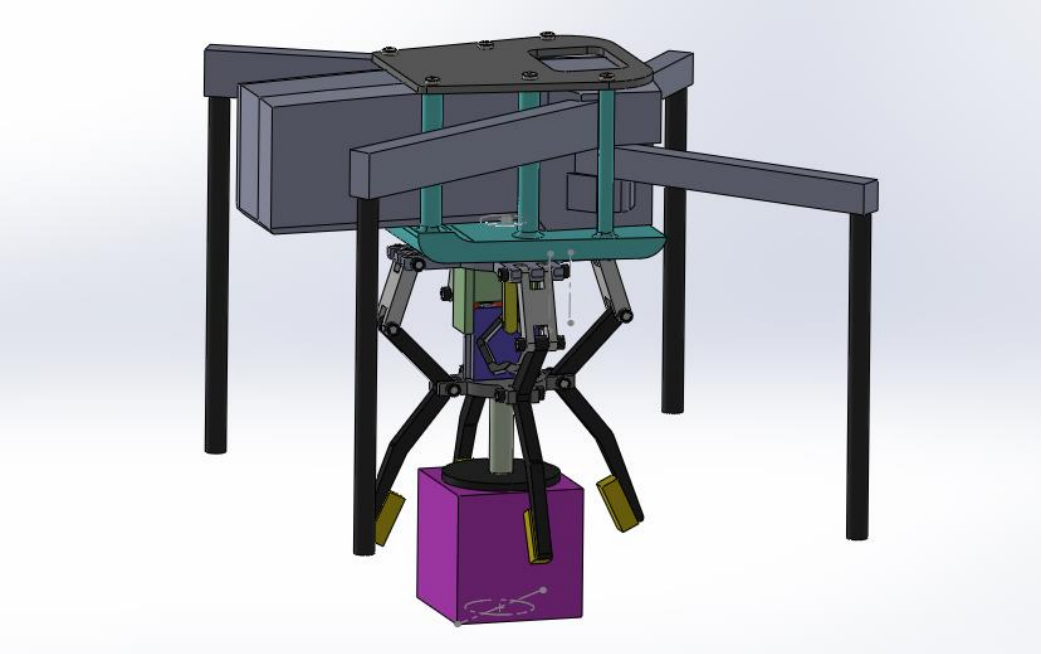

Figure 64: CAD assembly of estimated gripper

Part thicknesses are given for a value which will make system both light and strong as possible under static and dynamic forces. It is also assumed hinge pins should be strong as possible under given thicknesses for system. Design is made for 3D printing, thus, parts created for gripper will not weight much for our quadcopter and it is assumed that weights will be under drone lifting and motion limitations.

3.6.3 Static Calculations for Motion Stages of Gripper

According to our design, we determined to manufacture parts from PLA (Polylactic Acid) material which is very common material in 3D printer world. PLA is widely used because of its lightness and capability of quick prototyping, and it can also be formed in any desired shape via 3D printer. Material weights are changeable due to PLA infill ratios. Most of time, under weak forces like in our project, %20 infill rate for parts is enough to provide optimized lightness and strongness. In our design, for sections like hinge pins, force transfer rod etc. in which forces are higher compare to other parts, %100 infill rates are given. Meanwhile strongness increases, weight numbers are not affected marginally with %100 infill rates. At our sample design,

material weights are calculated with Ultimaker Cura software according to infill rates before printing. Before static calculations, part weights are determined as;

Drone Upper Mount Plate: 17,7 grams

Drone Lower Mount Plate: 40,5 grams

Gripper Upper Plate: 10,5 grams

Gripper Upper Link (x4): 5,6 grams

Gripper Lower Link (Arm) (x4): 16,4 grams

Cam Slider Plate: 7 grams

Cam Plate: 4,8 grams

Gripper Lower Plate: 4,3 grams

Cam Follower Stick: 0,6 grams

Force Transfer Rod: 1,5 grams

Pressure Pad: 4,4 grams

Upper Hinge Pin (x4): 1,2 grams

Lower Hinge Pins (x8): 1,6 grams

Hinge Pin Cap (x24): <2,4 grams

M3x12 (x5): 5 grams

M3x35 (x2): 4,4 grams

M4x12 (x8): 14,4 grams

Loads (Cube and cylinder forms of load exist with empty and filled versions): 40, 53, 100, 113 grams

Leaf Spring (x4): 1,2 grams

Drone Foot Assembly (x4): 72 grams

Drone Foot Support Links: 31 grams (Total)

Cam Mechanism Springs: <0,1 gram

Total Weight on Drone (Without Load): 246,5 grams

Total Weight on Drone (With Max. Load): 359,5 grams

3.6.3.1 Static Friction Calculations

Static friction calculation is needed to determine load grasping capability of gripper arm surface. For determination of friction coefficients between load and gripper arm surface, referred inclined plane experiment can be applied for different surfaces with different materials. Due to inclined plane experiment, an object which is to be slided over a rotatable surface will be put to system. When object is placed on

rotatable surface, rotatable plane is gradually lifted. Tangent of angle at which object starts to slide on platform will give us friction coefficient between surfaces. According to applied experiment on different surfaces, maximum and minimum coefficients can be found as;

PLA-PLA: (Max: 0.58, Min: 0.26)

PLA-Pochette Nylon: (Max: 0.47, Min: 0.47)

PLA-Foamed Surface: (Max: 2.15, Min: 1.73)

PLA-Cardboard: (Max: 0.27, Min: 0.27)

PLA-MDF Wood Plaque: (Max: 0.58, Min: 0.58)

PLA-Steel Surface: (Max: 0.37, Min: 0.37)

PLA-Sandpaper: (Max: 1.43, Min: 1.19)

PLA-Beech Wood Plaque: (Max: 0.58, Min: 0.47)

PLA-Adhesive Band: (Max: 0.47, Min: 0.36)

As referred before, we will use this friction data for the case of gripper load grasping. Our gripper can hold the load under condition of $4\times\mu F > mg$ (μ=Static friction coefficient between load and arm, F=Normal force applied by arm to the load), μF = Friction force, $4\times\mu F$= Total static frictional force on four arms of gripper, mg = Load weight.

3.6.3.2 Gripper Force Calculations

After part weights are defined approximately, we need to calculate forces inside the gripper to estimate cam mechanism spring constant and sectional tensions. If calculations seem wrong or doesn't provide our assumptions, then design parameters can be changed quickly on CAD model.

3.6.3.2.1 Step 1: Position of Gripper Pad Presses the Load

For drone to grasp the load, gripper's pressure pad should press on load up to cam stick reaches locking position in cam mechanism. Calculations regarding this process can be summarized with equation as;

$$F_{Pres1} = k_{Eq} \times x1 + G_{Parts} + F_{MiddlePlate} + F_{S\ Hinges\ \&\ Cam\ Mechanism} \qquad (3.17)$$

x_1 = Spring first displacement amount

k_{Eq} = Equivalent spring coefficient

G_{parts} = Parts weights

$$G_{Parts} = G_{MiddlePlate} + G_{PressureRod} + G_{PressurePad} + G_{CamPlate} + G_{LowerRod} \times 4 + G_{Cap} \times 8 \quad (3.18)$$

$$F_{MiddlePlate} = 4 \times F_{MLy} \quad (3.19)$$

For one arm of gripper, moment of just before pressure pad touches the load is seen in Figure 65.

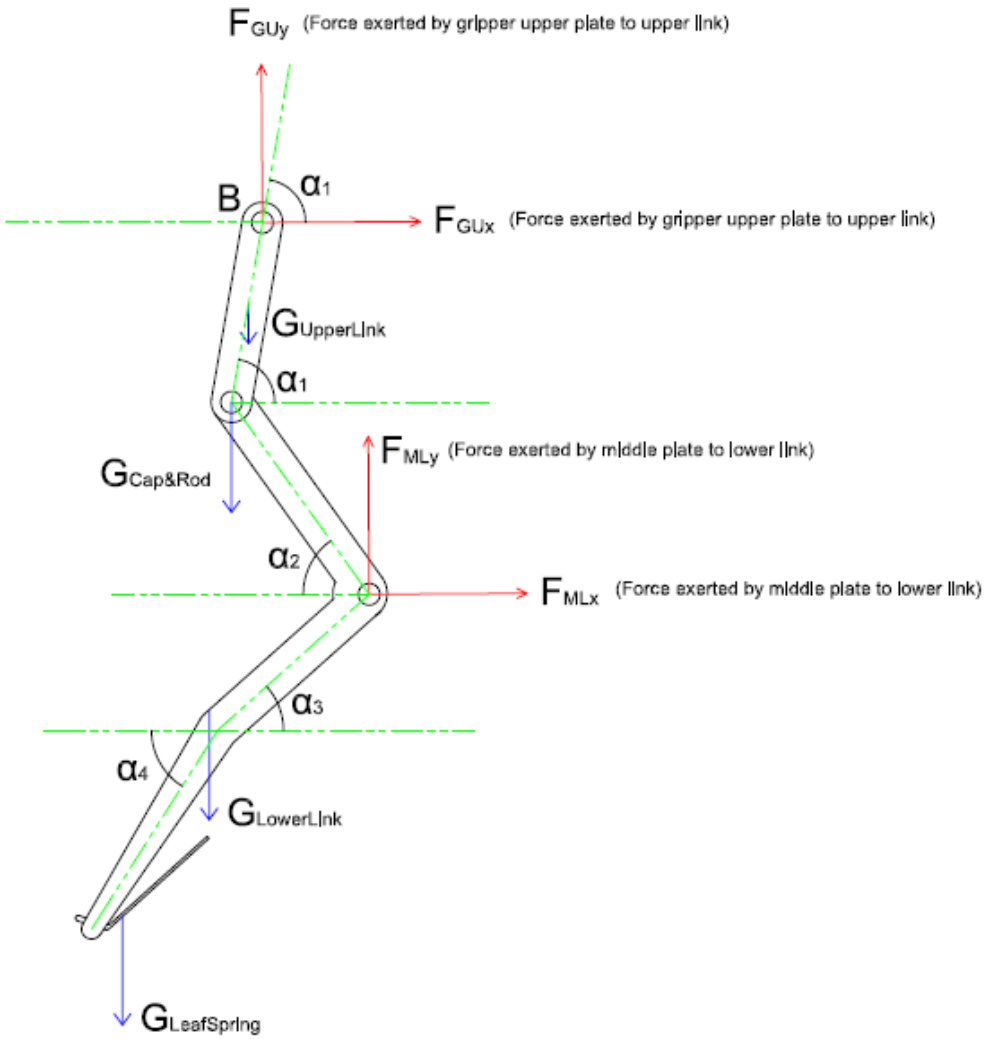

Figure 65: Force diagram for one arm, just before pressure pad touches the load

Table 7: Angle, mass and weight values for Step-1

Angle Values	Mass Values	Weight Values
$\alpha_1 = 80.43°$	$m_{UpperLink} = 1.4$ grams	$G_{UpperLink} = 0.013$ N
$\alpha_2 = 54.17°$	$m_{LowerLink} = 4.1$ grams	$G_{LowerLink} = 0.0402$ N
$\alpha_3 = 41.93°$	$m_{LeafSpring} = 0.3$ gram	$G_{LeafSpring} = 0.0029$ N
$\alpha_4 = 57.93°$	$m_{LowerRod} = 0.2$ gram	$G_{Cap\&Rod} = 3.924x10^{-3}$ N
	$m_{Cap} \leq 0.1$ gram	

Force Equations:

$$\sum F_X = 0 \ \rightarrow^{+} F_{GU_X} + F_{ML_X} = 0 \ \rightarrow \ F_{ML_X} = -F_{GU_X} \quad (3.20)$$

$$\sum F_Y = 0 \ \uparrow^{+} F_{GU_Y} + F_{ML_Y} - 0.0600\ N = 0 \ \rightarrow F_{GU_Y} + F_{ML_Y} = 0.0600\ N \quad (3.21)$$

Moment Equations:

$$\sum M_B = 0\ CCW_{+} \ \rightarrow \ G_{UpperLink} \times (0.0022\ m) + F_{ML_Y} \times (0.016\ m) +$$

$$F_{ML_X} \times (0.055\ m) + \ G_{Cap\&Rod} \times (0.0044\ m) + G_{LowerLink} \times (0.0087\ m) +$$

$$G_{LeafSpring} \times (0.0172\ m) \ = 0 \quad (3.22)$$

$$G_{UpperLink} = 0.013\ N, G_{LowerLink} = \ 0.0402\ N, G_{LeafSpring} = \ 0.0029\ N$$

$$G_{Cap\&Rod} = 3.924 \times 10^{-3}\ N \quad (3.23)$$

$$F_{ML_Y} \times 0\ (0.016\ m) + F_{ML_X} \times (0.055\ m) = -4.45 \times 10^{-4} \quad (3.24)$$

$$F_{GU} \times \cos(80.43^{\circ}) = F_{GU_X},\ F_{GU} \times \sin(80.43^{\circ}) = F_{GU_Y} \quad (3.25)$$

$$F_{GU_X} \times tan(80.43^{\circ}) = F_{GU_Y}, -F_{ML_X} \times tan(80.43^{\circ}) = F_{GU_Y} \quad (3.26)$$

$(F_{ML_X} = \ -F_{GU_X})$ (From Equation) (3.20)

$$-F_{ML_X} \times tan(80.43^{\circ}) + F_{ML_Y} = 0.0600\ N \quad (3.27)$$

$$+107.81/F_{ML_X} \times (0.055\ m) + F_{ML_Y} \times (0.016\ m) = -4.45 \times 10^{-4}\ N \quad (3.24)$$

$$F_{ML_Y} + 1.72 \times F_{ML_Y} = 0.0120\ N \quad (3.28)$$

$$2.72 \times F_{ML_Y} = 0.0120\ N \quad (3.29)$$

$$F_{ML_Y} = 0.00441\ N, F_{GU_Y} = 0.055\ N, F_{GU_X} = 0.0092\ N, F_{ML_X} = -0.0092\ N \quad (3.30)$$

$F_{MiddlePlate} = 4 \times F_{ML_Y} = 0.0176\ N\ \downarrow$ (Force created by four arms of gripper on middle plate) (3.19)

(Forces which are defining F_{MLx} are neutralized on middle plate because we have four arms placed symmetrically. F_{MLx} forces act on each other oppositely.)

$G_{Parts} = G_{MiddlePlate} + G_{PressureStick} + G_{PressurePad} + G_{CamPlate} + G_{LowerRod} \times 4 + G_{Cap} \times 8$ (Parts connected to pressure pad directly or in other words lifting force applied to pressure pad should overcome these weights) (3. 18)

$G_{Parts} = 0.061\ N + 0.014\ N + 0.043\ N + 0.047\ N + 0.015\ N\ (G_{Cap\&Rod}) = 0.18\ N$ (3. 18)

Spring Selection:

$F_{Pres1} = k_{Eq} \times x1 + G_{Parts} + F_{MiddlePlate} + F_{S\ Hinges\ \&\ Cam\ Mechanism}$ (3. 31)

F_{pres1} is drone's pressing force on an object, which is also measured by hanging drone with precision scale in operating condition and it is found as 500 grams which is averagely equal to 4.905 N.

x_1: First spring displacement value, designed as 22.6 mm which is 0.0226 m

We can use equation for finding spring constant "k" for pressing spring as in equation (3.32).

$$k_{PressingSpring} = \frac{(d^4 \times G)}{(8 \times N_e \times D^3)} \quad (3.\ 32)$$

Here, after determination of spring constant, one can get spring dimensions as desired. However, in practical one cannot get a ready manufactured spring as what spring constant we have precisely. So, we manufactured softest possible spring, hardest possible spring and few springs in that range compatible to our designed slot in CAD. In rest, we need trial and error method to choose right spring in our range.

We have softest possible (To reach defined spring displacement value easier) spring which has spring coefficient 24 N/m which is 0.024 N/mm. We manufactured also springs in a range that having constants 0.03 N/mm, 0.075 N/mm, 0.122 N/mm (Highest spring constant)

If we substitute values into equation;

$$4.905\ N \geq \left(48 \frac{N}{m}\right) \times (0.0226\ m) + 0.18\ N + 0.0176\ N + Friction \quad (3.\ 31)$$

(Our pressing force on the load should be greater than right side of equation to make motion in smooth way) (48 N/m coefficient value comes from $k_{Eq} = k_1 + k_2$, we have two springs inside)

$$4.905\ N \geq (1.28\ N) + Friction \quad (3.31)$$

(Frictions on both hinges and cam mechanism)

Friction value can be maximum 3.625 N to make motion in smooth manner. (Which can be reduced as well by using machine oil and rasping for touching parts in case of we have over friction.)

3.6.3.2.2 Step 2: Gripper Load Grasping Position

In first step, we made calculations regarding gripper's pressure pad touches the load and drive the mechanism up to locking point. In Step 2, we will consider gripper arms grasp the load. For this calculation, we will benefit from free body diagram as well.

Table 8: Angle, mass and weight values for Step-2

Angle Values	Mass Values	Weight Values
$\alpha_1 = 54.13°$	$m_{UpperLink} = 1.4$ grams	$G_{UpperLink} = 0.013$ N
$\alpha_2 = 24.61°$	$m_{LowerLink} = 4.1$ grams	$G_{LowerLink} = 0.0402$ N
$\alpha_3 = 71.54°$	$m_{LeafSpring} = 0.3$ gram	$G_{LeafSpring} = 0.0029$ N
$\alpha_4 = 87.48°$	$m_{LowerRod} = 0.2$ gram	$G_{Cap\&Rod} = 3.924 \times 10^{-3}$ N
	$m_{Cap} \leq 0.1$ gram	

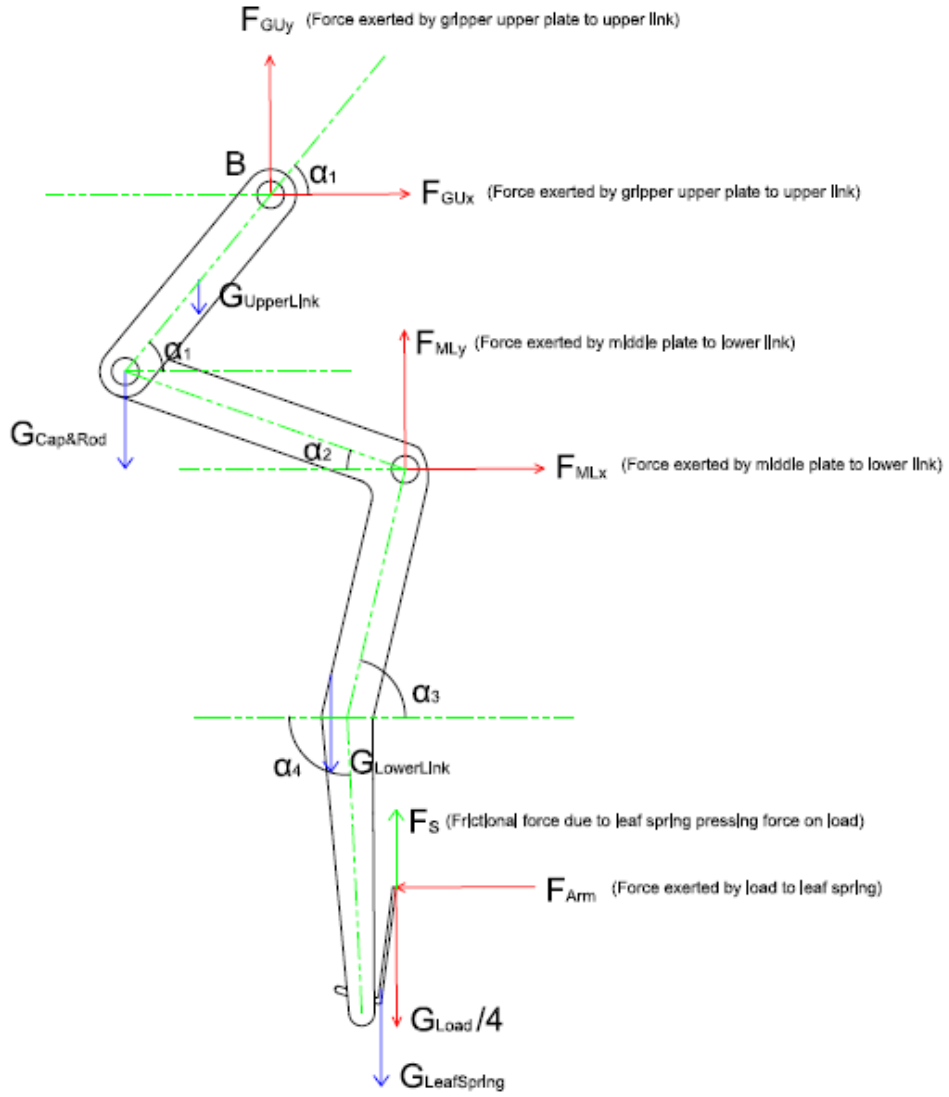

Figure 66: Force diagram for one arm when gripper grasping the load

Force Equations:

$$\sum F_X = 0 \ \rightarrow^{+} F_{GU_X} + F_{ML_X} - F_{Arm} = 0 \ \rightarrow F_{ML_X} + F_{GU_X} = F_{Arm} \quad (3.33)$$

$$\sum F_Y = 0 \ \uparrow^{+} F_{GU_Y} + F_{ML_Y} - 0.0600\ N - \frac{Gload}{4} + F_S = 0$$

$$\rightarrow F_{GU_Y} + F_{ML_Y} = 0 \quad (3.34)$$

$$F_S = F_{Arm} \times \mu_S \times F_S \geq G_{Load}/4 \text{ (Gripper load grasping condition)} \quad (3.35)$$

Moment Equations:

$$\sum M_B = 0\ CCW_{+} \rightarrow G_{UpperLink} \times (0.00816\ m) + F_{ML_Y} \times (0.016\ m) +$$
$$F_{ML_X} \times (0.035\ m) + G_{Cap\&Rod} \times (0.0163\ m) - G_{LowerLink} \times (0.0063\ m) -$$
$$G_{LeafSpring} \times (0.0138\ m) + F_S \times (0.013\ m) - F_{Arm} \times (0.078\ m) -$$
$$\frac{G_{Load}}{4} \times (0.013\ m) = 0 \quad (3.36)$$

$G_{UpperLink} = 0.013\ N, G_{LowerLink} = 0.0402\ N, G_{LeafSpring} = 0.0029\ N,$

$G_{Cap\&Rod} = 3.924\ \times 10^{-3}\ N, m_{LoadMax} = 113\ grams, G_{Load} = 1.108\ N$

$\rightarrow \frac{GLoad}{4} = 0.277\ N$ (3. 37)

$F_S \geq 0.277\ N$ (Load grasping condition for load not to slip over arm surface) (3. 35)

$F_S = F_{Arm} \times \mu_S$ (μ_s = Static friction coefficient between PLA leaf spring and PLA load) (3. 35)

$F_{Arm} \geq 0.477\ N$

(Least F_{arm} force for one arm when we have 113 grams PLA load) (3. 35)

Substituting values into force equations (3.33) and (3.34) respectively:

$F_{GU_X} + F_{ML_X} - 0.477\ N = 0$ (3. 33)

$F_{GU_X} + F_{ML_X} = 0.477\ N$ (3. 33)

$F_{GU_Y} + F_{ML_Y} - 0.0600\ N - 0.277\ N + 0.277\ N\ (F_S) = 0$ (3. 34)

$F_{GU_Y} + F_{ML_Y} = 0.0600\ N$ (3. 34)

Substituting values into moment equation (3.36):

$(0.013\ N) \times (0.00816\ m) + F_{ML_Y} \times (0.016\ m) + F_{ML_X} \times (0.035\ m) +$
$(3.924 \times 10^{-3}) \times (0.0163\ m) - (0.0402\ N) \times (0.0063\ m) - (0.0029\ N) \times$
$(0.0138\ m) + (0.277\ N) \times (0.013\ m) - (0.477\ N) \times (0.078\ m) - (0.277\ N) \times$
$(0.013\ m) = 0$ (3. 36)

$F_{ML_Y} \times (0.016\ m) + F_{ML_X} \times (0.035\ m) - 0.0371\ N = 0$ (3. 36)

$F_{ML_Y} \times (0.016\ m) + F_{ML_X} \times (0.035\ m) = 0.0371\ N$ (3. 36)

$F_{GU} \times cos(54.13^{\circ}) = F_{GU_X}, F_{GU} \times sin(54.13^{\circ}) = F_{GU_Y}$ (3. 38)

$F_{GU_X} \times tan(54.13^{\circ}) = F_{GU_Y} \rightarrow F_{GU_X} \times 1.382 = F_{GU_Y}$ (3. 39)

$-\frac{1.382}{F_{GU_X}} + F_{ML_X} = 0.477\ N$ (3. 40)

$F_{GU_X} \times 1.382 + F_{ML_Y} = 0.0600\ N$ (3. 41)

$-1.382 \times F_{ML_X} + F_{ML_Y} = -0.600\ N$ (3. 42)

$F_{ML_Y} = -0.600\ N + 1.382 \times F_{ML_X}$ (3. 43)

Substituting equation (3.43) into (3.36);

$\left(-0.600\ N + 1.382 \times F_{ML_X}\right) \times (0.016\ m) + F_{ML_X} \times (0.035\ m)$
$= 0.0371 N.m$ (3. 36)

$-9.6 \times 10^{-3} N.m + \left(0.022 \times F_{ML_X}\right) N.m + F_{ML_X} \times (0.035\ m)$
$= 0.0371 N.m$ (3.36)

$$0.057 \times \left(F_{ML_X}\right) N.m = 0.0467 N.m \quad (3.36)$$

$$F_{ML_X} = 0.819\ N, F_{GU_X} = -0.339\ N$$

$$F_{ML_Y} = 0.529\ N, F_{GU_Y} = -0.469\ N \quad (3.44)$$

3.6.3.2.3 Step 3: Gripper Load Releasing Position

For drone to release the load, a new force should be applied to pressure pad for unlocking the cam mechanism. Therefore, air vehicle should descend to press grasped load to the ground, in other words when load is under force, pressure pad will be under force too. This descend should continue up to cam mechanism to be unlocked. We can express this condition by writing equation;

$F_{Pres2} = k_{Eq} \times x2 + G_{Parts} + F_{MiddlePlate} + F_{S\ Hinges\ \&\ Cam\ Mechanism}$ (Friction on hinges and cam mechanism) (3.45)

x_2 = Spring second displacement amount

k_{Eq} = Spring coefficient

G_{parts} = Weight of parts in motion

$$G_{Parts} = G_{MiddlePlate} + G_{PressureRod} + G_{PressurePad} + G_{CamPlate} + G_{LowerRod} \times 4 + G_{Cap} \times 8 \quad (3.18)$$

$$F_{MiddlePlate} = 4 \times F_{ML_Y} \quad (3.19)$$

In this situation, x_2 is designed to be 2.60 mm to unlock the mechanism.

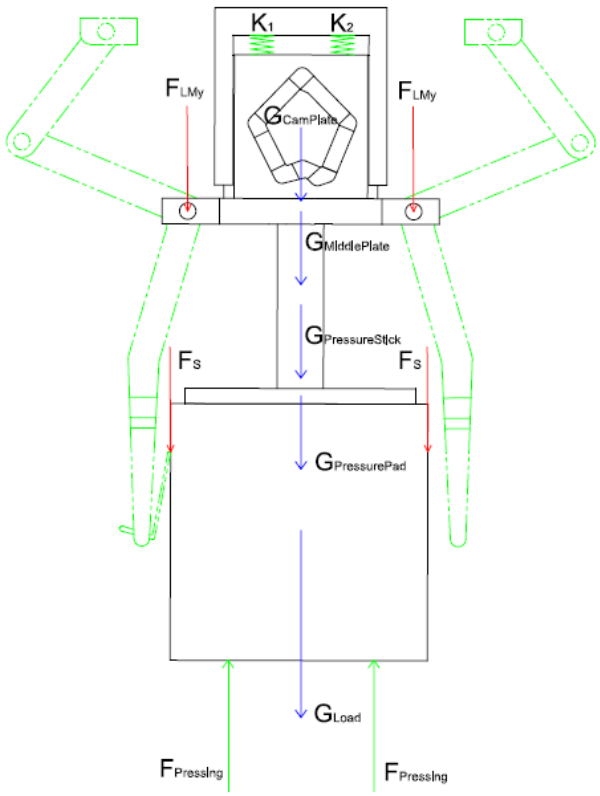

Figure 67: Force diagram for middle section when unlocking the load

Force Equation:

$\sum F_Y = 0 \ \uparrow^+$

$-F_{MLY} \times 4 - F_S \times 4 + 4.905\ N - 1.108\ N - 0.043\ N - 0.014\ N - 0.042\ N - 0.047\ N - F_S(Friction\ on\ hinges\ and\ cam\ mechanism) = k_{Eq} \times x2$ (3. 46)

Substituting values into equation (3.46):

$-0.529\ N \times 4 - 0.277\ N \times 4 + 4.905\ N - 1.108\ N - 0.043\ N - 0.014\ N - 0.042\ N - 0.047\ N - F_S\ (Friction\ on\ hinges\ and\ cam\ mechanism) = \left(48 \frac{N}{m}\right) \times (0.00260\ m)$ (3. 46)

$(k_{Eq} = k_1 + k_2)$ (3. 47)

$0.427\ N - F_S\ (Friction\ on\ hinges\ and\ cam\ mechanism) = 0.1248\ N$ (3. 48)

$0.3022 \geq F_{S\ Hinges\ \&\ Cam\ Mechanism}$ (Defined frictions should not be greater than this number when task is 113 grams load. As mentioned before friction in these sections can be reduced by machine oil and rasping.)

We can see whether chosen spring is enough to move gripper compounds after unlocking of cam mechanism easily;

$k_{Eq} \times x3 + G_{Parts} = F_{S\ Hinges\ \&\ Cam\ Mechanism} - F_{MiddlePlate}$ (In this situation there is no $F_{pressing}$ and F_S forces) (3. 49)

$x_3 = 20.05\ mm = 0.020\ m$ (3. 50)

$\left(48\frac{N}{m}\right) \times (0.020\ m) + 0.18\ N = F_{S\ Hinges\ \&\ Cam\ Mechanism} - 2.11\ N$ (3. 49)

3.25 N ≥ $F_{S\ Hinges\ \&\ Cam\ Mechanism}$ (Maximum friction force should be this number to move gripper compounds when releasing the load)

CHAPTER IV

FABRICATION OF DESIGN

4.1 PRODUCTION OF GRIPPER PARTS BY 3D PRINTER

In previous chapter, gripper part dimensions, related calculations and assembly placements are defined properly, then final design has been provided in computer environment. Although our gripper system works perfectly on computer simulations, most of time in real tests it is possible to have more errors or unwanted behaviours for many designs. For example, cam mechanism path profile or gripper arm shape has been changed many times after result of load lifting tests.

Figure 68: Reached final design after CAD stage

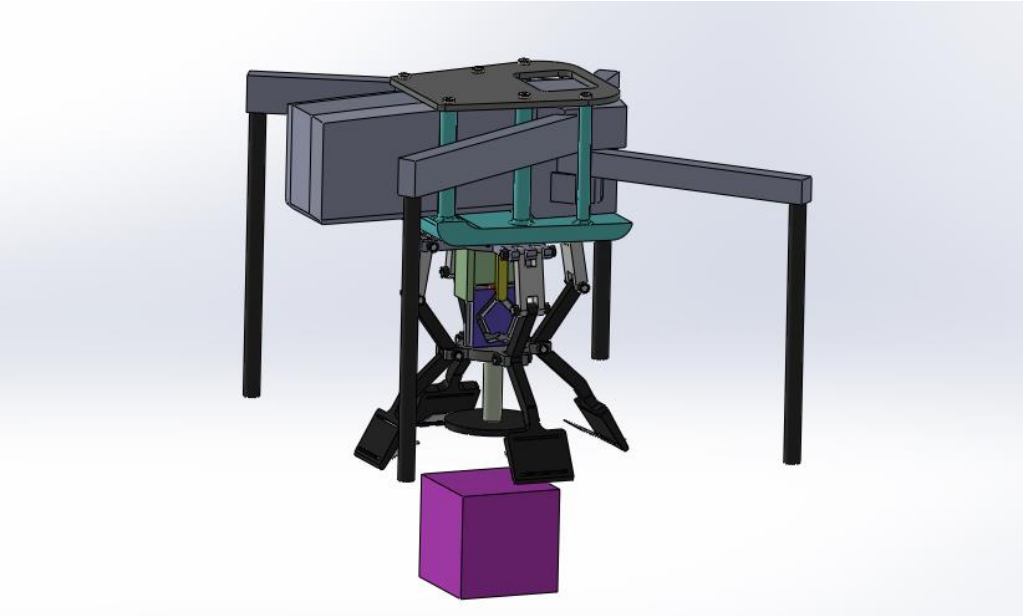

Figure 69: Designed gripper placement on reference drone

Every part in design has been sent to Ultimaker Cura slicer program to produce them with PLA (Polylactic Acid) material. Parts are produced with %20 infill ratio except pin, rod and cap structures in which they have %100 infill ratios. All parts are produced with 3D printer except cam mechanism springs which will be provided later for avoiding possible design changes. Besides, assembly members like different kind of screws will be get readily. Furthermore, for springs to work properly, machine oil will be used inside hinge structures and cam mechanism path.

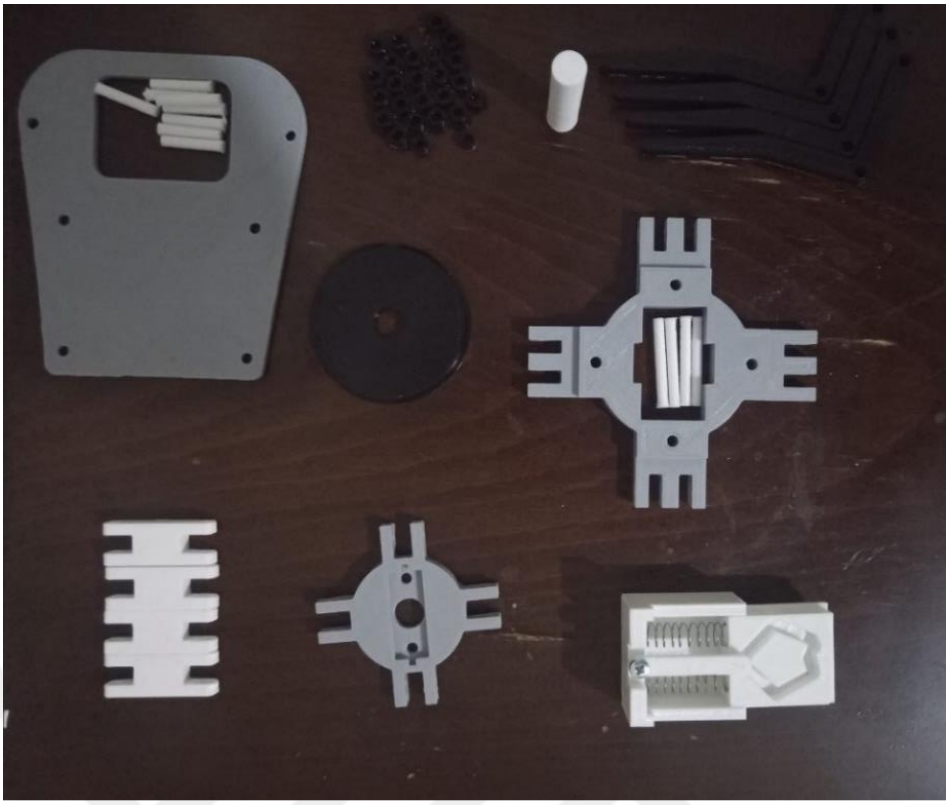

Figure 70: Manufactured parts just before assembly stage

Figure 71: Designed gripper mounting assembly for quadcopter (From top)

Figure 72: Designed gripper mounting assembly for quadcopter (From bottom)

4.2 PRODUCTION OF CAM MECHANISM SPRINGS

It is stated before that it is hard to get a precise manufactured spring for designed cam mechanism due to many reasons like changeable frictions on hinges, variable drone pressing force on the load or lack of sensitive raw spring material in industry. Also, unstable friction inside cam mechanism can play major role on spring motion. However, these technical disabilities will be reduced by using machine oil or rasping. As statically calculated before, there are three situations to define range for our springs. One is, spring should be able to collapse about 22.65 mm for cam mechanism to be locked in Step-1 under drone pressing force on the load. Second, spring needs to be collapsed about 2.60 mm to unlock cam mechanism in load releasing case. In third case, spring should push load and it should be able to move gripper middle plate to expand arms again when releasing the load. We ordered springs in a wide range possible that will fit to our cam mechanism slot (Which means spring outer diameter and spring length is known) from local spring manufacturer. We ordered softest possible spring which has spring coefficient 24 N/m and 122 N/m as hardest spring. We have also 30 N/m and 75 N/m springs as well in case we would need a more precise motions for cam mechanism.

Figure 73: Manufactured springs with same outer diameters and lengths made from spring steel having spring constants k=24 N/m, k=30 N/m, k=75 N/m, k=122 N/m from left to right respectively.

4.3 COMBINATION OF PARTS TO CREATE GRIPPER ASSEMBLY

All gripper parts, drone mounting parts and springs are produced as calculated in previous sections. So, final step is to merge them to create assembled mechanism.

Figure 74: Assembled gripper mechanism (From top)

Figure 75: Assembled gripper mechanism (From bottom)

CHAPTER V

TESTING THE GRIPPER

For test stage, gripper mechanism is tested with three different methods which are hand testing, robotic arm testing and flight test with quadcopter. Hand testing is made many times starting from gripper's born to end of this project to correct mistakes or design defects. Robotic arm testing is made alternatively for simulating drone movement to observe motions clearly when possible cases occur like drone is not able to lift whole mechanism properly or flight doesn't occur in stable behaviour. Tests are applied with two different shape of loads having 5 cm × 5 cm base dimensions (Arm expansion sizes determined minimum for loads having 5 cm × 5 cm base dimensions) as both having cubic and cylindrical shapes. Also, loads are designed for serving box function as well. By this way, loads will have a cap and body sides to allow for adding extra weights inside. Loads are manufactured via PLA material with %20 infill ratios and winded with adhesive tape to increase friction between leaf springs and load surface (Friction value between PLA arm surface and PLA load surface is found relatively smaller than PLA arm surface and adhesive band load surface.). For empty states, cubic box has 53 grams, cylindrical box has 40 grams. By adding additional weights to loads, cubic box reaches 113 grams while cylindrical one reaches 100 grams approximately. Thus, we will have applied tests approximately for 50 grams and 100 grams with different shape of loads.

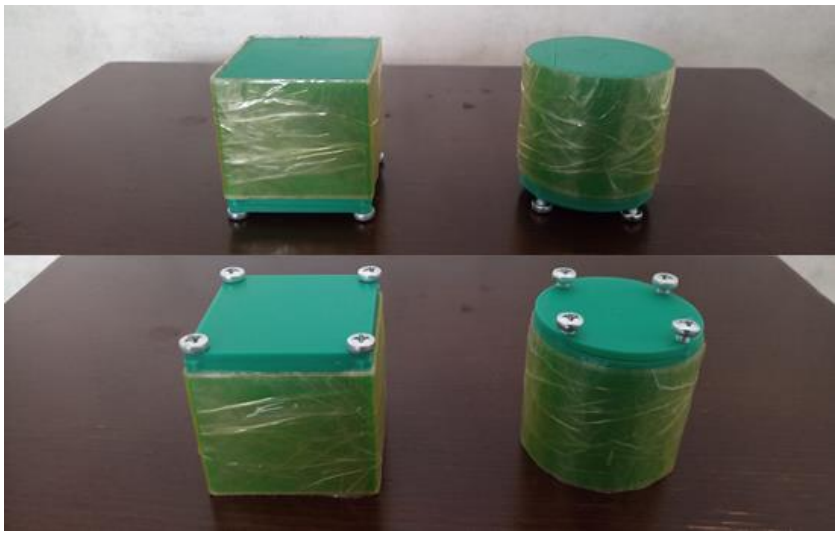

Figure 76: Box type loads having cubic and cylindrical shapes

5.1 TESTING GRIPPER WITH HAND TRIALS

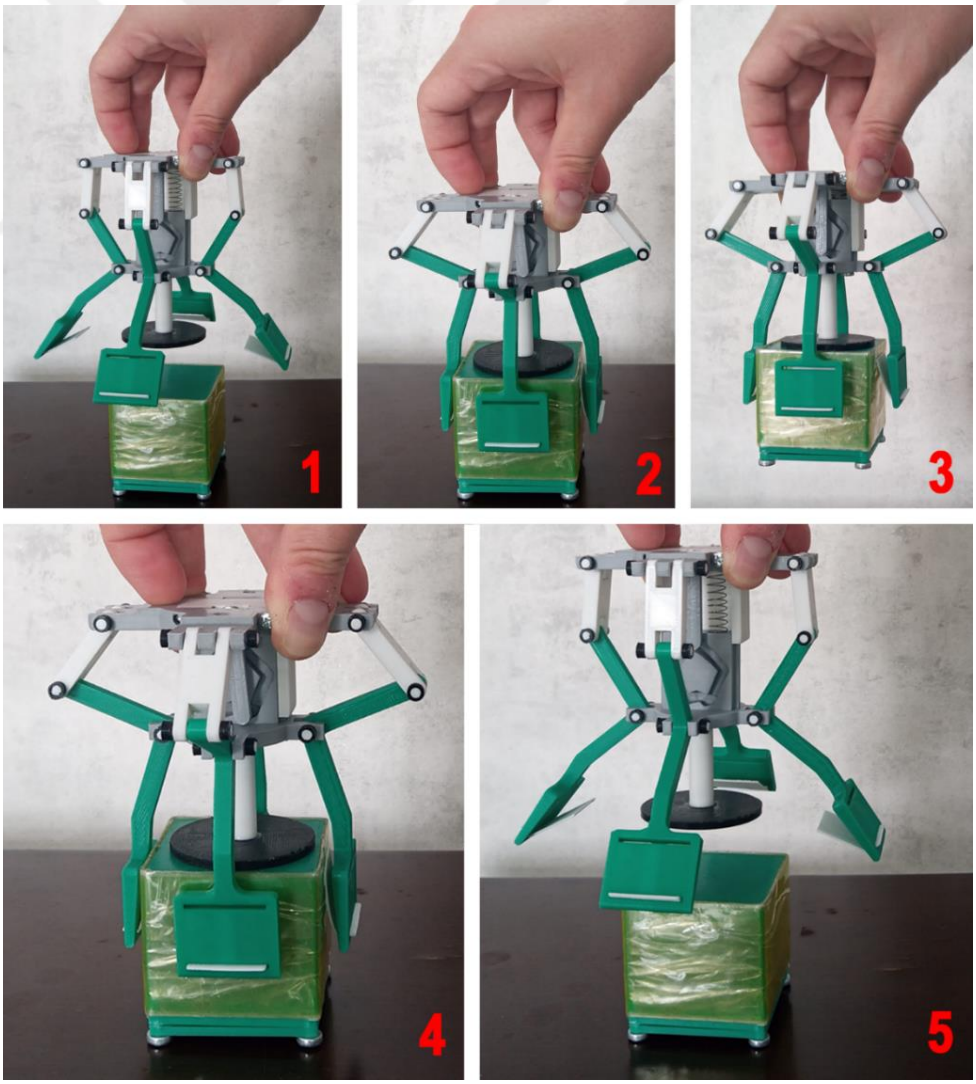

Figure 77: Hand trials with gripper for cubic load

Figure 78: Hand trials with gripper for cylindrical load

Regarding Figure 77 and Figure 78, hand trials basically include five steps to complete motion;

1- Gripper mechanism is approaching to target load.
2- Gripper pressure pad touched to load and applies a press on the load, this makes gripper arms to be collapsing. So, load is grasped.
3- Gripper holds the load on air.
4- For releasing the load, gripper is pressed again by touching the ground. This will release the mechanism to drop the load.
5- When gripper arms are expanded again, load is released and gripper can move away freely.

5.2 TESTING GRIPPER WITH ROBOTIC ARM

We have tested our gripper alternatively with also robotic arm to simulate drone motion on a manipulator. Before we made our test, we have designed a top box to put our previously designed Arduino-MPU6050 circuit inside. By this way, we can mount our gripper and Arduino-MPU6050 circuit together to robotic arm for measuring robotic arm motion characteristics to understand similarities and differences between robotic arm and our quadcopter drone. It is also aimed that applying a test with robotic arm that can imitate quadcopter's motion in case when our drone is not able to have flight with designed gripper fluently. Tests are done with pneumatically controlled Staubli Unimation Series robotic arm in university mechatronics laboratory by applying manual control. Test procedure is simply applied for gripper firstly to grab load, then to carry it for a while and finally to drop it. This procedure is applied for both cubic and cylindrical loads by using weights 40, 50, 100, 113 grams. During test procedure all motions are saved via MPU6050 module by sending acceleration parameters to notebook remotely. Throughout test process, our gripper could carry loads successfully without dropping it involuntarily in safe way.

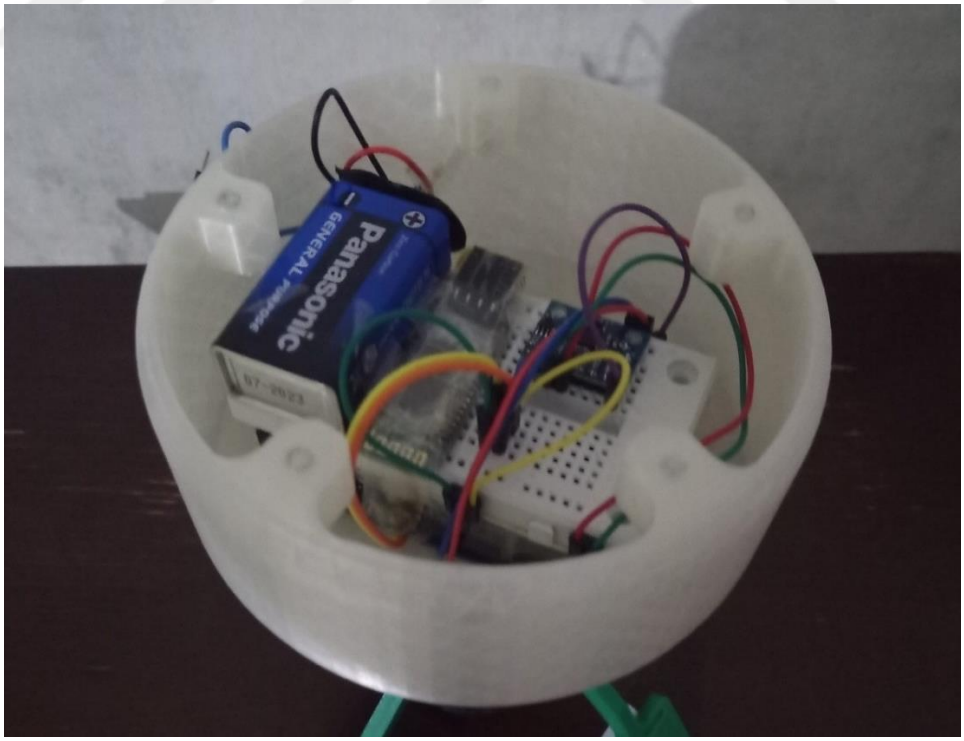

Figure 79: Top box for gripper to place Arduino-MPU6050 circuit inside

Figure 80: Mounted top box on upper the gripper

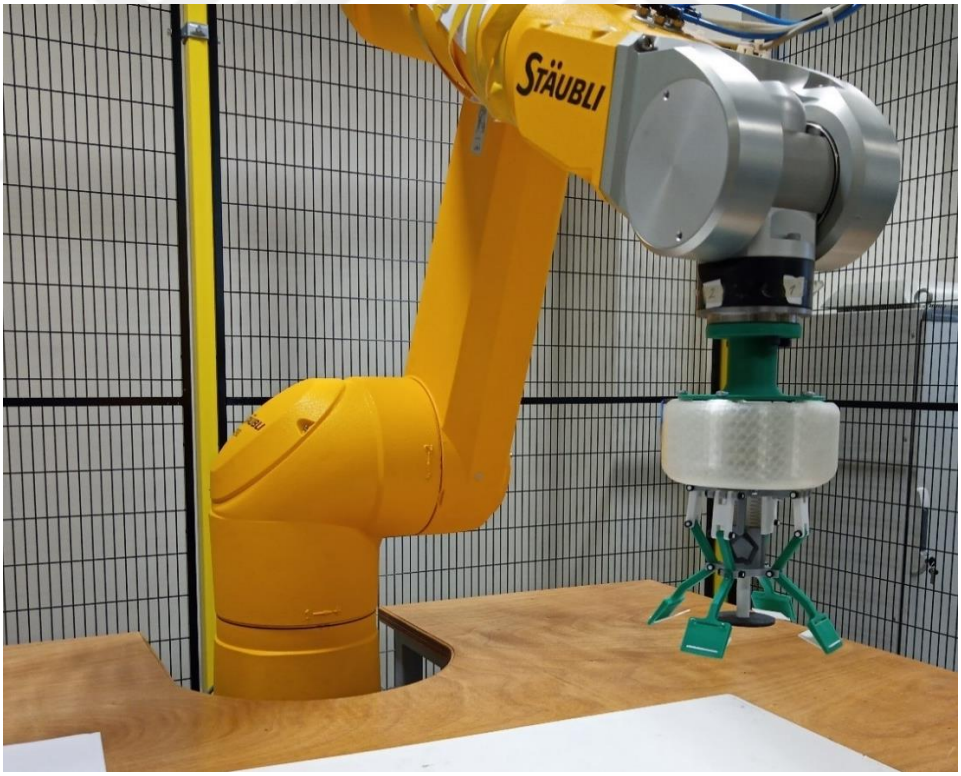

Figure 81: Mounted gripper-top box complex on robotic arm

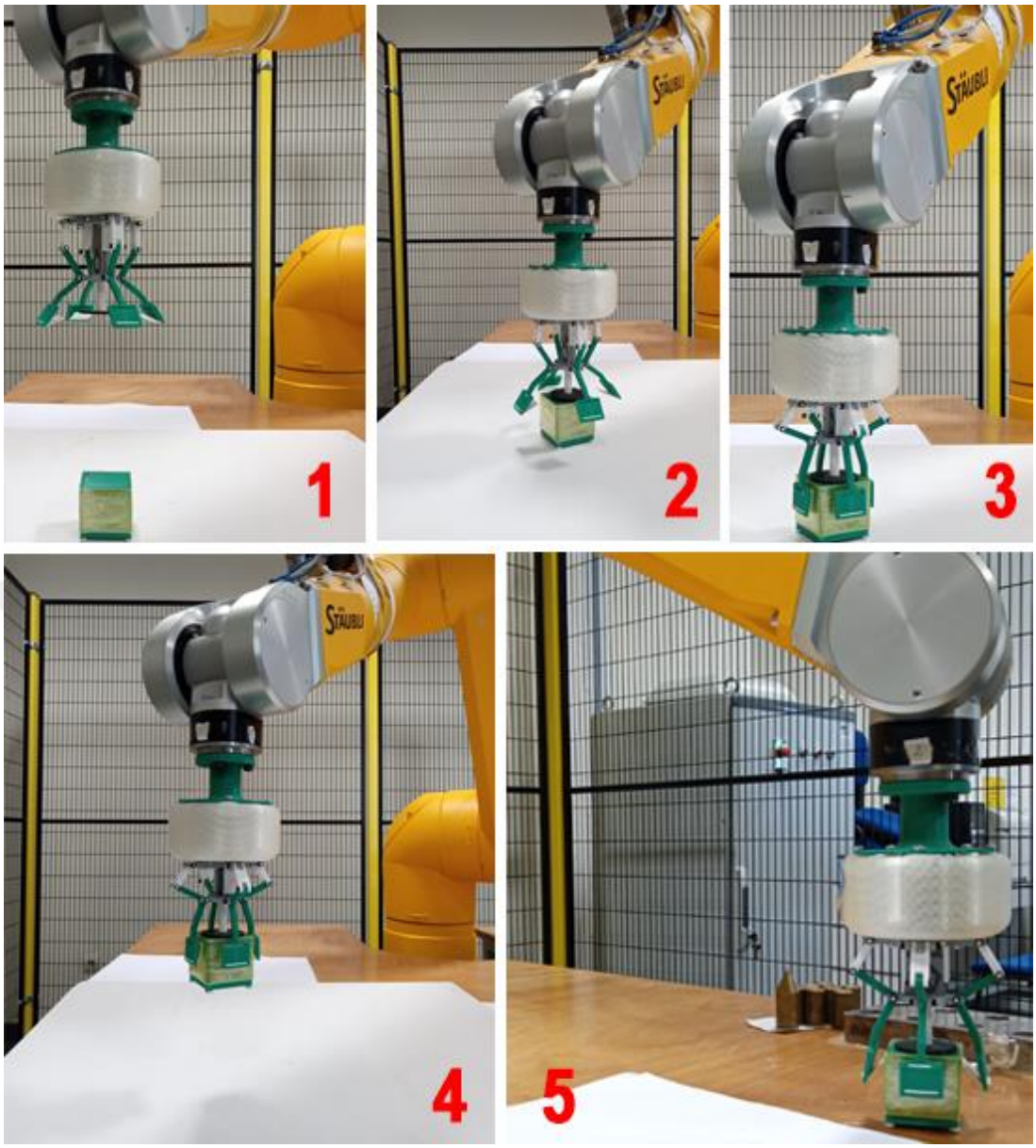

Figure 82: Gripper trial on robotic arm for cubic load

Regarding Figure 81 and Figure 82, robotic arm trials are basically including five steps to complete motion;

1- Gripper mechanism is approaching to target load.
2- Gripper pressure pad touched to load and applies a press on the load, this makes gripper arms to be collapsing.
3- Load is grasped properly.
4- Load is carried on air for a while for reaching the target point.
5- In final point, pressure pad is pushed by load for arms to be expanded again. After this stage, load is released and gripper can move away freely.

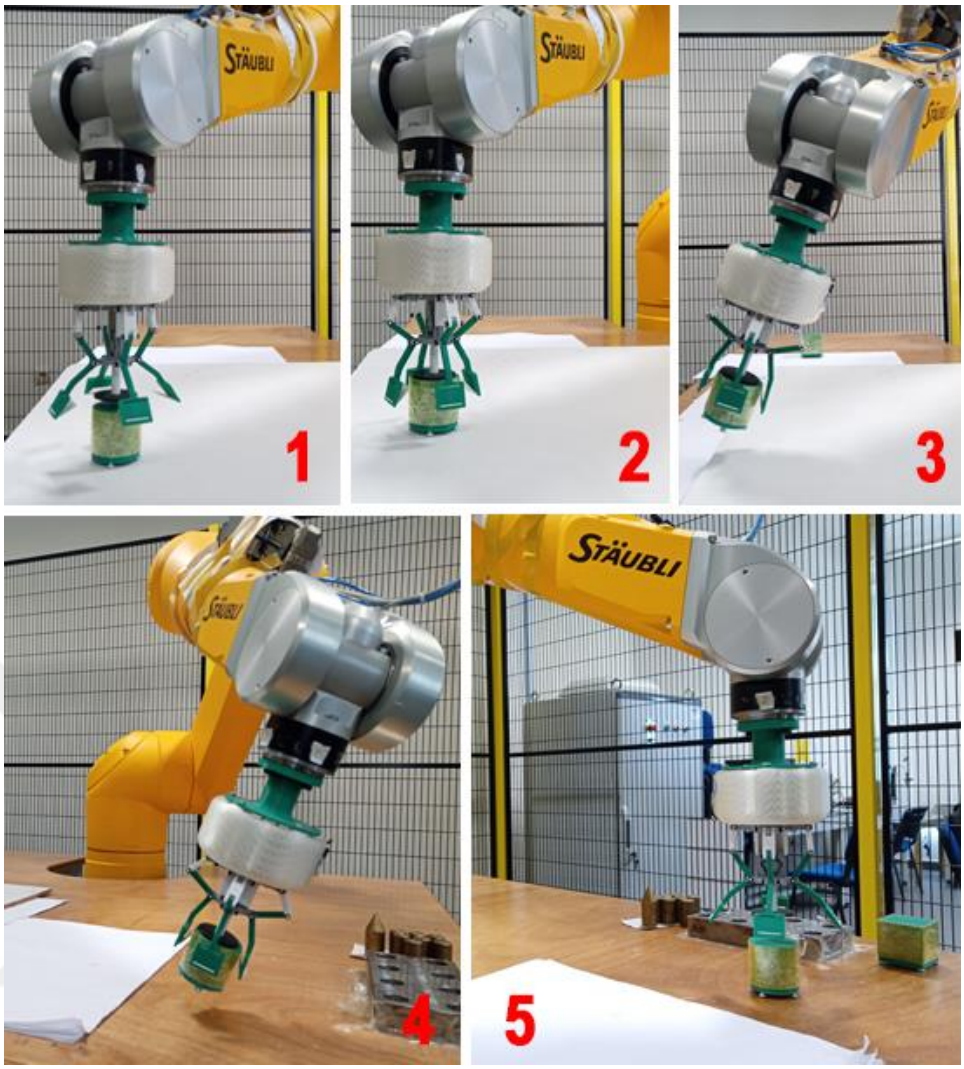

Figure 83: Gripper trial on robotic arm for cylindrical load

5.2.1 MPU6050 Robotic Arm Testing Parameters

As stated before, for mounting MPU6050 sensor, a top box is produced and attached to head of gripper. This top box is mounted to robotic arm end effector to measure robotic arm's linear acceleration, angular velocity and angular acceleration values in motion moment. These tests are applied for a shorter time compare to MPU6050 tests with drone itself. Test procedure is basically including load grasping, lifting, carrying, descending and releasing steps. Each procedure happens in shorter than twenty seconds because carrying step takes place through about 1-meter distance due to robotic arm operation area restrictions in laboratory. Robotic arm is controlled manually in maximum velocity to measure possible ultimate acceleration values. Manual control procedure is applied also for safety of our gripper to prevent potential crashes during test.

Robotic arm tests are applied in three different gripper conditions. One is without load, second one is with cubic load and last one is with cylindrical load. Also, for simulating quadcopter flight better, tests are carried out by giving a tilt angle to robotic arm end effector about 35º which is quadcopter's maximum tilt angle as well.

In the end of "Without Load" test, measurement results are;

Table 9: Ultimate values for "Without Load" Trials

	Linear Acceleration (m/s^2)		
	aX(m/s^2)	aY(m/s^2)	aZ(m/s^2)
Maximum	3.35	-0.68	1.74
Minimum	2.45	-3.42	-1.82
	Angular Velocity (rad/s)		
	RotX(rad/s)	RotY(rad/s)	RotZ(rad/s)
Maximum	0.05	0.01	0.00
Minimum	0.01	-0.02	-0.02
	Angular Acceleration (rad/s^2)		
	AngAX(rad/s^2)	AngAY(rad/s^2)	AngAZ(rad/s^2)
Maximum	0.30	0.20	0.10
Minimum	-0.30	-0.30	-0.20

In the end of "Cubic Load" test, measurement results are;

Table 10: Ultimate values for "Cubic Load" Trials

	Linear Acceleration (m/s^2)		
	aX(m/s^2)	aY(m/s^2)	aZ(m/s^2)
Maximum	0.30	-1.85	0.86
Minimum	-0.29	-3.17	-1.88
	Angular Velocity (rad/s)		
	RotX(rad/s)	RotY(rad/s)	RotZ(rad/s)
Maximum	0.04	0.01	-0.01
Minimum	0.02	-0.01	-0.02
	Angular Acceleration (rad/s^2)		
	AngAX(rad/s^2)	AngAY(rad/s^2)	AngAZ(rad/s^2)
Maximum	0.20	0.20	0.10
Minimum	-0.10	-0.20	-0.10

In the end of "Cylindrical Load" test, measurement results are;

Table 11: Ultimate values for "Cylindrical Load" Trials

	Linear Acceleration (m/s^2)		
	aX(m/s^2)	aY(m/s^2)	aZ(m/s^2)
Maximum	0.30	-1.85	0.86
Minimum	-0.29	-3.17	-1.88
	Angular Velocity (rad/s)		

Table 11 Cont.

	RotX(rad/s)	RotY(rad/s)	RotZ(rad/s)
Maximum	0.04	0.01	-0.01
Minimum	0.02	-0.01	-0.02
	Angular Acceleration (rad/s^2)		
	AngAX(rad/s^2)	AngAY(rad/s^2)	AngAZ(rad/s^2)
Maximum	0.20	0.20	0.10
Minimum	-0.10	-0.20	-0.10

5.3 TESTING GRIPPER WITH QUADCOPTER

Finally, as planned initially, we also tested our gripper model with quadcopter. For testing the gripper model with quadcopter, we added additional legs to raise quadcopter from ground for gripper to hold loads as in desired way and to maintain take-off and landing motions safe. Also, support beams are added between legs to reinforce structure during test procedure.

Test procedure is carried out by mounting load on drone at start, without drone remote controlling to grab the load manually during flight. This is because, our quadcopter is moving in very dynamic behaviour and it is not able to grab the load throughout the flight as desired way like planned at start. Test is applied for gripper on drone just to see whether gripper conveyance for loads during flight is safe. It is also targeted that understanding of flight characteristics of drone when our gripper mechanism mounted during test process.

Figure 84: Created leg chassis and support beams for quadcopter and mounted gripper mechanism to middle (From front)

Figure 85: Created leg chassis and support beams for quadcopter and mounted gripper mechanism on middle (From back)

Figure 86: Flight stage including quadcopter is lifting the load

Figure 87: Flight stage including quadcopter is transporting the load

5.4 RESULTS AND DISCUSSION

5.4.1 Evaluation of Tests

When desired gripper design process is completed, we had three types of tests. One test was performed with hand including grabbing, locking and releasing the load stages. Furthermore, designed gripper is shaked several times to be sure load is grasped properly and whether load is carried in flight case safely. Hand tests are applied successfully with cubic and cylindrical shape loads.

In some hand trials, mechanism experienced jammings due to cam profile's characteristics. It is believed that jamming can be reduced after some further modifications about cam profile. Additionally, load grasping friction can be increased or decreased by adjusting leaf spring angle by user's preferences. It is also possible to cover leaf spring with additional materials to enhance grasping feature far better.

For simulating a real drone flight, we also had robotic arm trials by mounting our gripper to end-effector of the arm. Test is basically including grabbing, carrying and releasing stages for cubic and cylindrical loads. Also, loads are tried with 50 grams and 115 grams averagely for a better flight projection. Besides, 35º inclination angle is given to the end effector to model quadcopter's inclined situation while moving forward. Tests are applied pursuant to manual manipulation of robotic arm to do tests in safe and controlled manner. Manipulation is done with maximum possible speed of arm in allowed restricted area of bench. While motions were being carried out, MPU6050 module gave acceleration parameters from the gripper with mounted top cap. Thereby, after robotic arm test procedure completed, it is observed that ultimate linear acceleration values in these tests show similarities with MPU6050 tests with drone itself. For example, in robotic arm tests maximum linear acceleration occurs around 3-4 m/s^2 values. When we look at single drone flight tests, especially considering free flight tests, we can see linear acceleration takes place maximum around 4 m/s^2 as well. This shows us we could model one similar environment with real drone flight by using our pneumatic robotic arm. These experiments can be expanded to larger acceleration values if arm is programmed to be autonomously for doing tests itself.

Gripper was tested with actual quadcopter flight as well. For this test, gripper was mounted to bottom of drone as planned before. Extra legs are attached to drone legs to raise drone from ground in proper length for making take off and landings

possible. Between legs, supporter beam structures are added to reinforce aerial vehicle. As stated before, load is mounted just before flight with hand and load is carried by drone for a while whether to see quadcopter is holding the load safely. Normal grabbing, locking and releasing steps couldn't be applied in this test, because, our quadcopter is moving in very dynamic behaviour and it is not able to grab the load throughout the flight as desired way like planned at start. It is supposed that having aerial vehicles providing more stable flight dynamics can result more accurate motions we can have for gripper during flight process. Besides, quadcopters providing higher lifting capacities will give better performance for this gripper concept. It is also advised to mount this gripper model for automated air vehicles or AI supported aerial platforms to do tasks whose conveyance path previously defined by users. Particularly; in factories, logistics storage facilities (Like internet shopping web site storage centers) or in environments require an automated load stowing processes, designed work will be more beneficial as an alternative to current load conveyance systems.

5.4.2 Fourier Transform Comparison for Acceleration Parameters of Robotic Arm and Actual Drone Flight

Fourier Transform calculations are applied for converting of datas which include waves versus time into separated sinus waves in frequency base. Fourier transform method is often used in signal processing, data analysis and data manipulations.

Basically, "Fast Fourier Transform" (FFT) is fast computation algorithm for "Discrete Fourier Transform" (DFT) method. In other words, they can be used in same purposes. DFT method can be summarized in a formulation as;

$$x[k] = \sum_{n=0}^{N-1} x[n] e^{(-j2\pi kn)/N} \quad (5.\ 1)$$

where x[n] shows discrete signal and N shows size of its domain. To find x[n] we multiply that value by n's function exponential value of "e". These values are then summed as seen in equation.

For calculation of this phenomenon, we need $O(N^2)$ operations (N multiplications and N additions. Shortly, FFT enables us to reduce this number of operations from $O(N^2)$ to O(NlogN).

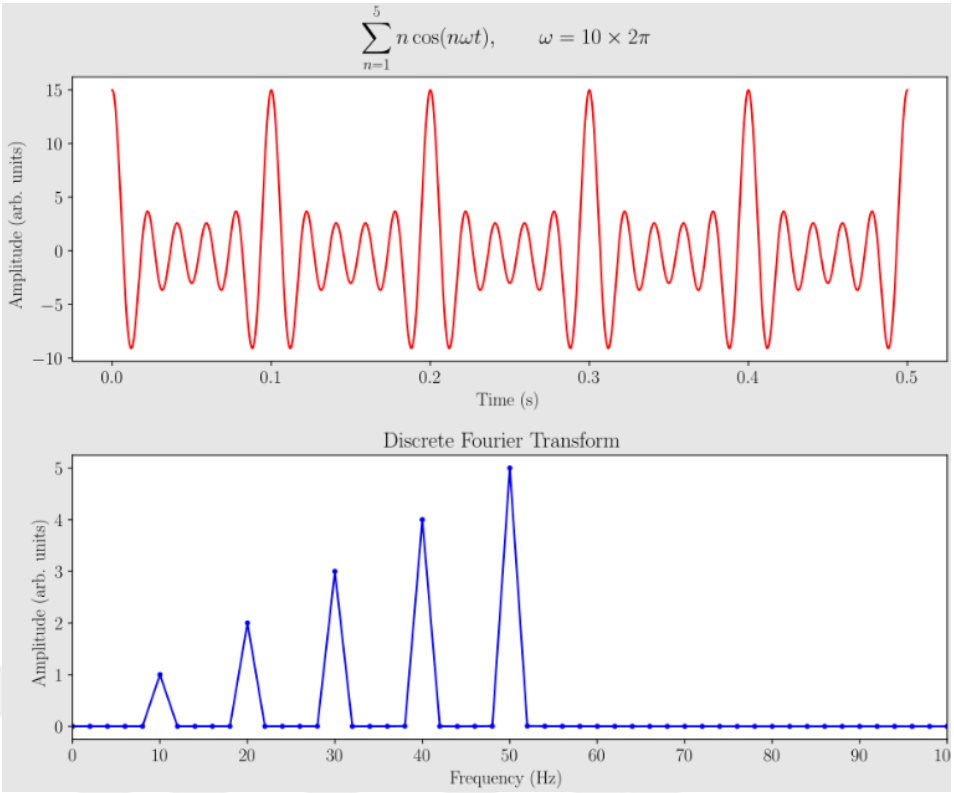

Figure 88: Application of "Discrete Fourier Transform" for a time domain waveform and getting frequency domain waveform version in the end [29]

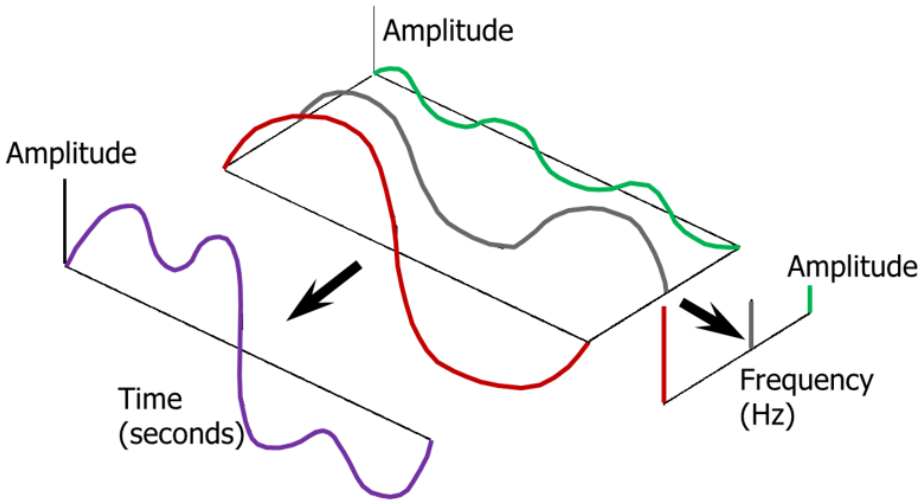

Figure 89: Fourier Transform allows conversion of complex time signal in frequency domain [30]

As mentioned before, we collected both flight parameters from robotic arm flight simulation and real drone flight by using MPU6050 module and then datas are rearranged with Excel. Collected datas are then used for creating of time domain waveforms graphs (Acceleration versus time, angular velocity versus time and angular acceleration versus time). Same procedure is applied also for robotic arm flight simulation as referred in robotic arm testing section. In our project, we also applied

Fourier Transform method to see frequency domains of already created graphs with time domain.

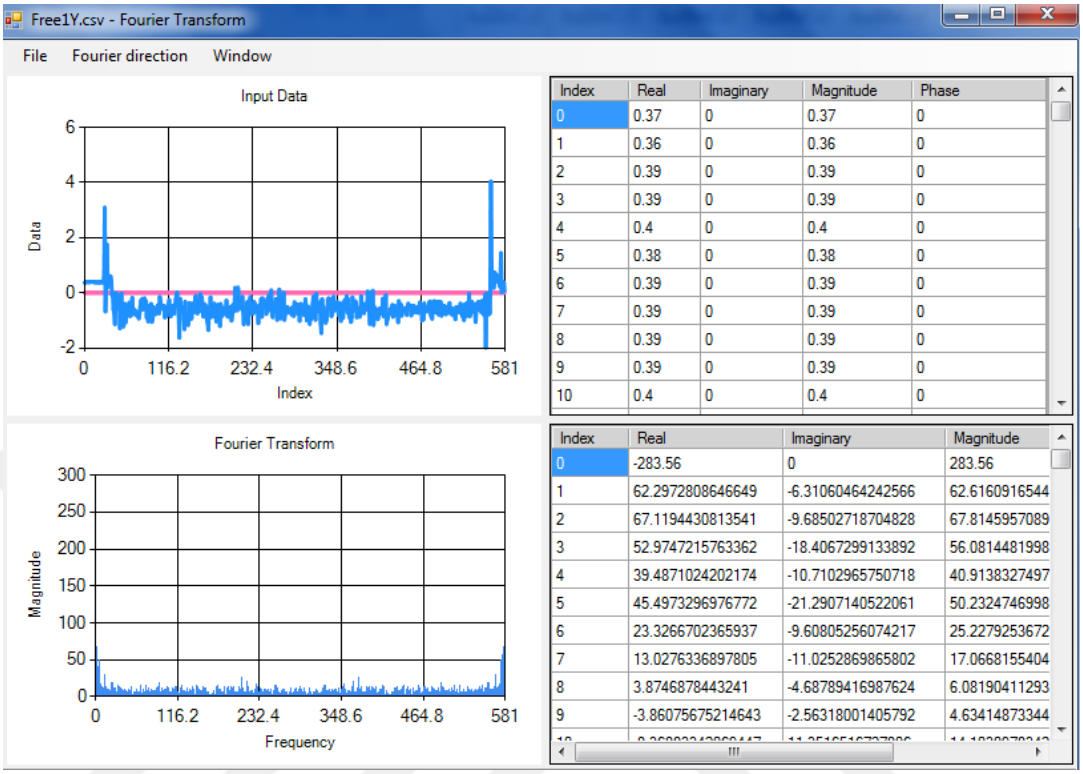

Index	Real	Imaginary	Magnitude	Phase
0	0.37	0	0.37	0
1	0.36	0	0.36	0
2	0.39	0	0.39	0
3	0.39	0	0.39	0
4	0.4	0	0.4	0
5	0.38	0	0.38	0
6	0.39	0	0.39	0
7	0.39	0	0.39	0
8	0.39	0	0.39	0
9	0.39	0	0.39	0
10	0.4	0	0.4	0

Index	Real	Imaginary	Magnitude
0	-283.56	0	283.56
1	62.2972808646649	-6.31060464242566	62.6160916544
2	67.1194430813541	-9.68502718704828	67.8145957089
3	52.9747215763362	-18.4067299133892	56.0814481998
4	39.4871024202174	-10.7102965750718	40.9138327497
5	45.4973296976772	-21.2907140522061	50.2324746998
6	23.3266702365937	-9.60805256074217	25.2279253672
7	13.0276336897805	-11.0252869865802	17.0668155404
8	3.8746878443241	-4.68789416987624	6.08190411293
9	-3.86075675214643	-2.56318001405792	4.63414873344

Figure 90: Computer program for application of "Fourier Transform"

Our purpose about applying this method is to clearly see and compare our parameters by separating unnecessary complex waves in time domain. This gives us brief idea about our flight parameters like how vibrations distributed throughout the flight. Therefore, we can distinctly observe stability states of a flight from Fourier Transform applied graphs in frequency domain. All transforms are made with computer software. Program is running FFT method for the cases when number of data is 2 to n. In rest conditions, program is calculating inputs according to DFT method.

For our case, we can compare Fourier analysis for linear acceleration in Y direction values because we mounted MPU6050 module's Y axis for placing to drone's front and robotic arm motion direction in testing stages.

"Free Flight 1" linear acceleration for Y direction in time domain:

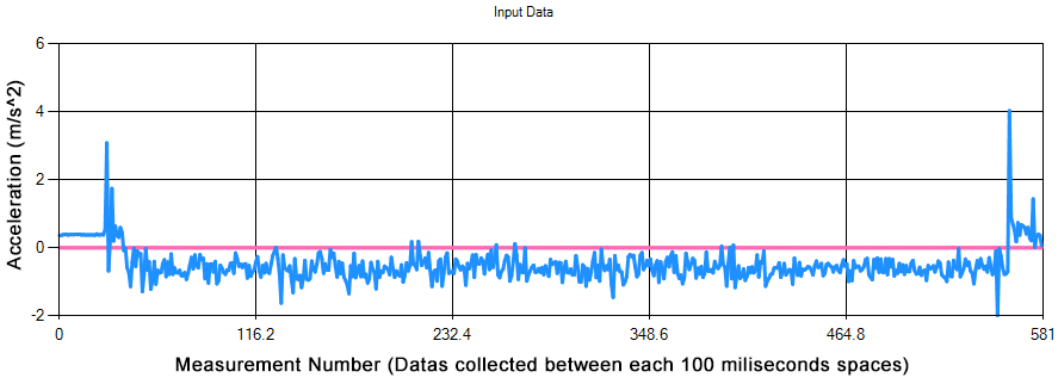

Figure 91: "Free Flight 1" linear acceleration in time domain

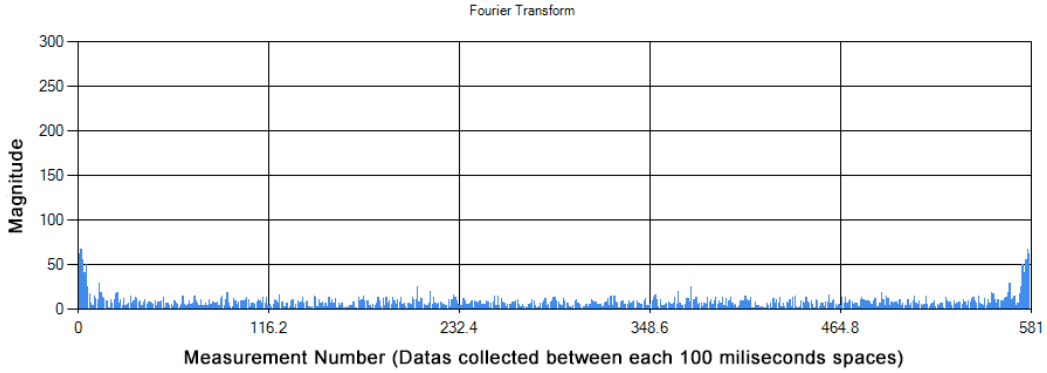

Figure 92: "Free Flight 1" linear acceleration in frequency domain through first moments of flight (Graph after Fourier Transformation applied)

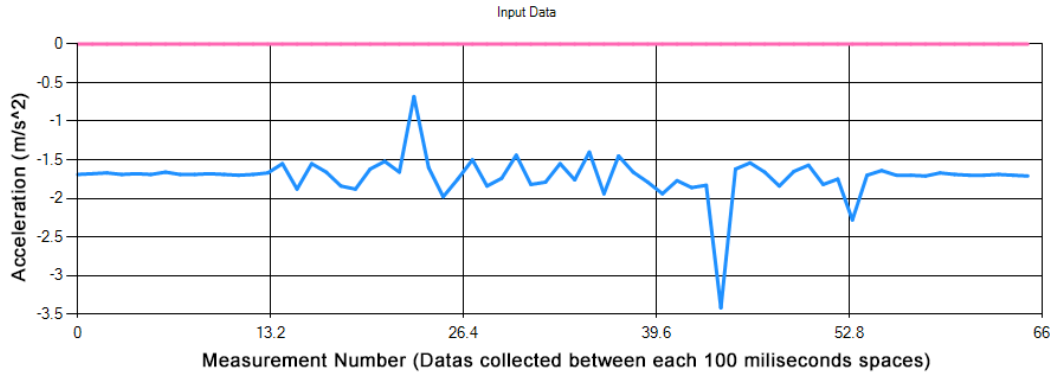

Figure 93: "Without Load" robotic arm test linear acceleration in time domain

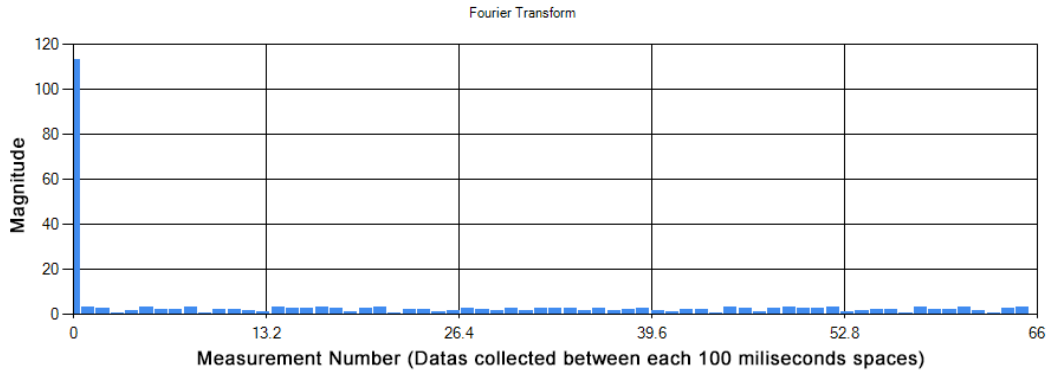

Figure 94: "Without Load" robotic arm test linear acceleration in frequency domain through first moments of flight (Graph after Fourier Transformation applied)

As seen in Figures 92 and 94, robotic arm tests have less vibration and instabilities while actual drone flight has more vibration and unstable behaviour. Meanwhile, we can see marginal explosions on start of each trial from Fourier charts because we have maximum acceleration jumps at take-offs. So, when we think about our gripper model, it is better to have more stable aerial vehicle to make happen grabbing function smoother.

5.4.3 Comparison the Project with Similar Works

The most similar thesis regarding our project is made in name of "Compliant Bistable Gripper for Aerial Perching and Grasping" which is also presented in 2019 International Conference on Robotics and Automation (ICRA). The project is developed mainly for small aerial robot's lack of energy continuity during flights. As solution to that, a perching capability is given for a mini quadcopter. With this capability, small aerial vehicles can perch or land on various places for recharging or resting a while. According to solution, three-legged perching system, three soft silicon tubes and connected contact pad system is created as in compliant manner [10].

Briefly, system does grasp function by touching between contact pad and object. When touching happens with an ideal force, compliant legs collapse to grip the object for perching. Releasing function is made with heating the resistance system to drive legs which are printed with thermoplastic material for expanding again [10].

Mentioned compliant system shows similarities with our project about pad system, related pad driven arms and needed ideal contact force with the object. Grasping function is used in both system with contact pad driven arm mechanism. When enough contact force happens, each gripper provides grasping function in same way.

There are differences about releasing system for both projects. While our system does release with a second contact with object and ground, compliant bistable gripper system does the same function by heating up resistance wire to soften thermoplastics legs for expansion. So, that perching system requires additional remote control to make it possible said functionality. While our system can be modified for all dimensioned vehicles, referred system mostly create a proper environment for small aerial vehicles. However, it provides more lightweight chassis design and perching feature as well [10].

CHAPTER VI

CONCLUSION

In this thesis, we have covered a design process of a gripper system which doesn't need an additional motorized control mechanism inside and will serve conveyence function mainly for rotary wing aerial vehicles to carry different kind of loads.

Before starting the project, in scope of literature search which includes current gripper systems for aerial vehicles, linkage synthesis and spherical grabbing systems topics are included to discover current applied technologies and techniques in the field. Then, main objectives are defined and design circle is restricted with following ideas. Ideas are created in form of sketches for determining basic lines of desired mechanism. With sketches and defined tasks, our non-motorized system is determined to be including two main functions which are powering the mechanism with drone's ascending or descending motion and providing self locking-unlocking feature for gripper arms. According to these two design parameters, again a literature search has been made this time for current linkages providing that two functions. Rotary wing vehicle can provide power for gripper from ascending and descending motions with a contact system and can provide locking and unlocking functions with a ball pencil mechanism like system by using same ascending-descending motions of aerial vehicle. In other words, our vehicle should provide both load grasping and locking functions with same movement in same time, because we have neither any motorized driving system nor remotely controllable electronic component inside the mechanism. According to this, when we think reversely, mechanism should release the load and arms should be unlocked with same movement in same time. By considering these main features, a sample template gripper mechanism is designed and produced from wood material to lift a small box. That wood gripper created a reference template for our final design. After this point, wood gripper is planned to be modified without changing main lines

To simulate drone's flight, we also mounted acceleration sensor on drone to catch acceleration parameters during flight. These datas are used for comparing drone flight characteristics with robotic arm test characteristics as well.

Due to we have main lines about our gripper, we started to design our final gripper with CAD software by taking reference of our load and initial dimensional limitations. Our design is mainly produced with 3D printer in the end of design process. Produced gripper had revisions before final mechanism after we made hand trials.

When we assembled our final gripper model, we had three types of tests to measure characteristics of the design. These tests are applied as hand trials, robotic arm trials and quadcopter flight trials respectively. Hand trials were applied whether to see our gripper is working as in desired way. Robotic arm trials were utilized to simulate an ideal drone motion while our gripper mounted on the system. Robotic arm tests also show us similarities and differences with actual drone tests as well. After robotic arm tests completed, we tried our gripper with actual drone flight tests too.

In the end of test procedure, it is observed that gripper could easily grab, lock and release the load in two motions of gripper in hand and robotic arm tests. In drone flight tests, it was hard to apply grab, lock and release functions during flight because of quadcopter's high dynamic characteristics, so, it was hard to control the drone manually to do previously defined tasks. Drone flight tests are done for being sure whether gripper is grasping the load properly during flight of quadcopter and it is detected the vehicle could provide conveyance for load with our gripper design successfully.

Our thesis can be enhanced by using more powerful and precise motion provider drones to make healthier trials for manipulating objects. Furthermore, for exact lock and unlock function, cam mechanism and its components can be produced with metal material to reduce frictions more. Besides, trials showed us that mentioned load grasping and releasing procedure with human controlled air vehicle is relatively harder in cases when load is not seen clearly by operator or chosen drone moves in too dynamic manner like we experienced. Instead, we can propose that designed new gripper can also be mounted on automated air vehicles, robotic manipulators or AI supported aerial platforms to complete tasks. Besides, for situations of aerial vehicle pilot doesn't see load brightly, it is possible to mount a camera to bottom of aerial vehicle as well to locate the vehicle better while grasping and releasing the object.

It is considered that, this thesis will lead works to be extended along new ideas in the field. Especially, it is believed, benefits of thesis will widen the horizon of people who work on grasping techniques for aerial vehicles or robotic manipulators in non-motorized way. Designed gripper will be also advantageous for linkage creators who work in different disciplines of mechanical science.

REFERENCES

[1] Amazon (2013). *Amazon Prime Air* [Video file]. Retrieved from https://www.youtube.com/watch?v=98BIu9dpwHU (Date of Access: 07.05.2022).

[2] Rajashekhar V. S., Vibha M. R., Das K. & Ghose D. (2021), "A Robust Aerial Gripper for Passive Grasping and Impulsive Release using Scotch Yoke Mechanism", *5th International Conference of The Robotics Society*, p. 1-7, Kanpur, India.

[3] Mantis Engineer Team (2015), *Mantis Claw Tests* [Video file]. Retrieved from, https://www.youtube.com/watch?v=4gJVcfd98bg (Date of Access: 07.05.2022)

[4] Kruse L.& Bradley J.(2018), "A Hybrid, Actively Compliant Manipulator/Gripper for Aerial Manipulation with a Multicopter", *2018 IEEE International Symposium on Safety, Security, and Rescue Robotics (SSRR)*, Philadelphia, PA, USA.

[5] Bellicoso C. D., Buonocore L. R., Lippiello V. & Siciliano B. (2015), "Design, Modelling and Control of a 5-DoF Light-Weight Robot Arm for Aerial Manipulation", *2015 23rd Mediterranean Conference on Control and Automation, MED 2015-Conference Proceedings*, p. 853–858, Torremolinos, Spain.

[6] Adafruit Industries (2018), *Drone Claw* [Video file]. Retrieved from, https://www.youtube.com/watch?v=93u8R_UpoCw (Date of Access: 07.05.2022).

[7] Mantis Engineer Team (2016), *Mantis Carbon Drone Claw* [Video file]. Retrieved from, https://www.youtube.com/watch?v=swspg2VEPHY (Date of Access: 07.05.2022).

[8] Kim Sukjun, Lee Dae-Young, Jung Gwang-Pil & Cho Kyu-Jin. (2018), "An Origami-Inspired, Self-Locking Robotic Arm That Can Be Folded Flat", *Science Robotics*, p. 1–11.

[9] PRODRONE (2016), *Dual Robot Arm Large-Format Drone PD6B-AW-ARM* [Video file]. Retrieved from, https://www.youtube.com/watch?v=T6ka U2sgPqo (Date of Access: 07.05.2022).

[10] Zhang H., Sun J. & Zhao, J. (2019), "Compliant Bistable Gripper for Aerial Perching and Grasping", *IEEE International Conference on Robotics and Automation*, p. 1248–1253, Montreal, QC, Canada.

[11] Fiaz U. A., Abdelkader M. & Shamma, J. S. (2018), "An Intelligent Gripper Design for Autonomous Aerial Transport with Passive Magnetic Grasping and Dual- Impulsive Release", *IEEE/ASME International Conference on Advanced Intelligent Mechatronics*, p. 1027–1032, Auckland, New Zealand.

[12] The GrabCAD Community Library (2022). *Pneumatic / Hydraulic Gripper*. Retrieved from https://grabcad.com/library/pneumatic-hydraulic-gripper-1 (Date of Access: 07.05.2022).

[13] The GrabCAD Community Library (2022). *Gripper*. Retrieved from https://grabcad.com/library/gripper-230 (Date of Access: 07.05.2022).

[14] The GrabCAD Community Library (2022). *Robot Gripper*. Retrieved from https://grabcad.com/library/robot-gripper-24 (Date of Access: 07.05.2022).

[15] The GrabCAD Community Library (2022). *Gripper*. Retrieved from https://grabcad.com/library/gripper-234 (Date of Access: 07.05.2022).

[16] The GrabCAD Community Library (2022). *Plunger Activated Gripper*. Retrieved from https://grabcad.com/library/plunger-activated-gripper-1 (Date of Access: 09.05.2022).

[17] The GrabCAD Community Library (2022). *Pneumatic Gripper*. Retrieved from https://grabcad.com/library/pneumatic-gripper-4 (Date of Access: 09.05.2022)

[18] The GrabCAD Community Library (2022). *Robot Gripper*. Retrieved from https://grabcad.com/library/robot-gripper-1 (Date of Access: 09.05.2022).

[19] The GrabCAD Community Library (2022). *Gripper*. Retrieved from https://grabcad.com/library/gripper-148 (Date of Access: 09.05.2022).

[20] engineerguy (2015), *How a Retractable Ballpoint Pen Works* [Video file]. Retrieved from, https://www.youtube.com/watch?v=MhVw-MHGv4s (Date of Access: 07.05.2022).

[21] thang010146 (2015), *Push-push button 2* [Video file]. Retrieved from, https://www.youtube.com/watch?v=5JzjSsxSsb8 (Date of Access: 07.05.2022)

[22] thang010146 (2015), *Push-push button 1a* [Video file]. Retrieved from, https://www.youtube.com/shorts/Meltd5Kclqs (Date of Access: 07.05.2022).

[23] thang010146 (2016), *Push-push button 3* [Video file]. Retrieved from, https://www.youtube.com/watch?v=kJ0BlovBWtk (Date of Access: 07.05.2022).

[24] thang010146 (2016), *Push-turn button mechanism* [Video file]. Retrieved from, https://www.youtube.com/watch?v=Iq3ICLRWXf8 (Date of Access: 07.05.2022).

[25] Omni Calculator (2021). *Drone Motor Calculator*. Retrieved from https://www.omnicalculator.com/other/drone-motor (Date of Access: 07.05.2022).

[26] IVC WIKI (2012). *Center of Gravity*. Retrieved from https://beta.ivc.no/wiki/index.php/TBS_Discovery_setup (Date of Access: 07.05.2022).

[27] Brunner D. (2016), *Setting the PID controller of a drone properly*. Retrieved from, https://www.technik-consulting.eu/en/optimizing/drone_PID-optimizing.html (Date of Access: 07.05.2022).

[28] Last Minute Engineers (2020). *Interface MPU6050 Accelerometer and Gyroscope Sensor with Arduino*. Retrieved from https://lastminuteengineers.com/mpu6050-accel-gyro-arduino-tutorial/ (Date of Access: 09.05.2022).

[29] Wikimedia Commons (2020), FFT of Cosine Summation Function.svg [File]. Retrieved from, https://commons.wikimedia.org/wiki/File:FFT_of_Cosine_Summation_Function.svg (Date of Access: 15.05.2022).

[30] Siemens DISW (2022). *What is the Fourier Transform*. Retrieved from https://community.sw.siemens.com/s/article/what-is-the-fourier-transform (Date of Access: 09.05.2022).

APPENDICES

1. Arduino Written Code

```
#include <Adafruit_MPU6050.h>
#include <Adafruit_Sensor.h>
#include <Wire.h>
Adafruit_MPU6050 mpu;
#include <SoftwareSerial.h>
SoftwareSerial mySerial(3,4);
void setup(void) {
mySerial.begin(9600);
Serial.begin(115200);
mySerial.println("Adafruit MPU6050 test!");
if (!mpu.begin()) {
mySerial.println("Failed to find MPU6050 chip");
while (1) {
delay(10);
}
}
mySerial.println("MPU6050 Found!");
mpu.setAccelerometerRange(MPU6050_RANGE_8_G);
mpu.setGyroRange(MPU6050_RANGE_500_DEG);
mpu.setFilterBandwidth(MPU6050_BAND_21_HZ);
}
```

```
void loop() {
sensors_event_t a, g, temp;
mpu.getEvent(&a, &g, &temp)
mySerial.print("Acceleration X: ");
mySerial.print(a.acceleration.x);
mySerial.print(", Y: ");
mySerial.print(a.acceleration.y);
mySerial.print(", Z: ");
mySerial.print(a.acceleration.z);
mySerial.println(" m/s^2");
mySerial.print("Rotation X: ");
mySerial.print(g.gyro.x);
mySerial.print(", Y: ");
mySerial.print(g.gyro.y);
mySerial.print(", Z: ");
mySerial.print(g.gyro.z);
mySerial.println(" rad/s");
//////////////
Serial.print("Acceleration X: ");
Serial.print(a.acceleration.x);
Serial.print(", Y: ");
Serial.print(a.acceleration.y);
Serial.print(", Z: ");
Serial.print(a.acceleration.z);
Serial.println(" m/s^2");
Serial.print("Rotation X: ");
Serial.print(g.gyro.x);
Serial.print(", Y: ");
Serial.print(g.gyro.y);
Serial.print(", Z: ");
Serial.print(g.gyro.z);
Serial.println(" rad/s");
Serial.print("Temperature: ");
Serial.print(temp.temperature);
```

```
Serial.println(" degC");
  //////////
mySerial.println("");
delay(100);
}
```